ROLE OF TUMOR MICROENVIRONMENT IN BREAST CANCER METASTASIS

by

Aparna Shinde

A Dissertation

Submitted to the Faculty of Purdue University

In Partial Fulfillment of the Requirements for the degree of

Doctor of Philosophy

Department of Medicinal Chemistry and Molecular Pharmacology

West Lafayette, Indiana

May 2019

THE PURDUE UNIVERSITY GRADUATE SCHOOL
STATEMENT OF COMMITTEE APPROVAL

Dr. Michael Wendt, Chair

Department of Medicinal Chemistry and Molecular Pharmacology

Dr. Jennifer Freeman

School of Health Sciences

Dr. Tony Hazbun

Department of Medicinal Chemistry and Molecular Pharmacology

Dr. Dorothy Teegarden

Department of Nutrition Science

Approved by:

Dr. Andy Hudmon

Head of the Graduate Program

This dissertation is dedicated to my Mom, Dad and my Husband.

ACKNOWLEDGMENTS

I would like to express my gratitude to my mentor, Dr. Michael Wendt for his advice, and guidance about research, thesis and beyond. He encouraged and supported me in all my challenging times at Purdue. I am thankful to all my committee members Dr. Jennifer Freeman, Dr. Dorothy Teegarden and Dr. Tony Hazbun for all their support and guidance.

I want to thank all my collaborators, Dr. Robert Geahlen, Dr. Luis Solorio, Dr. Dorothy Teegarden, and Dr. Dykhuizen for providing me wonderful opportunity to work with them on their projects. I am thankful to Dr. James Schaber for helping me with confocal microscopy. I am thankful to Purdue University for providing all the research facilities, which I used to complete all my projects.

I want to thank Dr. Wen-Hung Wang for teaching me CRISPR/CAS9 technique. I want to thank my collaborator and my dear friend Dr. Tomasz Wilmanski for his support, great ideas and discussions. I want to thank all Wendt lab members.

I am thankful to all my friends I have met in Purdue. I am very thankful to my life partner and my best friend Dr. Ruchit Mehta for all the love, advice, emotional support, patience, fun and lot more. Thank you Apeksha (Mom), Bhagwan (Dad), Avanti (Sister) and Anirudha (Brother). You make my life complete. Most of all, I thank God for all the blessings and for making this possible.

TABLE OF CONTENTS

LIST OF TABLES

LIST OF FIGURES

ABBREVIATIONS

EMT, Epithelial-Mesenchymal Transition

MET, Mesenchymal-Epithelial Transition

ECM, Extracellular Matrix

CRISPR, clustered regularly interspaced short palindromic repeats

FN, Fibronectin

TGM2, Tissue Transglutaminase 2

TGF-β, Transforming growth factor -β

FGFR, Fibroblast growth factor receptor

EGFR, Epidermal growth factor receptor

PDGFR, Platelet derived growth factor receptor

TNS1, Tensin

Ecad, E-cadherin

HMLE, Human mammary epithelial

HPF, Human pulmonary fibroblasts

HEK, Human embryonic kidney

SNAIL, Zinc finger protein SNAI1

SLUG, Zinc finger protein SNAI2

PARP1, Poly (ADP-Ribose) Polymerase 1

NF-κB, Nuclear factor kappa-light-chain-enhancer of activated B cells

ZEB1, Zinc finger E-box-binding homeobox 1

ZO-1, Zonula occludens-1

STAT3, Signal transducer and activator of transcription 3

CD, cluster of differentiation

WT, wild type

SEM, Standard error of the mean

TEM, Transmission electron microscopy

NC9, N-alpha-Carbobenzyloxy-N-epsilon-acryloyl-L-lysine(2 -(2dansylaminoethoxy)ethoxy)ethanamide

HIF-1, hypoxia-inducible factor-1

AKT, serine-threonine kinase 1

ERK, Extracellular Signal-Regulated Kinase

FAK, Focal Adhesion Kinase

ABSTRACT

Author: Shinde, Aparna Bhagwan. PhD
Institution: Purdue University
Degree Received: May 2019
Title: Role Of Tumor Microenvironment in Breast Cancer Metastasis
Committee Chair: Michael Wendt

Metastasis of primary mammary tumors to vital secondary organs is the primary cause of breast cancer-associated death, with no effective treatment. Metastasis is a highly selective process that requires cancer cells to overcome multiple barriers to escape the primary tumor, survive in circulation, and eventually colonize distant secondary organs. One of the important aspects of metastatic cancers is the ability to undergo epithelial-mesenchymal transition (EMT) and the reverse process mesenchymal-epithelial transition (MET) process. Constant interconversion of tumor cells between these phenotypes creates epithelial-mesenchymal heterogeneity (EMH) and interaction between these tumor cell types and the stromal cell compartment is clearly important to metastasis. In healthy tissues, stromal cells maintain the composition and structure of the tissue through the production of extracellular matrix (ECM) proteins and paracrine signaling with epithelial cells. However, little is known about how EMH promotes changes in the ECM to promote breast cancer progression and metastasis. Cancer cells also secret exosomes, nano-size extracellular vesicles, to establish intercellular communication with distant organs in order to induce metastasis. These exosomes contain a plethora of different proteins including extracellular matrix proteins and matrix crosslinking enzymes. Fibronectin, an important ECM protein, plays an active role in tumor progression and is often crosslinked by tissue transglutaminase 2 (TGM2) to promote fibrosis in cancer. Both FN and TGM2 exist in

exosomes and are expressed by heterogenous breast tumors. Although FN and TGM2 have been reported to play essential roles in cancer, their involvement in metastasis remains unclear. This work utilizes a variety of approaches to investigate the role of tumor heterogeneity and ECM proteins in promoting breast cancer metastasis. In this dissertation, we establish that mesenchymal cells expressing intracellular FN are held in a stable non-metastatic mesenchymal phenotype and produce cellular fibrils containing functionalized FN capable of supporting the growth of metastatic competent epithelial cells. We introduce a novel 3D culture system consisting of a tessellated scaffold which is capable of recapitulating cellular and matrix phenotypes *in vivo.* Further, we also demonstrate breast tumor cells secrete exosomes containing TGM2 crosslinked FN fibrils to promote premetastatic niche formation and induction of metastasis. Using genetic approaches, we establish TGM2 is essential and sufficient to drive metastasis. Finally, we demonstrate pharmacological inhibition of TGM2 offers a potential therapeutic strategy to treat metastatic breast cancer. Altogether, our research provides insights into the mechanism through which TGM2 promotes metastatic breast cancer. This work will help in developing new drugs to target TGM2 aimed at reducing breast cancer metastasis.

CHAPTER 1. INTRODUCTION

1.1 Breast Cancer Metastasis

Cancer is the second leading cause of death worldwide. Among women, breast cancer is the most commonly diagnosed and second leading cause of cancer-related death. Globally each year there is 23% growth in breast cancer cases among women [1,2]. The first line of treatment for early stage breast cancer patients is surgical removal of primary mammary tumors. The five-year survival rate for breast cancer patients is 99%, but there is a drastic drop to 22% for patients with a metastatic form of disease[3,4]. In addition, patients that undergo primary tumor removal can relapse several years later with metastatic disease. It is still extremely challenging to precisely recognize patients at higher risk of recurrence and cure patients with metastasis.

Biologically, metastasis is made up of several processes in which primary tumor cells spread to distant organs to form secondary tumors. There are multiple barriers for cancer cells to successfully metastasize. These barriers include sufficient invasion, migration, intravasation, extravasation, adaptation, and outgrowth[5]. Further, the microenvironment surrounding the tumor tissue plays an essential role in tumor progression and metastasis. Therefore, it is of utmost importance to understand the underlying mechanisms of metastatic breast cancer to develop a correct treatment to patients. In this study, we sought to understand the role of fibronectin, an extracellular matrix protein, in the metastatic progression of breast cancer. Understanding the factors that are key to the development of distant metastases will help to design effective strategies for diagnosis and develop better therapy for breast cancer patients with distant metastases.

1.2 Epithelial-Mesenchymal Transition

Epithelial-Mesenchymal Transition (EMT) is an evolutionarily conserved developmental program[6]. It also plays an important role in cancer progression and promotes metastasis by conferring properties like increased migration, invasion, proliferation and apoptotic resistance to cancer cells (Figure 1.1)[7]. In addition, EMT helps tumor cells to acquire stem cell properties and become more resistant to therapy[8,9]. Since EMT plays an essential role in metastasis, it has become one of the key hallmarks of cancers and a promising target in cancer therapy[10,11]. Nevertheless, the functional contribution of EMT to metastasis remains ambiguous and requires the creation of new *in vivo* and *in vitro* model system studies to achieve complete understanding.

The signaling pathways that are implicated in the maintenance of EMT comprise of transforming growth factor (TGF-β), bone morphogenic protein, fibroblast growth factor, epidermal growth factor, hepatocyte growth factor, Wnt/β-catenin, and Notch pathways[7]. Cancer cells that have undergone EMT are morphologically and epigenetically different as distinguished by augmented expression of mesenchymal markers like N-cadherin, vimentin, fibroblast-specific protein, and fibronectin (FN) and diminished expression of epithelial markers like E-cadherin, Zo-1, and occludin (Figure 1.1)[12]. Whether or not EMT influence copy number changes in gene mutation rates is interesting but not yet established. Cancer cells also exhibit enhanced expression of EMT-associated transcription factors such as Snail, Zeb, Twist, and Slug. Finally, EMT contributing miRNA's and epigenetic regulators contribute to cellular plasticity essential during metastasis and drug resistance[13].

Mechanistically, EMT promotes intravasation of cancer cells (Figure 1.2). Intravasation is the process where cancer cells cross the endothelial barrier to enter the circulatory system. These cells in circulation are required to exit from the circulation

system into distant tissues to form secondary tumors. After circulating tumor cells home to distant organs, they can undergo MET to colonize and form metastatic lesions. These outcomes, therefore, do not rule out the possibility of epithelial-mesenchymal plasticity (EMP) that allows tumor cells to undergo EMT or MET as needed. Modern CTC capture methods have detected both epithelial and mesenchymal CTCs in the circulation[14–17] and suggested CTCs exhibit heterogeneity and express EMT transcription factors[18,19]. In order to utilize EMT as a target for cancer therapy, it is very important to understand how EMT causes heterogeneity in primary and circulating tumor cells to promote metastasis.

1.2.1 Extracellular matrix proteins in EMT

The extracellular matrix is a complex network of proteins and polysaccharides that surrounds cells like a meshwork and is critical for cell survival, growth, proliferation, and tissue organization[20]. Structural studies suggest that ECM are rich in proteins including collagens, fibronectin, tissue transglutaminases, proteoglycans, laminins, and glycosaminoglycans; and that these elements are arranged in domains[20,21]. These domains are supportive of conserved structure-function relationships like oligomerization, engagement of certain cell surface receptors by FN, or the association of small leucine-rich proteoglycans to collagen[20,22]. It is further noteworthy that extracellular matrix is a vibrant structure where homeostasis is achieved by regulating the degradation and deposition processes, which is performed by families of endopeptidases, transglutaminases, matrix metalloproteinases (MMPS) under various physiological conditions[20,23]. Along with the alterations in the extracellular matrix architecture, various growth factors and bioactive fragments are released due to the degradation of extracellular matrix constituents by MMPs,

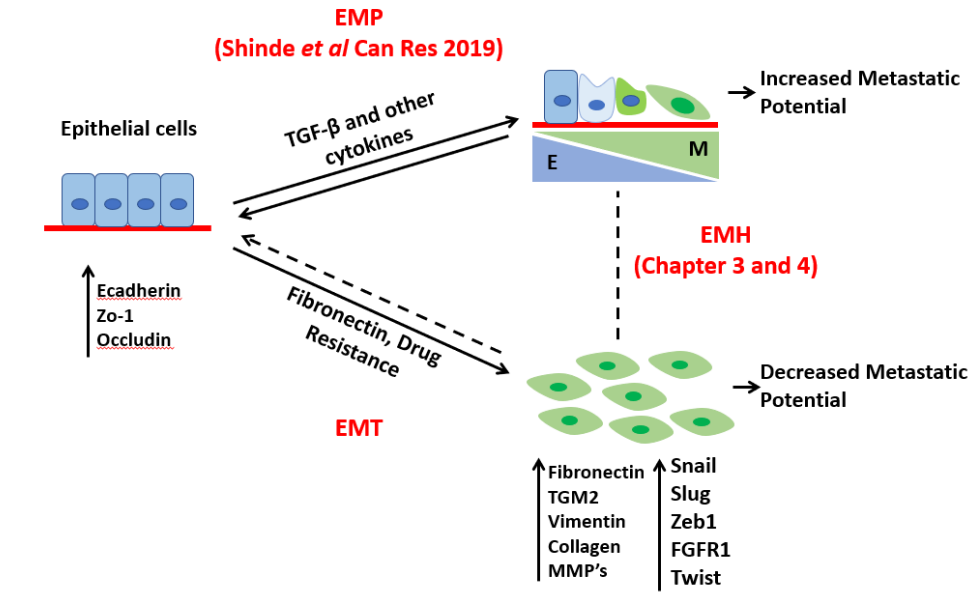

Figure 1.1: Illustration of Epithelial-Mesenchymal Transition (EMT) and Mesenchymal-Epithelial Transition (MET) processes[24]. Adapted from Mittal.V Annual Review of Pathology: Mechanism of Disease.

Induction of EMT in cancer cells causes them to undergo molecular and cellular changes resulting in mesenchymal phenotype. These mesenchymal cells have fibroblasts like morphology and can secrete extracellular matrix proteins including FN, collagen, and MMPs. Incomplete reversion to epithelial phenotype supports epithelial-mesenchymal heterogeneity (EMH). Cells that fail to undergo MET result in a permanent non-metastatic mesenchymal phenotype.

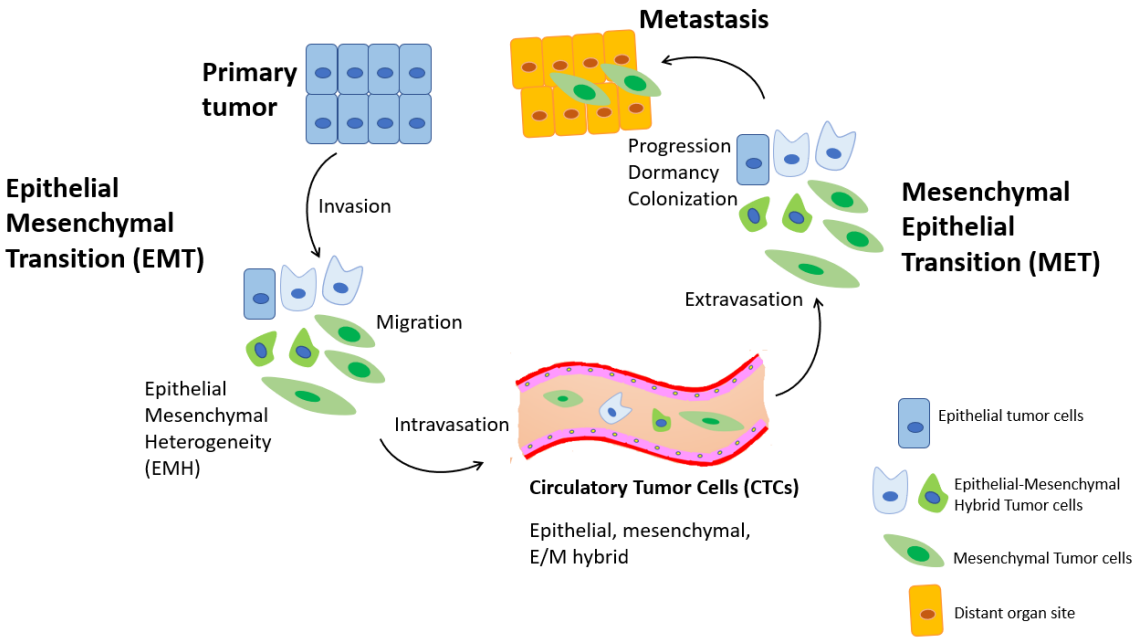

Figure 1.2: Illustration of epithelial-mesenchymal plasticity in tumor progression and metastasis[24]. Adapted from Mittal.V Annual Review of Pathology: Mechanism of Disease.

Induction of EMT in cancer cells causes them to undergo molecular and cellular changes resulting in mesenchymal phenotype that fosters local migration and invasion, intravasation, and extravasation. Upon arriving at metastatic sites, these cells can undergo MET by interacting with the tumor microenvironment to form macrometastases.

which significantly influences cell behavior. Given the importance of the extracellular matrix in driving major cell processes like cell growth, survival, differentiation, and EMT, it plays a major role in cancer progression and metastasis[21,22,25].

1.2.2 Fibronectin and fibrillogenesis

Fibronectin is an important component of ECM that promotes communication of cells with ECM via integrins and other receptors and regulates cell adhesion, migration, and differentiation[25]. Cells secret FN as a dimeric glycoprotein containing subunits ranging from 230 kDa and 270 kDa dependent on alternate splicing [26,27]. Fibronectin exists in different forms including plasma FN and cellular FN. Plasma FN was discovered 60 years ago in blood[28]. Cellular FN is mainly found in fibrillar matrices of most tissues and is one of the major forms of FN.

Fibronectin is mainly made of three modules termed type I, II and III repeats that have unique structures. Type I and II repeats exist in conformations due to disulfide bonds between modules whereas type III repeat consists of 7 stranded barrel arrangement and is deficient in disulfide bonds allowing conformational changes[29,30]. These set of modules form binding domains for many proteins and carbohydrates. Fibronectin consists of RGD-dependent cell binding domain in III_{10} and CS1 segment of the alternatively spliced V region[27]. Integrins can bind to either of these regions. Fibronectin communicates with cells through integrin receptors, αβ heterodimers containing two transmembrane domains[31]. Syndecans, a different family of cell surface receptors, connect with FN through the association of their glycosaminoglycan (GAG) chains with the carboxy-terminal heparin-binding domains of FN[32]. The carboxy-terminal heparin-binding domains of FN can also

bind heparin, heparan sulfate and chondroitin sulfate GAGs[33,34]. These associations play an important role in integrin-mediated cell spreading and intracellular signaling[35].

Fibronectin can associate with itself (self-association) using the amino-terminal assembly domain present in the first five types I repeats[34,36]. The amino-terminal assembly domain plays an important part in FN fibrillogenesis[37]. Being the crucial blood protein, FN interacts with fibrin using this domain during blood coagulation. The gelatin/collagen-binding domain is located adjacent to the amino-terminal assembly domain and is comprised of type I and type II modules[33]. This domain acts as a binding site for TGM2. Tissue transglutaminase 2 facilitates dimerization of FN by forming antiparallel disulfide bonds between the cysteine residues at the carboxy-terminal of FN[38]. These dimers are very important for the formation of FN fibrils. Apart from crosslinking FN, TGM2 also promotes FN assembly mediated by α5β1 and operates as integrin-binding adhesion coreceptor for FN[39]. The integrin receptors are concomitantly associated with the actin cytoskeleton via their cytoplasmic domains. This association allows FN-FN interactions outside the cell and activates signaling cascades important in cell adhesion, proliferation, and survival[39–41]. The initiation of the assembly of FN fibrils depends on FN binding to integrins which causes the development of FN multimers and soluble FN fibrils from FN dimers. Soluble and insoluble FN are distinguished based on their solubility in deoxycholate (DOC) detergent[42,43]. Eventually, FN dimers continue to associate from end to end that leads to lengthening and thickening of fibrils resulting in DOC insoluble FN matrix[44]. The strength of these insoluble FN fibrils is contingent on resilient non-covalent protein-protein interactions[45]. A dock and lock process can lead to the development of FN matrix in which FN dimers bind to fibrils in an irreversible fashion and then become

irreversibly integrated into fibrils by undergoing conformational transformations[46]. Thus, the distinct form of binding domains gives FN the capability to establish connections concurrently with other FN molecules, different ECM proteins including collagen, proteoglycans, various cell surface receptors, and extracellular enzymes. This multitasking of FN is crucial in the process of embryogenesis[47].

1.2.3 Fibronectin matrix deposition

Fibronectin bound to integrins is important for the formation of adhesion complexes in which integrins communicate with the actin cytoskeleton of cells through their cytoplasmic tails[48]. This interaction of FN with actin cytoskeleton via integrins is crucial for the assembly of FN matrix. Contractile actin-myosin filaments in stress fibers create tension at the location of contacts between integrins and FN[31,49]. The engagement of α5β1 integrins with actin induces translocation of these receptors away from the contact sites resulting in the induction of FN fibrillogenesis. These ECM contact complexes also contain tensin that binds to actin and β1 integrins simultaneously[40,48,50]. Other integrins that promote FN fibrillogenesis include αvβ3, αvβ5, αvβ6, α4β1, α4β7, αIIbβ3, α8β1, and α9β1[20]. Binding of integrins to FN also causes activation of focal adhesion kinase (FAK), which is essential in FN matrix assembly[34]. Further, Rho GTPase also regulates FN matrix assembly through activation of downstream Rho kinase instigating cell contractility and fibrillogenesis[51,52].

1.2.4 Fibronectin in cancer-associated EMT

Fibronectin regulates EMT signaling pathways like FAK/JAK/STAT3 pathway, which is dependent on β1-integrin activation[53]. Augmented expression of FN regulates EMT partially in mammary epithelial cancer cells and lung cancer[12,54]. Fibronectin can also

upregulate the molecular expression of mesenchymal genes like Snail, N-cadherin, vimentin, MMP-2, and p-Smad2, and stimulate an EMT response in these cancer cells[54,55]. Furthermore, FN signaling is based on Src, Erk1/2, and PI3-K activation and associated with diminished junctional E-cadherin expression[56]. Fibronectin promotes its own expression by driving expression of mesenchymal genes such as Snail1-NF-κB-PARP1 complex that binds to the FN promoter and induces FN expression[57]. Cytokines like TGF-β induce FN expression and drive EMT in breast cancer cells[54]. In addition, decrease in expressions of FN and vimentin result in reduced cell motility and inhibition of EMT[58]. Thus, increased FN expression is associated with tumor aggressiveness and EMT processes.

1.2.5 Tissue transglutaminase 2

One of the most complicated and global members of the transglutaminase family of enzymes is tissue transglutaminase 2 (TGM2). In the abundance of Ca^{2+}, TGM2 modifies proteins post-translationally by crosslinking stable ε-(γ-glutamyl)lysine isopeptide or polyamines at specific peptide bound glutamine residues[59]. Other functions of TGM2 include guanine triphosphate (GTP) hydrolysis and protein disulfide isomerization[59]. Further, TGM2 can also act as kinase and scaffold protein[60–62]. Surface TGM2 is involved in cell adhesion and integrin signaling since it is capable of engaging various ECM proteins including FN, laminin, vitronectin, and collagen. Its interaction with FN and integrins is critical for cell-ECM adhesion, cell migration, and formation of fibrillar FN networks[61]. Tissue transglutaminase 2 has high affinity to the gelatin-binding region of FN[41,63,64]. Further, TGM2 can also bind β1, β3, and β5 integrins subunits to stabilize integrin-FN interactions essential for driving different cellular processes[64]. Because of its modest affinity for integrin-FN complex and robust non-covalent association with both

proteins, it acts as a bridge between integrin and FN thereby strengthening the cell-ECM interactions[64]. Subsequently, the implication of TGM2 in integrin-mediated FN matrix deposition, cell adhesion, spreading, survival, differentiation, and ECM contraction was discovered in both normal and cancer cells[65,66]. As TGM2 can remodel ECM and induce fibrosis in many cancers, TGM2-FN interaction has become a new promising target for emerging innovative cancer drugs to block tumor cells attachment to ECM and curb associated signaling pathways[67,68].

Abnormal upregulation of TGM2 is observed in multiple cancers including glioblastoma, ovarian cancer, breast cancer, osteosarcomas, lung, malignant melanomas, and pancreatic ductal carcinomas[69–74]. Often, aberrant TGM2 expression is associated with chemotherapeutic resistance and metastasis. In mammary cancer cells, TGM2 induces drug resistance and augments invasiveness through EMT[66]. Both its expression and enzymatic activity alter pathways important in cancer progression including the establishment of NF-κB, HIF-1α, AKT, epidermal growth factor-mediated carcinogenesis, and suppression of PTEN (phosphatase and tensin homolog deleted on chromosome 10)[75]. Further, TGM2 can also promote EMT [66,76]. Overexpression of TGM2 induces EMT in mammary cancer cells and upregulates expression of mesenchymal markers like Snail1, Twist1, and Zeb1 to increase anchorage-independent growth, migration, and invasiveness[65]. Further, loss of TGM2 promotes MET in drug-resistant breast cancer cells accompanied with increased expression of E-cadherin at junctions and diminished levels of Snail1 and Zeb1[76]. In addition, TGM2 acts downstream of TGF-β and is required for TGF-β induced EMT in mammary epithelial cells[66]. Together these data suggest the importance of TGM2 in EMT, which is crucial for metastatic dissemination and tumor development.

1.2.6 Tissue transglutaminase 2 as an emerging therapeutic target for cancer

Since TGM2 plays an active role in different cancers [59,75], a possible strategy to treat cancers would be impeding its active site. Also, this offers a distinct prospect to manage different types of cancer at different stages. Since TGM2 can modulate multiple signaling pathways and functions in cancer cells important for their growth and survival, its inhibition offers a single target for cancer therapeutics.

Tissue transglutaminase 2 inhibitors are classified into three types depending on their mode of action. These three classes consist of a) competitive amine inhibitors 2) reversible inhibitors and 3) irreversible inhibitors. The most commonly used TGM2 inhibitors are competitive inhibitors because of their commercial availability, chemical stability, and non-toxicity in living cells. These inhibitors include putrescine, monodansylcadaverine, and 5-(biotinamido) pentylamine and they impede TGM2 transamidase activity by competing with natural amine substrates such as protein-bound lysine residues[77]. Reversible TGM2 inhibitors include GTP, and compounds with thieno[2,3-d] pyrimidine-4-one acyl hydrazide backbones. These inhibitors block the substrate access to the active site of TGM2 without covalently altering the enzyme[78,79]. Irreversible TGM2 inhibitors impede enzymatic activity through covalent modification of the enzyme thereby preventing the substrate binding. These include iodoacetamide, 3-halo-4,5-dihydroisoxazoles, and carbobenzyloxy-L-glutaminylglycine (Cbz-gln-gly) as backbone[80–85]. Recently, Keillor group developed (6-acrylamido-1-(4-((5-(dimethylamino)naphthalen-1-yl)sulfonyl)piperazin-1-yl)- 1-oxohexan-2-yl)carbamate (VA4), and (S)-Benzyl (6-acrylamido-1-(4-(7-hydroxy-2-oxo-2H-chromene-3-carbonyl)piperazin-1-yl)- 1-oxohexan-2-yl)carbamate (VA5) and N-alpha-Carbobenzyloxy-N-epsilon-acryloyl-L-lysine(2-(2dansylaminoethoxy)ethoxy)ethanamide

(NC9) as effective TGM2 irreversible inhibitors[86,87]. Effective inhibition of TGM2 by NC9 is reported in many cancers including glioblastoma, ovarian, epidermal, leukemia, and prostate and therefore it is a promising inhibitor of TGM2[86,88–93]. TTGM5826, a recently developed inhibitor for TGM2, stabilizes the open conformation of TGM2 in breast and brain cancer cells to induce cell death[94]. Thus, the application of different TGM2 inhibitors to biological systems has generated encouraging outcomes in various types of cancer. In this dissertation, we have used NC9 inhibitor obtained from Keillor group to examine its potential in TGM2 inhibition to treat breast cancer metastasis.

1.3 Exosomes

Prokaryotic and eukaryotic cells shed extracellular vesicles that can exist in micro or nano-sizes[95]. Nanosized vesicular structures that range from 30- 100 nm are termed as exosomes. Exosomes are formed from the luminal membranes of multivesicular bodies (MVBs)[96]. Most exosomes are released into the extracellular environment while some of them are secreted into neighboring cells through their fusion to the cell membrane. In addition, exosomes can activate multiple signaling pathways involved in important cellular processes or transfer specific information into targeted recipient cells upon their systemic transport to distant organs [97,98]. Cancer cells derived exosomes contain functional molecular cargo comprising of oncogenic virus derived molecules, miRNA, mRNA, DNA fragments, cytokines, ECM proteins like FN, laminins, integrins, enzymes like TGM2, kinases, transcription factors, growth factors including EGFR, FGFR, VEGF and other proteins like Dicer, therefore, capable of causing malignant transformation and promoting tumor progression; suggesting a probable evolutionary process through which tumor cells

utilize exosomes and protect their homeostasis for their own advantages like growth, drug resistance, and survival[99–102].

1.3.1 Role of exosomes in cancer

Recent studies have indicated the critical role of exosomes in invasion-metastasis cascade. Their role has been recognized in EMT induction, construction of a premetastatic niche and immune response modulation[103–106]. Through the delivery of necessary autocrine and paracrine signals, cancer cells derived exosomes can induce EMT in neoplastic cells, which allows them to invade the surrounding tissue of the primary tumor, intravasate and arrive into the circulatory system. In contrast to exosomes secreted under normoxic conditions, those secreted under hypoxic conditions exhibit increased expression of EMT-inducing moieties including FN, integrins, TGF-β1, TGM2, vimentin, tumor necrosis factor α (TNF-α), HIF-1α, interleukin-6, and platelet-derived growth factors (PDGF)[107,108]. Consequently, cells present in the tumor microenvironment end up taking the above molecules that cause modifications of their transcriptome and proteome.

Secondly, cancer cells derived exosomes nurture a premetastatic niche in distant organs, which helps metastatic cells to extravasate, survive dormancy, or ultimately form secondary tumors (Figure 1.3). They create a premetastatic niche by stimulating reactive, myofibroblast-rich stroma, ECM remodeling, proliferation and angiogenesis [109–112]. Further, activation of TGF-β-SMAD pathway by exosomes causes differentiation of mesenchymal stem cells and normal stromal fibroblasts into myofibroblast-like cells[113–115]. In addition, TGF-β from exosomes causes generation of myofibroblasts that have increased fibroblast growth factor and are more proangiogenic[114]. Interestingly, non-cancerous cells

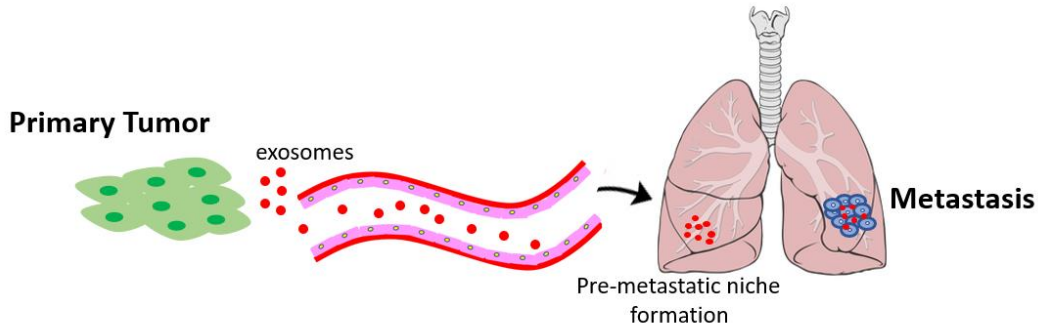

Figure 1.3: Illustration of premetastatic formation by exosomes secreted by primary tumor.

derived exosomes may also help circulating tumor cells in adapting to unfavorable conditions; thereby promoting dynamic and bidirectional crosstalk within the tumor microenvironment. Cancer cells derived exosomes can also promote pre-metastatic niche establishment by modifying tumor-penetrating lymphocytes to promote immune evasion and destruction within the tumor microenvironment, an essential event for metastasis[100,104,108,116]. Further, exosomes can promote organotropism[106,117]. Cancer cells derived exosomes are also capable of tempering immune response to promote metastatic progression and can trigger inflammatory pathways that force immune players to cultivate a prometastatic microenvironment[116,118]

1.4 Research Questions

As detailed above, metastatic breast cancer is the most lethal disease among women worldwide[3]. Metastasis is a cascade of sequential events. Upon transformation, primary tumor cells undergo EMT and MET to form metastatic lesions in distant organs[7]. Cells that are incapable of undergoing a complete transition from mesenchymal to epithelial phenotype or vice versa results in tumor heterogeneity. Recent information insinuates that influential inducers of EMT can drive epithelial tumor cells into a highly mesenchymal, stromal-like state. These mesenchymal cells are incapable of undergoing MET or have limited capacity and therefore, can act as cancer-associated fibroblasts[119]. The inducers of these more stable mesenchymal phenotypes and the mechanism through which these stromal-like tumor cells continue to contribute to the metastatic process are unknown. Therefore, further studies are essential to elucidate the role of heterogeneity in metastatic breast cancer. Similarly, the impact of matrix proteins secreted by these mesenchymal

tumor cells in metastatic breast cancer remains poorly understood and continues to be a topic of investigation in breast cancer research.

Fibronectin is overexpressed in many cancers and actively involved in multiple steps of tumor progression[20]. Also, FN expression is known to increase during EMT. Although, several studies suggest the role of abnormal FN expression in cancer cell survival, invasion, proliferation and metastasis[120–122], how FN expressed by mesenchymal tumor cells in heterogenous tumors supports tumor progression and metastasis remains unclear. Further, FN is functional only in its fibrillar form and cells expressing FN like fibroblasts mainly deposit FN matrix[36]. Whether mesenchymal tumor cells expressing FN are capable of producing functionalized FN fibrils or depositing FN matrix to act in stromal capacity, still remains under-investigated.

Tissue transglutaminase 2 is abnormally overexpressed in metastatic and drug-resistant tumor cells. It is a multi-functional enzyme and important for various biological processes including extracellular matrix formation and integrin-mediated signaling[69,123]. However, its role in metastatic breast cancer is ambiguous. Further, extracellular vesicles isolated from cancer cells contain TGM2 and can transform non-cancerous cells to support cancer cells growth and survival[124]. Whether these exosomes can construct a premetastatic niche to foster metastasis of breast cancer cells has not been investigated.

This dissertation specifically focuses on investigating the role of epithelial-mesenchymal heterogeneity (EMH) and extracellular matrix proteins in promoting breast cancer metastasis. ***We hypothesize that mesenchymal breast cancer cells in epithelial-mesenchymal heterogenous tumors secrete extracellular matrix proteins or exosomes containing extracellular matrix proteins to establish intercellular communication***

important for tumor progression and distant metastasis. To test our hypothesis, we designed three specific aims. The first aim focuses on determining the role of EMH in breast cancer metastasis. In the second aim, we investigate how mesenchymal cells utilize intracellular FN to support the growth of metastatic competent epithelial cells. The last aim examines the role of exosomes secreted by metastatic breast cancer cells in the development of the premetastatic niche to foster tumor progression and metastasis.

To accomplish our first aim, we used Ca1h and Ca1a models to create primary mosaic tumors and tracked their individual metastasis capacity using bioluminescence technique (chapter 3). Our study suggests that mesenchymal cells promote metastasis of epithelial breast cancer cells. We demonstrate epithelial breast cancer cells interact with mesenchymal breast cancer cells to support their own growth and proliferation (chapter 3).

The second aim investigated the autocrine and paracrine role of FN using a novel 3D scaffold system that accurately recapitulated *in vivo* tumor microenvironment conditions. To determine the function of FN, we used gain or loss of function approaches and performed both *in vitro and in vivo* assays. As a result of our investigation, it was identified that cells expressing FN get locked into a non-metastatic mesenchymal phenotype and act in a stromal fashion to support the growth of metastatic competent cells by producing functionalized fibrils (chapter 3).

To achieve our third aim, we used a HER2-driven (HME2) metastatic progression series developed in the Wendt lab [125]. Using gain and loss of function approaches and *in vivo* metastasis assays, we report that TGM2 is not only required for breast cancer progression but also adequate to modify non-metastatic tumor cells into metastatic tumor cells (chapter 4). Next, we investigated the role of exosomes containing FN and TGM2 in

driving metastatic breast cancer. Results of our study demonstrate that TGM2 crosslinks FN on the surface of exosomes to induce premetastatic niche formation and promotes metastatic breast cancer. Further, our study reveals that TGM2 upregulates tensin expression to promote FN fibrillogenesis on the surface of exosomes. We also establish that genetic depletion of TGM2 inhibits metastasis and therefore, can be an effective therapeutic target to treat metastatic breast cancer.

Collectively, the studies reported in this dissertation shed new light on tumor growth promoting functions of FN within the ECM and its autocrine role in inhibiting the metastatic potential of mesenchymal tumor cells. Results of our investigations also establish that TGM2 is essential and sufficient to promote metastasis of breast cancer cells. Further, our studies contribute to the growing knowledge of FN and TGM2-mediated mechanisms in metastatic breast cancer, particularly the development of TGM2 as a therapeutic target.

1.5 References

1. DeSantis, C., Ma, J., Bryan, L. & Jemal, A. Breast cancer statistics, 2013. *CA. Cancer J. Clin.* (2014). doi:10.1039/b614914f
2. Ghoncheh, M., Pournamdar, Z. & Salehiniya, H. Incidence and Mortality and Epidemiology of Breast Cancer in the World. *Asian Pacific J. Cancer Prev.* (2016). doi:10.7314/APJCP.2016.17.S3.43
3. F. Bray *et al.* Global Cancer Statistics 2018: GLOBOCAN Estimates of Incidence and Mortality Worldwide for 36 Cancers in 185 Countries. *CA. Cancer J. Clin.* (2018). doi:10.3322/caac.21492
4. Breastcancer.org. U.S. Breast Cancer Statistics. *Web Page* (2018). doi:10.1080/14786437308217452

5. Hanahan, D. & Weinberg, R. A. Hallmarks of cancer: The next generation. Vol. 144, Cell. 2011. p. 646–74. llmarks of cancer: The next generation. *Cell* (2011). doi:10.1016/j.cell.2011.02.013
6. Thiery, J. P., Acloque, H., Huang, R. Y. J. & Nieto, M. A. Epithelial-Mesenchymal Transitions in Development and Disease. *Cell* (2009). doi:10.1016/j.cell.2009.11.007
7. Brabletz, T., Kalluri, R., Nieto, M. A. & Weinberg, R. A. EMT in cancer. *Nature Reviews Cancer* (2018). doi:10.1038/nrc.2017.118
8. Brown, W. S., Akhand, S. S. & Wendt, M. K. FGFR signaling maintains a drug persistent cell population following epithelial-mesenchymal transition. *Oncotarget* (2016). doi:10.18632/oncotarget.13117
9. Mani, S. A. *et al.* The Epithelial-Mesenchymal Transition Generates Cells with Properties of Stem Cells. *Cell* (2008). doi:10.1016/j.cell.2008.03.027
10. Hanahan, D. & Weinberg, R. A. Hallmarks of cancer: The next generation. *Cell* (2011). doi:10.1016/j.cell.2011.02.013
11. Hanahan, D. & Weinberg, R. A. The hallmarks of cancer. *Cell* (2000). doi:10.1016/S0092-8674(00)81683-9
12. Willis, B. C. & Borok, Z. TGF-β-induced EMT: mechanisms and implications for fibrotic lung disease. *Am. J. Physiol. Cell. Mol. Physiol.* (2007). doi:10.1152/ajplung.00163.2007
13. Díaz-López, A. *et al.* Zeb1 and Snail1 engage miR-200f transcriptional and epigenetic regulation during EMT. *Int. J. Cancer* (2015). doi:10.1002/ijc.29177
14. Alix-Panabières, C., Mader, S. & Pantel, K. Epithelial-mesenchymal plasticity in circulating tumor cells. *Journal of Molecular Medicine* (2017). doi:10.1007/s00109-016-1500-6
15. Alix-Panabieѐres, C. & Pantel, K. Circulating tumor cells: Liquid biopsy of cancer. *Clinical Chemistry* (2013). doi:10.1373/clinchem.2012.194258
16. Yu, M. *et al.* Circulating breast tumor cells exhibit dynamic changes in epithelial and mesenchymal composition. *Science (80-.).* (2013). doi:10.1126/science.1228522

17. Liu, H. Y. & Yin, Z. F. Epithelial-mesenchymal transition and circulating tumor cells. *Tumor* (2013). doi:10.3781/j.issn.1000-7431.2013.09.015
18. Khoo, B. L. *et al.* Short-term expansion of breast circulating cancer cells predicts response to anti-cancer therapy. *Oncotarget* (2015). doi:10.18632/oncotarget.3903
19. Barriere, G. *et al.* Circulating tumor cells and epithelial, mesenchymal and stemness markers: characterization of cell subpopulations. *Ann. Transl. Med.* (2014). doi:10.3978/j.issn.2305-5839.2014.10.04
20. Theocharis, A. D., Skandalis, S. S., Gialeli, C. & Karamanos, N. K. Extracellular matrix structure. *Advanced Drug Delivery Reviews* (2016). doi:10.1016/j.addr.2015.11.001
21. Hynes, R. O. & Naba, A. Overview of the matrisome-An inventory of extracellular matrix constituents and functions. *Cold Spring Harb. Perspect. Biol.* (2012). doi:10.1101/cshperspect.a004903
22. Lu, P., Weaver, V. M. & Werb, Z. The extracellular matrix: A dynamic niche in cancer progression. *Journal of Cell Biology* (2012). doi:10.1083/jcb.201102147
23. Hynes, R. O. The extracellular matrix: Not just pretty fibrils. *Science* (2009). doi:10.1126/science.1176009
24. Mittal, V. Epithelial Mesenchymal Transition in Tumor Metastasis. *Annu. Rev. Pathol. Mech. Dis.* doi:doi.org/10.1146/annurev-pathol-020117-043854
25. Bonnans, C., Chou, J. & Werb, Z. Remodelling the extracellular matrix in development and disease. *Nature Reviews Molecular Cell Biology* (2014). doi:10.1038/nrm3904
26. Liwnicz, B. H. & Sawaya, R. Fibronectin. in *Immunodiagnosis of Cancer: Second Edition* (2017). doi:10.1201/9780203751268
27. Pankov, R. Fibronectin at a glance. *J. Cell Sci.* (2002). doi:10.1242/jcs.00059
28. Edsall, J. T. SOME EARLY HISTORY OF COLD- INSOLUBLE GLOBULIN. *Ann. N. Y. Acad. Sci.* (1978). doi:10.1111/j.1749-6632.1978.tb16788.x
29. Hynes, R. O. Fibronectins. *Scientific American* (1986). doi:10.1038/scientificamerican0686-42

30. Sechrist, J., Loredo, G., Peters, J., Bronner-Fraser, M. & Luetolf, S. Spatial Expression of the Alternatively Spliced EIIIB and EIIIA Segments of Fibronectin in the Early Chicken Embryo. *Cell Commun. Adhes.* (2003). doi:10.1080/15419060216015
31. Johansson, S., Svineng, G., Wennerberg, K., Armulik, A. & Lohikangas, L. Fibronectin-integrin interactions. *Front. Biosci.* (1997).
32. Stepp, M. A. *et al.* Syndecan-1 regulates cell migration and fibronectin fibril assembly. *Exp. Cell Res.* (2010). doi:10.1016/j.yexcr.2010.05.020
33. Mao, Y. & Schwarzbauer, J. E. Fibronectin fibrillogenesis, a cell-mediated matrix assembly process. *Matrix Biology* (2005). doi:10.1016/j.matbio.2005.06.008
34. Singh, P., Carraher, C. & Schwarzbauer, J. E. Assembly of Fibronectin Extracellular Matrix. *Annu. Rev. Cell Dev. Biol.* (2010). doi:10.1146/annurev-cellbio-100109-104020
35. Roy, D. C. & Hocking, D. C. Recombinant Fibronectin Matrix Mimetics Specify Integrin Adhesion and Extracellular Matrix Assembly. *Tissue Eng. Part A* (2013). doi:10.1089/ten.tea.2012.0257
36. Schwarzbauer, J. E. & Sechler, J. L. Fibronectin fibrillogenesis: A paradigm for extracellular matrix assembly. *Current Opinion in Cell Biology* (1999). doi:10.1016/S0955-0674(99)00017-4
37. Halliday, N. L. & Tomasek, J. J. Mechanical properties of the extracellular matrix influence fibronectin fibril assembly in vitro. *Exp. Cell Res.* (1995). doi:10.1006/excr.1995.1069
38. Akimov, S. S. & Belkin, A. M. Cell-surface transglutaminase promotes fibronectin assembly via interaction with the gelatin-binding domain of fibronectin: a role in TGFbeta-dependent matrix deposition. *J. Cell Sci.* (2001).
39. Akimov, S. S., Krylov, D., Fleischmana, L. F. & Belkin, A. M. Tissue transglutaminase is an integrin-binding adhesion coreceptor for fibronectin. *J. Cell Biol.* (2000). doi:10.1083/jcb.148.4.825
40. Mierke, C. T., Frey, B., Fellner, M., Herrmann, M. & Fabry, B. Integrin {alpha}5{beta}1 facilitates cancer cell invasion through enhanced contractile forces. *J Cell Sci* (2011). doi:10.1242/jcs.071985

41. Wang, Z. *et al.* RGD-independent cell adhesion via a tissue transglutaminase-fibronectin matrix promotes fibronectin fibril deposition and requires syndecan-4/2 and α5β1 integrin co-signaling. *J. Biol. Chem.* (2010). doi:10.1074/jbc.M110.123703
42. Choi, M. G. & Hynes, R. O. Biosynthesis and processing of fibronectin in NIL.8 hamster cells. *J. Biol. Chem.* (1979).
43. McKeown Longo, P. J. & Mosher, D. F. Binding of plasma fibronectin to cell layers of human skin fibroblasts. *J. Cell Biol.* (1983). doi:10.1083/jcb.97.2.466
44. Chen, H. & Mosher, D. F. Formation of Sodium Dodecyl Sulfate-stable Fibronectin Multimers. *J. Biol. Chem.* (2002). doi:10.1074/jbc.271.15.9084
45. Main, A. L., Harvey, T. S., Baron, M., Boyd, J. & Campbell, I. D. The three-dimensional structure of the tenth type III module of fibronectin: An insight into RGD-mediated interactions. *Cell* (1992). doi:10.1016/0092-8674(92)90600-H
46. Esler, W. P. *et al.* Alzheimer's disease amyloid propagation by a template-dependent dock- lock mechanism. *Biochemistry* (2000). doi:10.1021/bi992933h
47. Rozario, T., Dzamba, B., Weber, G. F., Davidson, L. A. & DeSimone, D. W. The physical state of fibronectin matrix differentially regulates morphogenetic movements in vivo. *Dev. Biol.* (2009). doi:10.1016/j.ydbio.2008.12.025
48. Pankov, R. *et al.* Integrin dynamics and matrix assembly: Tensin-dependent translocation of α5β1 integrins promotes early fibronectin fibrillogenesis. *J. Cell Biol.* (2000). doi:10.1083/jcb.148.5.1075
49. Leiss, M., Beckmann, K., Girós, A., Costell, M. & Fässler, R. The role of integrin binding sites in fibronectin matrix assembly in vivo. *Current Opinion in Cell Biology* (2008). doi:10.1016/j.ceb.2008.06.001
50. McCleverty, C. J., Lin, D. C. & Liddington, R. C. Structure of the PTB domain of tensin1 and a model for its recruitment to fibrillar adhesions. *Protein Sci* (2007). doi:10.1110/ps.072798707
51. Zhang, Q., Magnusson, M. K. & Mosher, D. F. Lysophosphatidic acid and microtubule-destabilizing agents stimulate fibronectin matrix assembly through Rho-dependent actin stress fiber formation and cell contraction. *Mol. Biol. Cell* (2013). doi:10.1091/mbc.8.8.1415

52. Yoneda, A., Ushakov, D., Multhaupt, H. A. B. & Couchman, J. R. Fibronectin Matrix Assembly Requires Distinct Contributions from Rho Kinases I and -II. *Mol. Biol. Cell* (2006). doi:10.1091/mbc.e06-08-0684
53. Balanis, N. *et al.* Epithelial to mesenchymal transition promotes breast cancer progression via a fibronectin-dependent STAT3 signaling pathway. *J. Biol. Chem.* (2013). doi:10.1074/jbc.M113.475277
54. Park, J. & Schwarzbauer, J. E. Mammary epithelial cell interactions with fibronectin stimulate epithelial-mesenchymal transition. *Oncogene* (2014). doi:10.1038/onc.2013.118
55. Freire-de-Lima, L. *et al.* Involvement of O-glycosylation defining oncofetal fibronectin in epithelial-mesenchymal transition process. *Proc. Natl. Acad. Sci.* (2011). doi:10.1073/pnas.1115191108
56. Meng, X. N. *et al.* Characterisation of fibronectin-mediated FAK signalling pathways in lung cancer cell migration and invasion. *Br. J. Cancer* (2009). doi:10.1038/sj.bjc.6605154
57. Stanisavljevic, J., Porta-de-la-Riva, M., Batlle, R., de Herreros, A. G. & Baulida, J. The p65 subunit of NF-κB and PARP1 assist Snail1 in activating fibronectin transcription. *J. Cell Sci.* (2011). doi:10.1242/jcs.078824
58. Wu, Y.-M. *et al.* Inhibition of ERRalpha suppresses epithelial mesenchymal transition of triple negative breast cancer cells by directly targeting fibronectin. *Oncotarget* (2015). doi:10.18632/oncotarget.4436
59. Belkin, A. M. Extracellular TG2: Emerging functions and regulation. *FEBS Journal* (2011). doi:10.1111/j.1742-4658.2011.08346.x
60. Nurminskaya, M. V. & Belkin, A. M. Cellular Functions of Tissue Transglutaminase. *Int. Rev. Cell Mol. Biol.* (2012). doi:10.1016/B978-0-12-394305-7.00001-X
61. Collighan, R. J. & Griffin, M. Transglutaminase 2 cross-linking of matrix proteins: Biological significance and medical applications. *Amino Acids* (2009). doi:10.1007/s00726-008-0190-y

62. Odii, B. O. & Coussons, P. Biological functionalities of transglutaminase 2 and the possibility of its compensation by other members of the transglutaminase family. *The Scientific World Journal* (2014). doi:10.1155/2014/714561
63. Lortat-Jacob, H. *et al.* Transglutaminase-2 interaction with heparin: Identification of a heparin binding site that regulates cell adhesion to fibronectin-transglutaminase-2 matrix. *J. Biol. Chem.* (2012). doi:10.1074/jbc.M111.337089
64. Hang, J., Zemskov, E. A., Lorand, L. & Belkin, A. M. Identification of a novel recognition sequence for fibronectin within the NH2-terminal β-sandwich domain of tissue transglutaminase. *J. Biol. Chem.* (2005). doi:10.1074/jbc.M503323200
65. Agnihotri, N., Kumar, S. & Mehta, K. Tissue transglutaminase as a central mediator in inflammation-induced progression of breast cancer. *Breast Cancer Research* (2012). doi:10.1186/bcr3371
66. Kumar, A. *et al.* Tissue transglutaminase promotes drug resistance and invasion by inducing mesenchymal transition in mammary epithelial cells. *PLoS One* (2010). doi:10.1371/journal.pone.0013390
67. Agnihotri, N. & Mehta, K. Transglutaminase-2: evolution from pedestrian protein to a promising therapeutic target. *Amino Acids* (2017). doi:10.1007/s00726-016-2320-2
68. Siegel, M. & Khosla, C. Transglutaminase 2 inhibitors and their therapeutic role in disease states. *Pharmacology and Therapeutics* (2007). doi:10.1016/j.pharmthera.2007.05.003
69. Huang, L., Xu, A. M. & Liu, W. Transglutaminase 2 in cancer. *Am. J. Cancer Res.* (2015).
70. Oh, K., Moon, H.-G., Lee, D.-S. & Yoo, Y.-B. Tissue transglutaminase-interleukin-6 axis facilitates peritoneal tumor spreading and metastasis of human ovarian cancer cells. *Lab. Anim. Res.* (2015). doi:10.5625/lar.2015.31.4.188
71. Mangala, L. S., Fok, J. Y., Zorrilla-Calancha, I. R., Verma, A. & Mehta, K. Tissue transglutaminase expression promotes cell attachment, invasion and survival in breast cancer cells. *Oncogene* (2007). doi:10.1038/sj.onc.1210035
72. Akar, U. *et al.* Tissue Transglutaminase Inhibits Autophagy in Pancreatic Cancer Cells. *Mol. Cancer Res.* (2007). doi:10.1158/1541-7786.MCR-06-0229

73. Fok, J. Y. Implications of tissue transglutaminase expression in malignant melanoma. *Mol. Cancer Ther.* (2006). doi:10.1158/1535-7163.mct-06-0083
74. Tucholski, J., Lesort, M. & Johnson, G. V. W. Tissue transglutaminase is essential for neurite outgrowth in human neuroblastoma SH-SY5Y cells. *Neuroscience* (2001). doi:10.1016/S0306-4522(00)00482-6
75. Kumar, S. & Mehta, K. Tissue transglutaminase, inflammation, and cancer: How intimate is the relationship? *Amino Acids* (2013). doi:10.1007/s00726-011-1139-0
76. He, W., Sun, Z. & Liu, Z. Silencing of TGM2 reverses epithelial to mesenchymal transition and modulates the chemosensitivity of breast cancer to docetaxel. *Exp. Ther. Med.* (2015). doi:10.3892/etm.2015.2679
77. Wodzinska, J. Transglutaminases as Targets for Pharmacological Inhibition. *Mini-Reviews Med. Chem.* (2012). doi:10.2174/1389557053175416
78. Lai, T.-S., Slaughter, T. F., Peoples, K. a, Hettasch, J. M. & Greenberg, C. S. Regulation of Human Tissue Transglutaminase Function by Magnesium-Nucleotide Complexes. *J. Biol. Chem.* (1998).
79. Duval, E., Case, A., Stein, R. L. & Cuny, G. D. Structure-activity relationship study of novel tissue transglutaminase inhibitors. *Bioorganic Med. Chem. Lett.* (2005). doi:10.1016/j.bmcl.2005.02.005
80. Marrano, C. *et al.* Synthesis and evaluation of novel dipeptide-bound 1,2,4-thiadiazoles as irreversible inhibitors of guinea pig liver transglutaminase. *Bioorg. Med. Chem.* (2001). doi:10.1016/S0968-0896(01)00228-0
81. Marrano, C., De Macédo, P. & Keillor, J. W. Evaluation of novel dipeptide-bound α,β-unsaturated amides and epoxides as irreversible inhibitors of guinea pig liver transglutaminase. *Bioorganic Med. Chem.* (2001). doi:10.1016/S0968-0896(01)00101-8
82. Halim, D., Caron, K. & Keillor, J. W. Synthesis and evaluation of peptidic maleimides as transglutaminase inhibitors. *Bioorganic Med. Chem. Lett.* (2007). doi:10.1016/j.bmcl.2006.10.061
83. De Macédo, P., Marrano, C. & Keillor, J. W. Synthesis of dipeptide-bound epoxides and α,β-unsaturated amides as potential irreversible transglutaminase inhibitors. *Bioorganic Med. Chem.* (2002). doi:10.1016/S0968-0896(01)00292-9

84. Castelhano, A. L., Billedeau, R., Pliura, D. H., Bonaventura, B. J. & Krantz, A. Synthesis, chemistry, and absolute configuration of novel transglutaminase inhibitors containing a 3-halo-4,5-dihydroisoxazole. *Bioorg. Chem.* (1988). doi:10.1016/0045-2068(88)90019-3

85. Folk, J. E. & Cole, P. W. Identification of a functional cysteine essential for the activity of guinea pig liver transglutaminase. *J. Biol. Chem.* (1966).

86. Gundemir, S., Monteagudo, A., Akbar, A., Keillor, J. W. & Johnson, G. V. W. The complex role of transglutaminase 2 in glioblastoma proliferation. *Neuro. Oncol.* (2017). doi:10.1093/neuonc/now157

87. Keillor, J. W. *et al.* The bioorganic chemistry of transglutaminase-from mechanism to inhibition and engineering. *Can. J. Chem.* (2008). doi:10.1139/V08-024

88. Kerr, C. *et al.* Transamidase site-targeted agents alter the conformation of the transglutaminase cancer stem cell survival protein to reduce GTP binding activity and cancer stem cell survival. *Oncogene* (2017). doi:10.1038/onc.2016.452

89. Akbar, A. *et al.* Structure-Activity Relationships of Potent, Targeted Covalent Inhibitors That Abolish Both the Transamidation and GTP Binding Activities of Human Tissue Transglutaminase. *J. Med. Chem.* (2017). doi:10.1021/acs.jmedchem.7b01070

90. Adhikary Gautam, Grun Daniel, Alexander Richard, Friedberg Joseph S., Xu Wen, Keillor Jeffrey W, Kandasamy Sivaveera, and E. L. Transglutaminase is a mesothelioma cancer stem cell survival protein that is required for tumor formation. *Oncotarget* **9**, 34495–34505. (2018).

91. Fisher, M. L., Keillor, J. W., Xu, W., Eckert, R. L. & Kerr, C. Transglutaminase Is Required for Epidermal Squamous Cell Carcinoma Stem Cell Survival. *Mol. Cancer Res.* (2015). doi:10.1158/1541-7786.MCR-14-0685-T

92. Jambrovics, K. *et al.* Transglutaminase 2 programs differentiating acute promyelocytic leukemia cells in all-trans retinoic acid treatment to inflammatory stage through NF-kB activation. *Haematologica* (2018). doi:10.3324/haematol.2018.192823

93. Fisher, M. L. *et al.* Type II transglutaminase stimulates epidermal cancer stem cell epithelial-mesenchymal transition. *Oncotarget* (2015).
94. Katt, W. P. *et al.* A small molecule regulator of tissue transglutaminase conformation inhibits the malignant phenotype of cancer cells. *Oncotarget* (2018). doi:https://doi.org/10.18632/oncotarget.26193
95. Simons, M. & Raposo, G. Exosomes - vesicular carriers for intercellular communication. *Current Opinion in Cell Biology* (2009). doi:10.1016/j.ceb.2009.03.007
96. Stoorvogel, W., Kleijmeer, M. J., Geuze, H. J. & Raposo, G. The biogenesis and functions of exosomes. *Traffic* (2002). doi:10.1034/j.1600-0854.2002.30502.x
97. Colombo, M., Raposo, G. & Théry, C. Biogenesis, Secretion, and Intercellular Interactions of Exosomes and Other Extracellular Vesicles. *Annu. Rev. Cell Dev. Biol.* (2014). doi:10.1146/annurev-cellbio-101512-122326
98. Li, K., Chen, Y., Li, A., Tan, C. & Liu, X. Exosomes play roles in sequential processes of tumor metastasis. *International Journal of Cancer* (2018). doi:10.1002/ijc.31774
99. Atay, S. & Godwin, A. K. Tumor-derived exosomes: A message delivery system for tumor progression. *Commun. Integr. Biol.* (2014). doi:10.4161/cib.28231
100. Iero, M. *et al.* Tumour-released exosomes and their implications in cancer immunity. *Cell Death and Differentiation* (2008). doi:10.1038/sj.cdd.4402237
101. Minciacchi, V. R., Freeman, M. R. & Di Vizio, D. Extracellular Vesicles in Cancer: Exosomes, Microvesicles and the Emerging Role of Large Oncosomes. *Seminars in Cell and Developmental Biology* (2015). doi:10.1016/j.semcdb.2015.02.010
102. Peinado, H., Lyden, D. & Bromberg, J. Transfer of cargo from exosomes to bone marrow progenitors promotes melanoma metastasis. *FEBS J.* (2012).
103. Syn, N., Wang, L., Sethi, G., Thiery, J. P. & Goh, B. C. Exosome-Mediated Metastasis: From Epithelial-Mesenchymal Transition to Escape from Immunosurveillance. *Trends in Pharmacological Sciences* (2016). doi:10.1016/j.tips.2016.04.006

104. Roma-Rodrigues, C., Fernandes, A. R. & Baptista, P. V. Exosome in tumour microenvironment: Overview of the crosstalk between normal and cancer cells. *BioMed Research International* (2014). doi:10.1155/2014/179486

105. Peinado, H. *et al.* Exosomes drive premetastatic nich formation. *Nat. Med.* (2012). doi:10.1038/nm.2753

106. Lyden, D. Exosomes: Tumor-derived exosomes promote pre-metastatic niche formation and organotropism. *SABCS* (2013).

107. Li, L. *et al.* Exosomes derived from hypoxic oral squamous cell carcinoma cells deliver miR-21 to normoxic cells to elicit a prometastatic phenotype. *Cancer Res.* (2016). doi:10.1158/0008-5472.CAN-15-1625

108. Ohyashiki, J. H., Umezu, T. & Ohyashiki, K. Exosomes promote bone marrow angiogenesis in hematologic neoplasia: The role of hypoxia. *Current Opinion in Hematology* (2016). doi:10.1097/MOH.0000000000000235

109. Peinado, H. *et al.* Melanoma exosomes educate bone marrow progenitor cells toward a pro-metastatic phenotype through MET. *Nat. Med.* (2012). doi:10.1038/nm.2753

110. Lesnik, J., Antes, T., Kim, J., Griner, E. & Pedro, L. Registered report: Melanoma exosomes educate bone marrow progenitor cells toward a pro-metastatic phenotype through MET. *Elife* (2016). doi:10.7554/eLife.07383

111. Christianson, H. C., Svensson, K. J., van Kuppevelt, T. H., Li, J.-P. & Belting, M. Cancer cell exosomes depend on cell-surface heparan sulfate proteoglycans for their internalization and functional activity. *Proc. Natl. Acad. Sci.* (2013). doi:10.1073/pnas.1304266110

112. Hoffman, R. M. Stromal-cell and cancer-cell exosomes leading the metastatic exodus for the promised niche. *Breast Cancer Res.* (2013). doi:10.1186/bcr3426

113. R Goulet, C. *et al.* Exosomes Induce Fibroblast Differentiation into Cancer-associated Fibroblasts through TGFβ Signaling. *Mol. Cancer Res.* (2018). doi:10.1158/1541-7786.MCR-17-0784

114. Chowdhury, R. *et al.* Cancer exosomes trigger mesenchymal stem cell differentiation into pro-angiogenic and pro-invasive myofibroblasts. *Oncotarget* (2015). doi:10.18632/oncotarget.2711

115. Webber, J., Steadman, R., Mason, M. D., Tabi, Z. & Clayton, A. Cancer exosomes trigger fibroblast to myofibroblast differentiation. *Cancer Res.* (2010). doi:10.1158/0008-5472.CAN-10-1722

116. Greening, D. W., Gopal, S. K., Xu, R., Simpson, R. J. & Chen, W. Exosomes and their roles in immune regulation and cancer. *Seminars in Cell and Developmental Biology* (2015). doi:10.1016/j.semcdb.2015.02.009

117. Hoshino, A. *et al.* Tumour exosome integrins determine organotropic metastasis. *Nature* (2015). doi:10.1038/nature15756

118. Bobrie, A. & Théry, C. Exosomes and communication between tumours and the immune system: are all exosomes equal? *Biochem. Soc. Trans.* (2013). doi:10.1042/BST20120245

119. Bani, D. & Nistri, S. New insights into the morphogenic role of stromal cells and their relevance for regenerative medicine. lessons from the heart. *J. Cell. Mol. Med.* (2014). doi:10.1111/jcmm.12247

120. Wang, J. P. & Hielscher, A. Fibronectin: How its aberrant expression in tumors may improve therapeutic targeting. *Journal of Cancer* (2017). doi:10.7150/jca.16901

121. Ruoslahti, E. Fibronectin in cell adhesion and invasion. *Cancer Metastasis Rev.* (1984). doi:10.1007/BF00047692

122. Li, C. L. *et al.* Fibronectin induces epithelial-mesenchymal transition in human breast cancer MCF-7 cells via activation of calpain. *Oncol. Lett.* (2017). doi:10.3892/ol.2017.5896

123. Mehta, K., Kumar, A. & Kim, H. I. Transglutaminase 2: A multi-tasking protein in the complex circuitry of inflammation and cancer. *Biochemical Pharmacology* (2010). doi:10.1016/j.bcp.2010.06.029

124. Antonyak, M. A. *et al.* Cancer cell-derived microvesicles induce transformation by transferring tissue transglutaminase and fibronectin to recipient cells. *Proc. Natl. Acad. Sci.* (2011). doi:10.1073/pnas.1017667108

125. Shinde, A. *et al.* Spleen tyrosine kinase-mediated autophagy is required for epithelial-mesenchymal plasticity and metastasis in breast cancer. *Cancer Res.* (2019). doi:10.1158/0008-5472.CAN-18-2636

CHAPTER 2. MATERIALS AND METHODS

2.1 Reagents

Ca1a and Ca1h cells were kindly provided by Dr. Fred Miller (Wayne St. University). These cells were cultured in DMEM containing 10% FBS and pen/strep and validated for lack of contamination by IDEXX Impact III testing. HMLE cells were kindly provided by Sendurai Mani (MD Anderson Cancer Center). These cells were cultured as previously described [1]. Luciferase expressing 4T1 and HMLE cells transformed via overexpression of Her2 and their variants were described previously[2,3]. Stable expression of the luciferase, eGFP or dTomato was achieved through lentiviral transduction and selection in puromycin or zeocin. For eGFP and dTomato expression, cells were sorted to increase uniform fluorescence across the entire population (Supplementary Fig. 1). Manipulation of FN expression was achieved through lentiviral-mediated transduction of TRCN0000064830, TRCN0000064832, a scrambled control shRNA (GE Dharmacon, Lafayette, CO), or pLV (VectorBuilder, Santa Clara, CA) encoding full-length human FN or GFP as a control. Manipulation of TGM2 expression was achieved through lentiviral-mediated transduction of TRCN0000000239, TRCN0000000241, a scrambled control shRNA, empty plko.1 vector (GE Dharmacon, Lafayette, CO), or pLV (VectorBuilder, Santa Clara, CA) encoding full-length human TGM2 or GFP as a control. Manipulation of Tns1 expression was achieved through lentiviral-mediated transduction of V2LMM_4992 or scrambled control. In all cases, stable genomic integration of constructs was selected for using puromycin. Primary human pulmonary fibroblasts were obtained from ATCC and cultured in the recommended fibroblast basal media supplemented with fibroblast growth factor low serum kit (ATCC). These cells were cultured in DMEM containing 10% FBS

and pen/strep. Cells were validated for lack of contamination using IDEXX Impact III testing on April 2nd, 2014 and cryogenically frozen. All cell lines were used within one month of thawing. All stable cell lines constructed during the course of the study are listed in Table 2.1.

2.2 Gene knockout studies using CRISPR-CAS

The dimeric CRISPR RNA-guided Fokl nuclease and Csy4-based multiplex gRNA expression system was used to generate the TGM2 knockout cell line. Two annealed target-site oligoduplexes designed by Zifit Targeter[4] and a constant region oligoduplex were assembled with BsmBI-digested pSQT1313 in a single-step ligation. Following are the sequences for the oligos used in the ligation step:

Target sites for Tgm2 mouse for CRISPR:

mtg2_LCOli1_set1

OLIGO 1: CACCGGTGCTGGGTGTTTGCAGCGGTGG

OLIGO 2: CCACGACCCACAAACGTCGCCACCCAAA

mtg2_LCOli2_set2

OLIGO 1: CACCGTGCACCCTTCGTGTTTGCCGAGG

OLIGO 2: CACGTGGGAAGCACAAACGGCTCCACAAA

Oligoduplex:

mTg2_LdRGN_Oli1: GCAGCGTGTGGTGGTCACGGCCATGTTTTAG

mTg2_LdRGN_Oli2: AGCTCTAAAACATGGCCGTGACCACCACACG

Table 2.1: Stable cell lines constructed during the course of the study

Cell Line name	**Plasmids used for transduction**	**Antibiotic resistance**	**Application**	**Location in Liquid Nitrogen Tank**
Ca1a-FF	pDestination-Blasticidin	Blasticidin	*In vitro* and *in vivo* imaging	Black Tank R1B7
Ca1a-FF dTom	pFFLuc2 Tomato Red	Zeocin	Confocal and *in vivo* imaging	Threw away
Ca1a-FF scram	pLKO.1 scram	Puromycin	β1-Integrin knockdown	Black Tank R1B9
Ca1a-FF shβ1-Integrin # 6	pLKO.1 shβ1-Intergrin # 6	Puromycin	β1-Integrin knockdown	Black Tank R1B9
Ca1a -FF GFP	pLV-eGFP	Hygromycin	FN overexpression	None left
Ca1a -FF FN	pLV-FN	Hygromycin	FN overexpression	Orange Tank R3B5
Ca1h-FF eGFP	pFFLuc2 GFP	Zeocin	Confocal and *in vivo* imaging	Orange Tank R3B5
Ca1h scram	pLKO.1 scram	Puromycin	FN knockdown	Black Tank R1B8
Ca1h shFN 30	pLKO.1 shFN 30	Puromycin	FN knockdown	Black Tank R1B8
Ca1h shFN 32	pLKO.1 shFN 32	Puromycin	FN knockdown	Black Tank R1B
Ca1h shFN 30 FF eGFP	pFFLuc2 GFP	Zeocin	Confocal and *in vivo* imaging	Orange Tank R3B5
Ca1h shFN 32 FF eGFP	pFFLuc2 GFP	Zeocin	Confocal and *in vivo* imaging	Threw away
Ca1h scram	pLKO.1 scram	Puromycin	β1-Integrin knockdown	Orange Tank R3B5
Ca1h shβ1-Integrin # 2	pLKO.1 shβ1-Intergrin # 2	Puromycin	β1-Integrin knockdown	Black Tank R1B9
T1K scram	pLKO.1 scram	Puromycin	β1-Integrin knockdown	Orange Tank R3B5
T1K shβ1-Integrin# 2	pLKO.1 shβ1-Intergrin#2	Puromycin	β1-Integrin knockdown	Orange Tank R3B5
Ca1h scram MT	pLKO.1 MT	Puromycin, Hygromycin	TGM2 knockdown	Black Tank R1B7
Ca1h scram shTGM2 239	pUC shTGM2 239	Puromycin, Hygromycin	TGM2 knockdown	Black Tank R1B7
Ca1h scram shTGM2 241	pUC shTGM2 241	Puromycin, Hygromycin	TGM2 knockdown	Black Tank R1B7
MDA-MB-231 MT	pLKO.1 MT	Puromycin	TGM2 knockdown	Orange Tank R3B5

Table 2.1 continued

MDA-MB-231 shTGM2 241	pLKO.1 shTGM2 241	Puromycin	TGM2 knockdown	Orange Tank R3B5
HMLE MT	pLV-MT	Puromycin	TGM2 overexpression	Black Tank R1B9
HMLE TGM2 (FGM)	pLV-TGM2	Puromycin	TGM2 overexpression	Black Tank R1B9
HME2-GFP	pLV-eGFP	Puromycin, Hygromycin	TGM2 overexpression	Black Tank R1B7
HME2-TGM2	pLV-TGM2	Puromycin, Hygromycin	TGM2 overexpression	Black Tank R1B7
HME2-BM MT	pLKO.1 MT	Puromycin, Hygromycin	TGM2 knockdown	Black Tank R1B7
HME2-BM shTGM2 # 3	pUC shTGM2 # 3	Puromycin, Hygromycin	TGM2 knockdown	Black Tank R1B9
HME2-BM shTGM2 # 239	pUC shTGM2 239	Puromycin, Hygromycin	TGM2 knockdown	Black Tank R1B7
HME2-BM shTGM2 # 241	pUC shTGM2 241	Puromycin, Hygromycin	TGM2 knockdown	Black Tank R1B7
4T1 FF scram	pLKO.1 scram	Puromycin	TNS1 knockdown	Black Tank R1B9
4T1 FF shTns1 # 20	pGIPZ shTns1 # 20	Puromycin	TNS1 knockdown	Black Tank R1B9
4T1 FF Tgm2KO	pBabe Puro pSQT1313 (ligated vector) and pSQT1601	Puromycin	TGM2 deletion	Orange Tank R3B5

Abbrevation: R= Rack#, B=Box#

mTg2_RdRGN_Oli1: GGCAGGAGAAACTGGTGCTGCGTCG

mTg2_RdRGN_Oli2: AAACCGACGCAGCACCAGTTTCTCC

Ultramer:

mTg2_ulm_OliF:/5Phos/AGCTAGAAATAGCAAGTTAAAATAAGGCTAGTCCGTT
ATCAACTTGAAAAAGTGGCACCGAGTCGGTGCGTTCACTGCCGTATA

mTg2_ulm_OliR:/5Phos/TGCCTATACGGCAGTGAACGCACCGACTCGGTGCCAC
TTTTTCAAGTTGATAACGGACTAGCCTTATTTTAACTTGCTATTTCT

PCR products were confirmed by running on native gel (0.375 M Tris-HCI pH:8.8, Acrylamide/Bis-acrylamide(30%/0.8%w/v), 10% (w/v) ammonium persulfate (APS) and TEMED) for 2 hours at 90 volts. After running the gel, the gel was immersed into ethidium bromide contained a 1X running buffer, shaken for 10 mins and imaged. The purified PCR product was extracted from the gel using a gel extraction kit. 3 µg of the ligated vector, 1 µg of pSQT1601 expressing Csy4 RNase and RNA-guided Fokl-dCas9 fusion nucleases, and 0.2 µg of pBABE Puro were transfected into luciferase-expressing 4T1 cells. pSQT1313 and pSQT1601 were gifts from Keith Joung (Addgene plasmids #53370 and #53369)[5]. After 48 hours, cells were treated with 5 µg/ml puromycin for clonal selection. Genomic DNA and cell lysates from selected colonies were analyzed by the PAGE-genotyping method[6] and immunoblot analyses to screen for clones with TGM2 knockout. Disruption of both alleles was confirmed by DNA sequencing. Following are the protein sequences for TGM2 WT and TGM2 KO clone # 33.

TGM2WT:

MAEELLLERCDLEIQANGRDHHTADLCQEKLVLRRGQRFRLTLYFEGRGYEASV
DSLTFGAVTGPDPSEEAGTKARFSLSDNVEEGSWS

TGM2KO # 33:

MAVASWSALPADSVLRGPWLRGQRGQPHVRCCD

Clone 33 was used for all the experiments.

2.3 METABRIC Data Analysis

We examined the data from 2,000 patient tumor biopsies available at the recent Molecular Taxonomy of Breast Cancer International Consortium (METABRIC) dataset[7]. Patients tumor samples were divided into subtypes according to PAM50 status and plotted for FN expression levels against overall survival. The dataset was further divided into 4 quartiles based on patient's samples expressing above the mean or median expression level of FN and plotted against overall survival.

2.4 Animal models

All *in vivo* assays were conducted under IACUC approval from Purdue University. Where indicated control or luciferase expressing Ca1a and Ca1h cells ($2x10^6$ / 50 μl) were injected into the second mammary fat pad of female 5-week old, nu/nu mice (Figure 2.1). Thirty-five days after engraftment tumors were surgically excised and metastasis was subsequently quantified by bioluminescent imaging. In other experiments, control and FN-depleted Ca1h cells ($5x10^5$ / 100 μl) were injected into the lateral tail vein of female 4-month-old, NSG mice. Pulmonary tumor growth was quantified by bioluminescence at the indicated time points. Based on previously established variability for bioluminescent imaging, 5 mice per group was chosen to adequately power our experiments to 0.80, with an α of 0.05. In separate experiments luciferase expressing HME2-GFP, HME2-TGM2,

HME2-BM MT or HME2-shTGM2 ($2x10^6$ / 50 µl) were injected into the second mammary fat pad of female 8-week old, NSG mice. Tumors were surgically excised after they achieved a size of 900 mm and metastasis was subsequently quantified by bioluminescent imaging. For exosome education experiments, 20ug of total exosome protein in 100 µl of sterile PBS was injected intraperitoneally into 3 months old NSG mice every other day for 3 weeks (Figure 2.2). Mice receiving 100 µl of sterile PBS acted as a control group. Luciferase expressing Ca1a ($7.5x10^5$ /100 µl) were injected into the lateral tail vein of exosome treated female NSG mice. Pulmonary tumor growth was quantified by bioluminescence at the indicated time points. Luciferase expressing 4T1-WT, 4T1-Tgm2KO, 4T1-scram or 4T1-shTns1 were resuspended in PBS (50 µl) and orthotopically engrafted onto the second mammary fat pad of 4 weeks old Balb/c mice ($2.5x10^4$ cells/mouse) (Jackson Labs, Bar Harbor, ME). Primary tumor growth and metastasis development were assessed via weekly bioluminescent imaging using the Advanced Molecular Imager (AMI) (Spectral Instruments, Tucson, AZ). Upon necropsy lungs from all animals were removed and fixed in 10% formalin and dehydrated in 70% ethanol for visualization of pulmonary metastatic nodules and histological analyses. Based on previously established variability for bioluminescent imaging, 4 or 5 mice per group was chosen to adequately power our experiments to 0.80, with an α of 0.05.

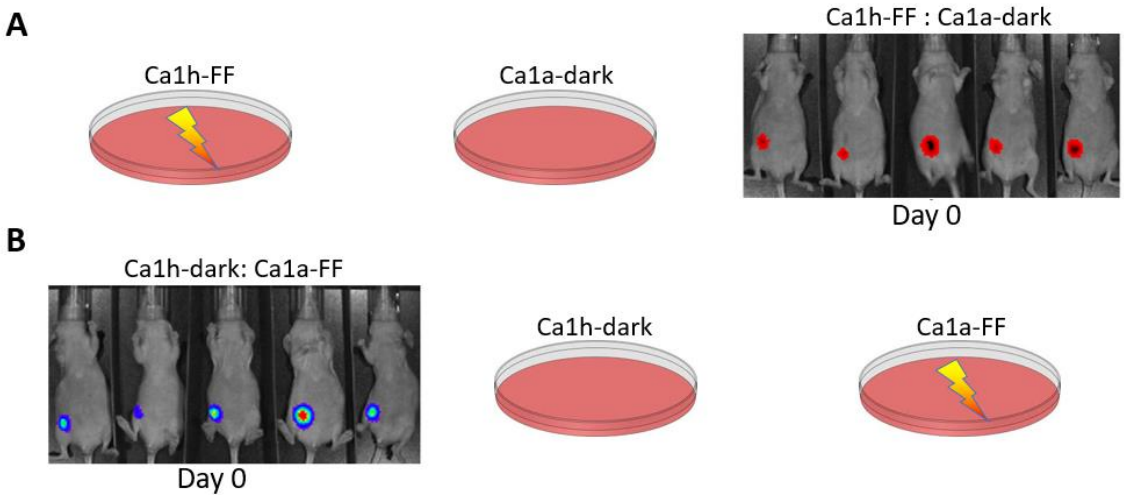

Figure 2.1: Schematic for Ca1h-Ca1a mixed *in vivo* assay.

(A) Ca1h-FF and Ca1a -dark cells were mixed in 1:1 ratio, engrafted on the mammary fat pad and imaged. (B) Ca1h-dark and Ca1a-FF cells were mixed in 1:1 ratio, engrafted on the mammary fat pad and imaged.

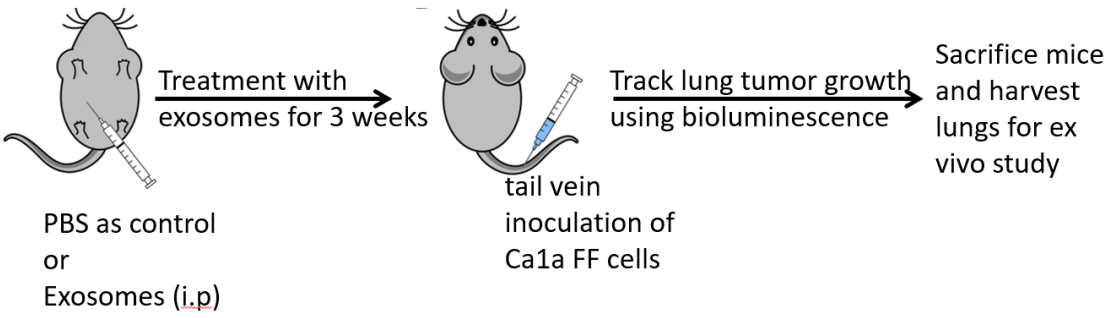

Figure 2.2: Schematic for *in vivo* assay using exosomes

2.5 Immunological assays

For immunoblot analyses cells were lysed using a modified RIPA lysis buffer containing 50 mM Tris, 150mM NaCl, 0.25% Sodium Deoxycholate, 1.0% NP40, 0.1% SDS, protease inhibitor cocktail, 10mM activated sodium ortho-vanadate, 40 mM β-glycerolphosphate and 20mM sodium fluoride. These lysates were separated by reducing 10% SDS PAGE and probed for β1 integrin, FGFR1 (Cell signaling technologies, Danvers, MA), fibronectin, E-cadherin, vimentin (BD biosciences, San Jose, CA), zeb1, actin (Santa Cruz Biotechnology, Santa Cruz, CA), zo-1 (Thermofisher Scientific), Ncad (RnD systems), TGM2 (Invitrogen CUB 7402, Mouse/Rat TGM2 antibody R & D systems , AF5418) or β-tubulin (DSHB, Iowa City, IA). To immunoblot FN dimers, lysates were separated by reducing 4-20% SDS PAGE and probed for FN. For immunofluorescence, cells were fixed in 4% paraformaldehyde (PFA), permeabilized in 0.1% Triton-X 100 and processed using fluorescently labeled phalloidin (Thermo Fisher, Waltham, MA) for visualization of the actin cytoskeleton, E-cadherin (BD biosciences) or FN (Abcam, Cambridge, MA). For immunostaining of cells on scaffolds, whole scaffolds were placed in 24 well plate using tweezers and the above steps were performed. To image, the scaffolds were placed in 6 cm dish containing PBS and imaged using dipping water objective for Zeiss confocal microscope. Where indicated, cellular monolayers were removed through incubation with 0.4% Triton, 1.5 NaCl, 50 mM, Tris pH 8 and 50mM EDTA for 48h in 4°C, washed with water, incubated with 0.5% sodium deoxycholate at 25°C and finally incubated with PBS (+Mgcl2) for 1 hour. Secreted proteins were precipitated from serum-free media by incubating 6 volumes of the sample with 1 volume of 50% trichloroacetic acid and 1 volume of 0.1% sodium deoxycholate on ice for 30 minutes. Protein was precipitated via centrifugation and the pellet was twice washed with acetone and finally

boiled at 95°C with 500 μl of the 4x laemmli buffer. For flow cytometry, cells were fixed in 1% PFA, blocked in 2.0% bovine serum albumin and stained with CD24 and CD44 (BioLegend, San Diego, CA) that were directly conjugated to the fluorescent probes. Patient samples stained for FN (DakoCytomation) by immunohistochemistry were obtained from the protein atlas[8,9]. Immunohistochemical analyses of formalin fixed paraffin embedded tissue sections from Ca1h pulmonary tumors were conducted by deparaffinization in xylene, rehydration, and antigen retrieval using 10mM sodium citrate (pH 6.0) under pressurized boiling. After inactivation of endogenous peroxidases in 3% H_2O_2, primary antibodies specific for Ecad (BD biosciences), human vimentin (BD biosciences), or Ki-67 (BD biosciences), or FN (BD biosciences) were added to serial sections and incubated overnight. Protein-specific staining was detected using appropriate biotinylated secondary antibodies in conjunction with ABC reagent (Vector, Burlingame, CA). These sections were counterstained with hematoxylin, dehydrated, and mounted. All antibodies used in the experiments are listed in Table 2.2.

Table 2.2: Antibodies used in the completion of these studies

Antigen	**Application**	**Vendor**	**Clone #**	**Concentration**	**Secondary**	**Storage Location**
FN	Western/ICC/IHC	Becton Dickenson	610078	1:1500	Goat αMS-HRP	20°C
FN3	ICC	Thermo Fisher	14-9869-82	1:50	Goat αMS-HRP	4°C
Ecad	Western/ICC/IHC	Becton Dickenson	610182	1:5000	Goat αMS-HRP	20°C
Vim	Western/IHC	Becton Dickenson	550513	1:1000	Goat αMS-HRP	4°C
TGM2	Western/IHC	Thermo Fisher	MA5-12739	1:1000	Goat αMS-HRP	4°C
TGM2	Western	R&D systems	AF5418	1: 500	Dnky αShp-HRP	20°C
TNS1	Western	Sigma	HPA036089	1:500	Goat αRbt-HRP	20°C
FGFR1	Western	Cell Signaling	2260	1:1000	Goat αRbt-HRP	20°C
β1 - Integrin	Western	Cell Signaling	3688	1:1000	Goat αRbt-HRP	20°C
β3 - Integrin	Western	Cell Signaling	3690	1:1000	Goat αRbt-HRP	20°C
β1 - Tubulin	Western	DSHB	E7	1:1000	Goat αRbt-HRP	20°C
CD63	Western/ICC	Santa Cruz	Sc-5275	1:250	Goat αMS-HRP	4°C
CD63	Western/ICC	Abcam		1:500/ 1:50	Goat αRbt-HRP	4°C
Ki67	IHC	Becton Dickenson	550609	1:100	Goat αMS-HRP	4°C
Snail	Western	Cell Signaling	6615	1:1000	Goat αMS-HRP	20°C
Zeb1	Western	Santa Cruz	Sc-25388	1:1000	Goat αRbt-HRP	4°C
Zo-1	Western	Thermo Fisher	61-7300	1:1000	Goat αRbt-HRP	20°C
p-STAT3	ICC	Cell Signaling	6774	1:2000	Goat αRbt-HRP	20°C
ErbB2	Western	Cell Signaling	2064	1:1000	Goat αRbt-HRP	20°C
Actin	Western	Santa Cruz	Sc-1616	1:1000	Dnky αGoat-HRP	4°C

Abbreviations: IHC= immunohistochemistry, ICC=immunocytochemistry, Dnky=donkey, MS=mouse, Rbt=rabbit, HRP=Horseradish Peroxidase

2.6 3D hydrogel assays

Fluorescent and bioluminescent Ca1a cells were mixed with non-labeled or fluorescent Ca1a, Ca1h control, and Ca1h cells depleted in FN in 1:1 ratio and grown under 3D culture conditions. Cell growth was quantified via the addition of luciferin (GoldBio, St. Louis, MO). Briefly, 2000 cells were plated in each well of a white-walled 96-well dish on top of a solidified 50µl bed of Cultrex basement membrane extract (BME) from (Trevigen, Gaithersburg, MD). These cells were suspended in growth media containing DMEM, 10% FBS and 5% of the BME. For confocal microscopy, differentially labeled cells were grown under 3D culture conditions using 50 mm Dish (MatTek**,** Ashland, MA) and images were taken at using Zeiss 40x water dipping objective lens. For 4T1 3D growth assays, 1000 cells were plated in each well of a white-walled 96-well dish on top of a solidified 50µl bed of Cultrex BME. These cells were suspended in growth media containing DMEM, 10% FBS and 5% of the BME. Growth was tracked every other day using bioluminescence and images were taken at Day 8.

2.7 Production of 3D scaffolds

Scaffolds were produced using a photolithography based approach, using the negative photo resist SU-8 2050 (Microchem, Westborough, MA). Silicon wafers were cleaned using a Glen 1000P plasma cleaner and dehydrated by baking at 120°C for 5 min. Omnicoat (Microchem, Westborough, MA) was used as a sacrificial layer. 3 layers of Omnicoat were applied for each wafer using a spin coater at a spread speed of 500 RPM for 5 s, followed by 30 s at 1000 RPM. After each layer was applied, the wafer was baked at 200°C for 1 min, then allowed to cool to RT. The SU-8 was then coated onto the wafer using a spread speed of 500 RPM for 5 s, followed by 1700 RPM for 30 s. A final thickness

of approximately 100 μm was attained. The wafer was then allowed to degass overnight at RT. After degassing, the wafers were baked at 65°C for 10 min, then the temperature was increased to 95°C for an additional 50 min bake. The wafers were then exposed to UV light using an MJB 45S mask aligner in hard contact mode, with a 20 second exposure time. A photomask was used to create the desired geometric pattern. After exposure, the wafer was baked for 5 min at 65°C followed by 10 min at 95°C. After cooling to RT, the wafers were developed in SU-8 developer for 11 min, rinsed in isopropanol (IPA), and then dried using compressed nitrogen gas. The developed scaffolds were then hard baked for 15 min at 150°C and then released from the wafer using fresh SU-8 developer. The scaffolds were subsequently washed 6 times in IPA and allowed to dry overnight before use.

2.8 Fibronectin coating of scaffolds

Scaffolds were coated with fibronectin by first mounting the scaffolds to a ferrous magnetic stainless-steel frame using a cyanoacrylate-based adhesive. The mounted scaffolds were then placed in a 100 μg/mL solution of fibronectin, and then magnetically suspended at the air-water interface. The scaffolds were rotated for 2 h on a rotisserie shaker that was maintained at 30°C with a rate of rotation of 8 RPM.

2.9 3D scaffold assays

Uncoated or fibronectin-coated 3D scaffolds were placed in ultralow attachment 24-well dishes. Cells (50,000) were added to the scaffolds for 24 hours at which point non-adherent cells were washed away. For immunofluorescence, at day 6 the scaffolds containing the cells were fixed and stained with the indicated antibodies using protocols described above. Images were taken using Zeiss 40x water dipping objective lens. For

exosomes experiments, cells (100,000) were added to the scaffolds. Cells were fed new media every 5 days for 2-3 weeks. Once the scaffolds were covered with HPF fibrils entirely, they were treated with 5ug of exosomes every other day for 3 weeks. Ca1a FF-dTomato cells were added to the exosomes treated scaffolds and tracked for growth by bioluminescence at indicated time points. On indicated time point, the scaffolds containing the cells were fixed and images were taken using a fluorescence microscope.

2.10 mRNA analyses

RNA was isolated using an RNA isolation kit (Omega bio-tek, Norcross, GA). Total RNA was reverse-transcribed using a cDNA synthesis kit from (Thermo Fisher) and semi-quantitative real-time PCR was performed using iQ SYBR Green (Thermo Fisher). GAPDH was used as reference gene. All primers used for the analysis are listed in Table 2.3.

2.11 RNA sequence analysis

Parental, Her2 transformed HMLE cells (HME2-parental), were treated every three days with TGF-β1 (5 ng/ml) for a period of 4 weeks to generate post-TGF-β mesenchymal cell conditions (Figure 2.3) [3]. Post-TGF-β mesenchymal cells were engrafted into fad pad of immunocompetent mice to acquire bone metastasis. These bone tumors were cultured *ex vivo* to obtain HME2-BM cells (Figure 2.3). Post-TGF-β mesenchymal cells were further sorted for a $CD44^{hi}$ phenotype (BioLegend) and total RNA was isolated using E.Z.N.A (Omega Bio-Tek). RNA sequencing was conducted using the Illumina HiSeq 2500 platform. These data have been deposited on the GEO database (GSE115255).

2.12 Isolation of exosomes from cells

Exosomes were isolated from serum-starved conditioned media of 10^7 cells (equivalent to four 150 mm dishes) as described previously[11,12]. 100 % confluent cell cultures were serum starved for 72h cultured to obtain conditioned media. The conditioned media was centrifuged at 300g for 10 minutes to remove live cells, 2000g for 10 minutes to remove cell debris and filtered through 0.22µM pore size Millipore filters. Filtered media was concentrated to 1 ml using 3KD MWCO Amicon ultra-15 centrifugal filters, followed by ultracentrifugation at 100,000 g for 2h. The pellet was washed with PBS using ultracentrifugation at 100,000 g for 2h and resuspended either in 3D RIPA buffer for immunoblot experiments or in PBS for other experiments. All the steps were carried out in cell culture hood and ultracentrifugation apparatus was cleaned with alcohol to avoid contamination.

Table 2.3: Primer sequences, product sizes, and conditions used to complete these studies

Gene name	Application	Forward primer (5’ to 3’)	Reverse primer (5’ to 3’)	Product size	Anneal Temp
GAPDH	RT-PCR	caactttggcattgtggaagggctc	acaaacactaatgttaattgccca	202	63°C
FN1	RT-PCR	acaaacactaatgttaattgccca	cctccagagcaaagggctta	200	63°C
CDH1	RT-PCR	gttcagactccagcccgc	aaattcactctgcccaggacg	250	63°C
VIM	RT-PCR	cgggagaaattgcaggagga	aaggtcaagacgtgccagag	105	63°C
hTGM2	RT-PCR	ataagttagcgccgctctcc	ctctaagaccagctcctcgg	124	63°C
mTGM2	RT-PCR	ggaggagcgacgggaatatg	attccatcctcgaactgccc	108	63°C

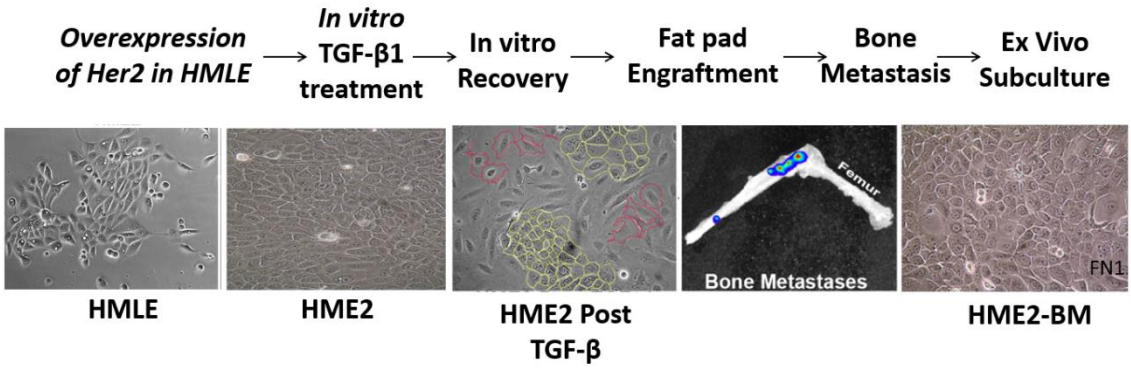

Note:
HMLE: Human Mammary Epithelial cells
HME2: HMLE expressing Her2 cells
HME2 Post TGF-β: TGF-β treated HMLE E2 cells
HME2-BM: Bone Mets

Figure 2.3: Diagram of development of HME2 model to study breast cancer metastasis. Modified from A. Shinde *et al* Cancer Research 2019

2.13 Immuno-Transmission Electron microscopy (TEM)

Protein expression on the surface of exosomes was examined using whole mount immunostaining staining. Thin formvar/carbon film coated 200 mesh copper EM grid were glow discharged for 30 seconds. Exosomes were fixed in 1 ml of paraformaldehyde (PFA) for 5 mins. 5-7 µl of fixed exosomes solution was loaded on the grids and incubated for 10 minutes. The grid was rinsed with 100 µl PBS three times each for 10 min, treated with 50 µl of 0.00M glycine to quench free aldehyde groups for 10 min, incubated with a 100 µl of blocking buffer (PBS containing 1% BSA) for 30 min and finally incubated with 100 µl of primary antibody (anti-FN3 (1:100) or anti-TGM2 (1:100) antibody) overnight at 4°C. Following day, grids were washed with 100 µl washing buffer (PBS containing 0.1% BSA) five times each for 10 min. Following incubation with secondary antibody (goat anti-mouse IgG (H+L) conjugated to 10 nm gold particle (ab39619, Abcam) diluted at 1:100 in PBS containing 0.1% BSA for 1h, grids were washed with washing buffer five times each for 10 min and 50µl of distilled water twice. Grids were air dried for 15 min and were observed by TEM at 200kV.

2.14 Confocal microscopy of Exosomes

For confocal microscopy imaging, exosomes samples were prepared as described previously[14]. 500 µl of PBS solution containing exosomes were incubated with simultaneously with 2 µl each of 0.587 mg/ml rabbit anti-CD63 (ab217345) or TGM2 (Invitrogen CUB 7402) and 0.5 mg/ml of FN3 (Invitrogen 14-9869-82) for 2h at room temperature. PBS replaced the primary antibody for blank control. Following incubation, the solution was purified by ultrafiltration (50KDa) at 600 rpm for 20 min. The filtrate was washed with PBS using ultrafiltration and resuspended in PBS. Next, a mixture of 0.5ul of

CM-dil, 1 ul of 2mg/ml of Alexa Fluor labeled 647 Goat anti-mouse IgG and 2mg/ml of Alexa Fluor 488 labeled Goat anti-rabbit IgG was added to exosomes solution, incubated for 1h with vigorous mixing and then purified again by ultrafiltration. Finally, the precipitate was resuspended in PBS and added on 35mm 1.5H glass coverslip bottom confocal dish and adsorbed for 15 minutes. The dishes were coated with 0.1% polyethyleneimine for 15 mins prior to the addition of the prepared sample. Samples were imaged using a Nikon confocal microscope.

2.15 Nanosight

Exosome size distribution and concentration were analyzed using semiautomated nanoparticle tracking-based analyses were performed using a NanoSight (NS300) apparatus (Malvern Instruments Ltd.). Samples were diluted to provide counts within the linear range of the instrument (i.e., 3 x 10^8 to 10^9 per mL). Three videos of 1-minute duration were documented for each sample, with a frame rate of 30 frames per second. Using NTA software (NTA 2.3; NanoSight Ltd.), particle movement was analyzed as per the manufacturer's protocol. The NTA software was adjusted to first identify and then track each particle on a frame-by-frame basis.

2.16 Statistical analyses

2-way ANOVA or 2-sided T-tests were used where the data met the assumptions of these tests and the variance was similar between the two groups being compared. P values of less than 0.05 were considered significant. No exclusion criteria were utilized in these studies.

2.17 References

1. Mani, S. A. *et al.* The Epithelial-Mesenchymal Transition Generates Cells with Properties of Stem Cells. *Cell* (2008). doi:10.1016/j.cell.2008.03.027
2. Smith, A., Wendt, M. K., Brown, W. S., Gray, N. S. & Tan, L. Covalent Targeting of Fibroblast Growth Factor Receptor Inhibits Metastatic Breast Cancer. *Mol. Cancer Ther.* (2016). doi:10.1158/1535-7163.mct-16-0136
3. Brown, W. S., Akhand, S. S. & Wendt, M. K. FGFR signaling maintains a drug persistent cell population following epithelial-mesenchymal transition. *Oncotarget* (2016). doi:10.18632/oncotarget.13117
4. Sander, J. D. *et al.* ZiFiT (Zinc Finger Targeter): An updated zinc finger engineering tool. *Nucleic Acids Res.* (2010). doi:10.1093/nar/gkq319
5. Wyvekens, N., Topkar, V. V., Khayter, C., Joung, J. K. & Tsai, S. Q. Dimeric CRISPR RNA-Guided FokI-dCas9 Nucleases Directed by Truncated gRNAs for Highly Specific Genome Editing. *Hum. Gene Ther.* (2015). doi:10.1089/hum.2015.084
6. Zhu, X. *et al.* An efficient genotyping method for genome-modified animals and human cells generated with CRISPR/Cas9 system. *Sci. Rep.* (2014). doi:10.1038/srep06420
7. Curtis, C. *et al.* The genomic and transcriptomic architecture of 2,000 breast tumours reveals novel subgroups. *Nature* (2012). doi:10.1038/nature10983
8. Malm, E. *et al.* A Human Protein Atlas for Normal and Cancer Tissues Based on Antibody Proteomics. *Mol. Cell. Proteomics* (2005). doi:10.1074/mcp.m500279-mcp200
9. Hober, S. *et al.* A Genecentric Human Protein Atlas for Expression Profiles Based on Antibodies. *Mol. Cell. Proteomics* (2008). doi:10.1074/mcp.r800013-mcp200
10. Shinde, A. *et al.* Spleen tyrosine kinase-mediated autophagy is required for epithelial-mesenchymal plasticity and metastasis in breast cancer. *Cancer Res.* (2019). doi:10.1158/0008-5472.CAN-18-2636
11. Kamerkar, S. *et al.* Exosomes facilitate therapeutic targeting of oncogenic KRAS in pancreatic cancer. *Nature* (2017). doi:10.1038/nature22341

12. Greening, D. W., Xu, R., Ji, H., Tauro, B. J. & Simpson, R. J. A protocol for exosome isolation and characterization: Evaluation of ultracentrifugation, density-gradient separation, and immunoaffinity capture methods. in *Methods in Molecular Biology* (2015). doi:10.1007/978-1-4939-2550-6_15
13. Jung, M. K. & Mun, J. Y. Sample Preparation and Imaging of Exosomes by Transmission Electron Microscopy. *J. Vis. Exp.* (2018). doi:10.3791/56482
14. Chen, C. *et al.* Imaging and Intracellular Tracking of Cancer-Derived Exosomes Using Single-Molecule Localization-Based Super-Resolution Microscope. *ACS Appl. Mater. Interfaces* (2016). doi:10.1021/acsami.6b09442

CHAPTER 3. AUTOCRINE FIBRONECTIN INHIBITS BREAST CANCER METASTASIS

The following chapter is reproduced and modified with permission from
Aparna Shinde, Sarah Libring, Aktan Alpsoy, Ammara Abdullah, James A Schaber, Luis Solorio, and Michael K. Wendt "Autocrine fibronectin inhibits breast cancer metastasis", Mol Cancer Res. 2018 Oct;16(10):1579-1589.

3.1 Abstract

Both epithelial-mesenchymal transition (EMT) and mesenchymal-epithelial transition (MET) are linked to metastasis via their ability to increase invasiveness and enhance tumor-initiating capacity. Growth factors, cytokines and chemotherapies present in the tumor microenvironment (TME) are capable of inducing EMT, but the role of the extracellular matrix (ECM) in this process remains poorly understood. Here, a novel tessellated three-dimensional (3D) polymer scaffolding is used to produce a fibrillar fibronectin matrix that induces EMT-like event that includes phosphorylation of STAT3 and requires expression of β1 integrin. Consistent with these findings, analysis of the METABRIC dataset strongly links high-level fibronectin (FN) expression to decreased patient survival. In contrast, *in vitro* analysis of the MCF-10A progression series indicated that intracellular FN expression was associated with non-metastatic cells. Therefore, differential bioluminescent imaging was used to track the metastasis of isogenic epithelial and mesenchymal cells within heterogeneous tumors. Interestingly, mesenchymal tumor cells do not produce FN matrix and cannot complete the metastatic process, even when grown within a tumor containing epithelial cells. However, mesenchymal tumor cells form FN containing cellular fibrils capable of supporting the growth and migration of metastatic-competent tumor cells.

Importantly, depletion of FN allows mesenchymal tumor cells to regain epithelial characteristics and initiate *in vivo* tumor growth within a metastatic microenvironment. Implications: In contrast to the tumor-promoting functions of fibronectin within the ECM, these data suggest that autocrine fibronectin production inhibits the metastatic potential of mesenchymal tumor cells.

3.2 Introduction

The ability of epithelial cells to transition into a more primitive, migratory phenotype is an important process that occurs during wound healing and development. However, this capacity of epithelial cells to transition between these different phenotypes also supports the metastatic progression of breast cancer. Numerous model systems suggest that cells undergo a transient EMT during invasion and dissemination, and then reverse that process through MET during the outgrowth of secondary metastatic tumors [106,119–121]. The importance of a highly plastic cell type to overcome the various stresses of the metastatic process is intuitively logical. However, the onset and reversal of EMT have also been linked to the increased tumor initiating capacity[122,123] These studies raise exciting possibilities that EMT:MET may reactivate a fundamental genetic program capable of producing cells with an enhanced potential for adaptation to metastatic microenvironments and initiation of secondary tumors. Concurrent with these single-cell autonomous notions of EMT:MET and stemness is a growing concept supporting the importance of EMT-induced tumor cell heterogeneity[124]. Heterogeneity within the stromal compartment of tumors is clearly important to metastasis as several critical paracrine signaling axes consisting of growth factors, hormones and adipokines have been described [125–127]. However, numerous inducers of EMT can result in subpopulations of tumor cells with

unique mechanical and molecular signatures that fall along a spectrum of epithelial to mesenchymal phenotypes[128,129]. Recent evidence suggests that more potent inducers of EMT can push epithelial tumor cells into a highly mesenchymal, stromal-like state and these cells have a reduced ability to undergo MET[102]. What the drivers of these more stable mesenchymal phenotypes are, and how and if these stromal-like tumor cells continue to contribute to the metastatic process remains to be established.

In healthy tissues, stromal cells maintain the composition and structure of the tissue through the production of extracellular matrix (ECM) proteins and paracrine signaling with epithelial cells[130]. Both compositional and structural changes in the ECM have been observed during metastasis[40]. One such ECM protein that can be produced by tumor cells following EMT is fibronectin (FN). Overall, increased FN expression in primary mammary tumors is strongly associated with decreased patient survival[106]. Herein, we utilize a novel 3D culture system consisting of a tessellated scaffold to demonstrate that fibrillar FN can drive an EMT-like morphological change, that allows for migration and proliferation of metastatic breast cancer cells independent of a hydrogel or polymer support. Counterintuitively, we find that breast cancer cells that constitutively express FN display an extremely stable mesenchymal phenotype and are not capable of completing metastasis. Therefore, we sought to address the hypothesis that autocrine production of FN by tumor cells limits their metastatic potential. Along these lines, genetic depletion of FN, but not its cognate receptor β1 integrin, allows tumor cells to regain epithelial characteristics and initiate tumor formation in the lungs.

Overall, our studies shed new light on the role of autocrine FN signaling during tumor growth and metastasis. Furthermore, we introduce a robust and versatile 3D cell

culture approach capable of accurately recapitulating tumor microenvironment conditions that allow for controlled studies that cannot be accomplished *in vivo* or with other systems.

3.3 Results

3.3.1 Fibronectin expression is associated with decreased patient survival

We have previously demonstrated an association between FN expression and decreased patient survival. Here we analyzed the recent Molecular Taxonomy of Breast Cancer International Consortium (METABRIC) dataset consisting of more than 2,000 patient tumor biopsies[112]. Significant outliers were observed in every subtype, with the claudin-low subtype having the outliers with the highest overall expression (Figure 3.1A). When the dataset is taken as a whole, those patients above the mean or median expression level of FN demonstrated decreased survival compared to those patients below the mean or median (Figure 3.1B and not shown). Finally, when separated into quartiles those patients with the highest levels of FN demonstrate the shortest survival time (Figure 3.1C). Overall, these data clearly indicate that high-level expression of the FN in primary tumors is strongly associated with decreased patient survival.

3.3.2 Non-metastatic mesenchymal tumor cells aid the metastasis of responder cells within heterogeneous tumors

The MCF10CA1a (Ca1a) and the MCF10CA1h (Ca1h) cells are variants derived from the RAS-transformed MCF-10AT cells. In culture, whole cell lysates obtained from Ca1h cells

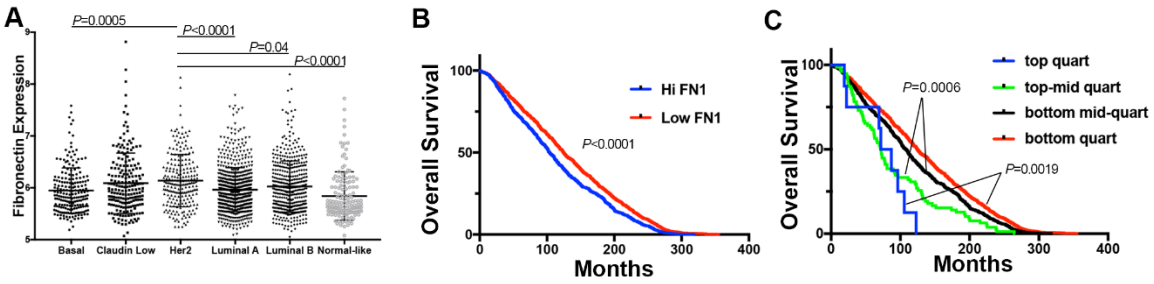

Figure 3.1: FN expression is associated with decreased patient survival.

(A) The METABRIC dataset was divided into breast cancer subtypes as determined by the PAM50 and analyzed for expression of *FN1*. Differences in FN1 expression between subtypes were analyzed by ANOVA resulting in the indicated *P* values. (B) Patients were separated into two groups based on the mean expression value of *FN1* and overall survival was plotted. (C) Patients were separated into quartiles based on FN1 expression and overall survival was plotted. Data in panels B and C were analyzed by a Log-rank test resulting in the indicated *P* value.

demonstrate constitutive expression of FN and low levels of the epithelial marker, Ecad (Figure 3.2A). In contrast, Ca1a cells fail to express detectable levels of FN but express robust amounts of Ecad (Figure 3.2A). Somewhat counter to the patient data presented in Figure 3.1, the FN-expressing Ca1h cells are considered to be invasive but not metastatic, while the Ca1a cells are considered to be fully metastatic[131]. However, it is difficult to directly compare the differential metastatic potential of the Ca1h and Ca1a cells *in vivo* due to drastic differences in primary tumor growth rates (Ca1h = 65.0 mg ± 17.32 mg; Ca1a = 983.4 mg ± 264 mg, 35 days post mammary fat pad engraftment of $2x10^6$ cells). Furthermore, the metastatic rate of Ca1a primary tumors is very low, making inhibition of this process statistically challenging (Figure 3.2B and 3.2C). Therefore, we sought to create mosaic tumors containing both Ca1h and Ca1a cells and track the metastasis of each cell type independently through differential labeling with firefly luciferase. Using this approach, 1:1 mixture of Ca1a and Ca1h cells were orthotopically engrafted onto the mammary fat pad of nu/nu mice and these mosaic tumors were grown for 35 days (Figure 3.2B). The primary tumors were surgically resected, and the subsequent metastasis of each cell type was tracked by firefly bioluminescence (Figure 3.2B and 3.2C). This approach indicated that even in a heterogeneous primary tumor, the Ca1a cells are clearly the cell type that forms metastatic lesions (Figure 3.2B and 3.2C and Figure 3.3). These studies also revealed a highly significant increase in the metastatic efficiency of the Ca1a cells when grown in a mosaic tumor with the highly mesenchymal Ca1h cells (Figure 3.2B and 3.2C). These data clearly indicate that while not competent for metastasis themselves, constitutively mesenchymal tumor cells can facilitate the metastasis of responder tumor cells in a paracrine manner.

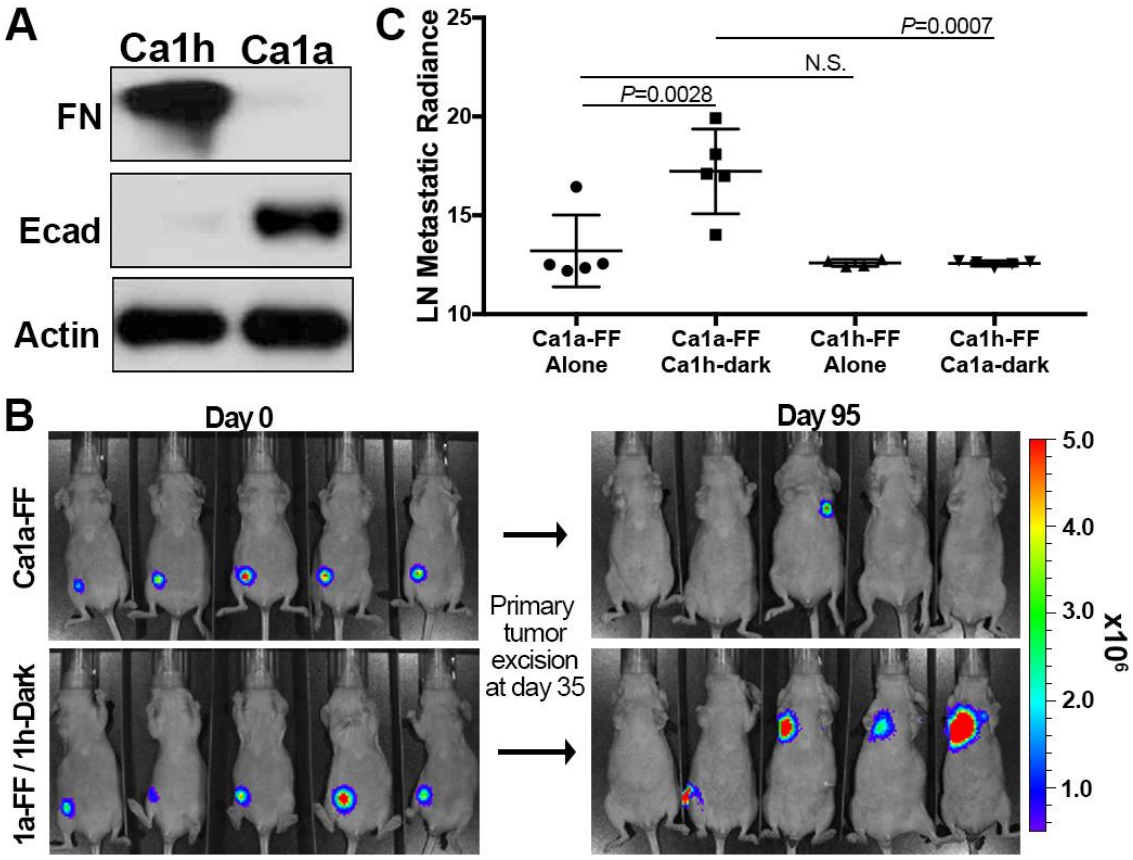

Figure 3.2: FN expressing tumor cells support the metastasis of epithelial cells from heterogeneous primary tumors.

(A) Immunoblot analyses for fibronectin (FN) and epithelial cadherin (Ecad) from nonmetastatic Ca1h cells and metastatic Ca1a cells. (B) Ca1a and Ca1h cells differentially expressing firefly luciferase were engrafted onto the mammary fat pad of two separate groups of mice. Bioluminescent images were taken immediately after engraftment (Day 0) and 95 days later (Day 95). (C) Primary mammary tumors were removed 35 days after engraftment and whole mouse bioluminescence at day 95 was used to quantify metastatic recurrence. Data are presented as the natural log (LN) of the bioluminescent radiance for each mouse (n=5 mice per group), resulting in the indicated P value.

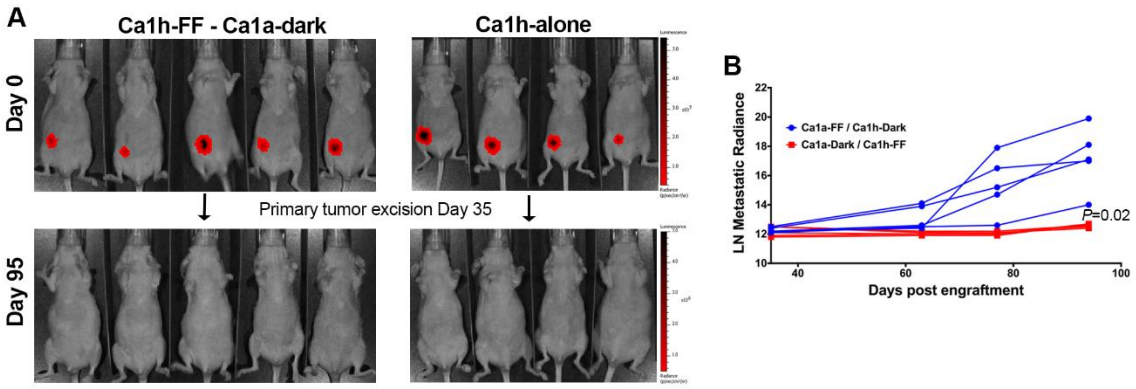

Figure 3.3: Ca1h cells are not metastatic.

(A) Firefly luciferase expressing Ca1h cells were engrafted onto the mammary fat pad. Bioluminescence was imaged immediately after engraftment (Day 0) and 95 days later (Day 95). Primary tumors were removed 35 days post engraftment. (B) Metastatic bioluminescent radiance was quantified at the indicated time points in mice bearing the indicated heterogeneous tumors. Data are expressed as the natural log (LN) of the metastatic radiance values for each individual animal resulting in the indicated *P* value.

3.3.3 Functionalized FN fibrils facilitate transient EMT and directional cellular migration

Previous studies suggest that FN contributes to metastasis through the induction of EMT[41,132] To further characterize the role of FN in facilitating the heterotypic interactions between Ca1a and Ca1h cells we initially attempted to use the Ca1h cells to create extracellular protein matrixes. However, consistent with previous studies we observed that unlike fibroblasts, Ca1h cells do not deposit FN into a matrix (Figure 3.4A and 3.4B). Therefore, we used a static adsorption coating method to coat tissue culture polystyrene (PS) with exogenous FN. Using this approach, we did observe increase cellular adhesion that was dependent on β1 integrin, a critical component of the FN receptor (Fig. 3.5A-3.5B)[133]. Consistent with previous reports, culturing the Ca1a cells on FN-coated PS did result in detectable modulation of EMT markers at the mRNA level (Figure 3.5C). However, using this approach we did not observe a morphological change in the Ca1a cells, and we did not observe detectable changes in E-cadherin protein levels in these cells even after six consecutive passages on FN-coated plates (Figure 3.5D-3.5E).

To achieve the fibrillar confirmation of FN that largely exists *in vivo*, we engineered a tessellated scaffold with 500 μm^2 square pores, made of SU-8, which are capable of supporting the growth of cells when placed in nonadherent culture wells (Figure 3.6A; Figure 3.7)[134,135]. In contrast to static adsorption to a growth surface, we were able to create fibrillar FN by utilizing a rotational method to coat our 3D cell culture scaffolds (Figure 3.6B). Importantly, only these FN fibrils contained cryptic binding domains, indicating enhanced functionalization of the ECM protein (Figure 3.6B). The FN fibrils crossed the

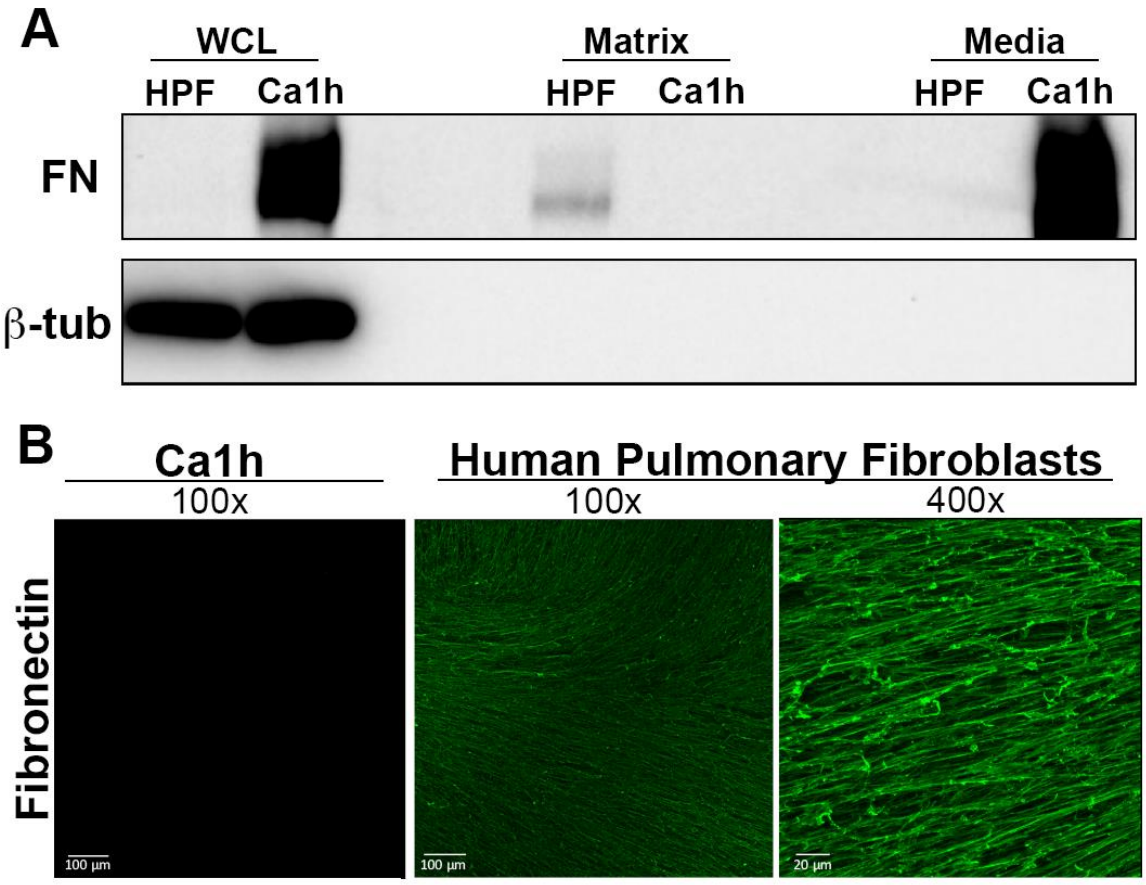

Figure 3.4: Tumor cells do not deposit fibronectin into a fibrillar matrix.

(A) Human pulmonary fibroblasts (HPF) and Ca1h cells were gathered via trypsinization, washed to remove extracellular proteins and subsequently lysed to obtain whole cell lysates (WCL). Separate, confluent cultures of HPFs or Ca1h cells were decellularized and deposited matrix proteins were gathered with SDS containing lysis buffer. Finally, serum-free media from confluent monolayers of HPFs and Ca1h cells were concentrated by protein precipitation. These three separate fractions were analyzed by immunoblot for the presence of FN. Expression of β-tubulin (β-tub) served as a loading control for the WCL. (B) Confluent cultures of Ca1h and HPFs were decellularized as in panel A and the remaining matrix was stained with antibodies specific for fibronectin.

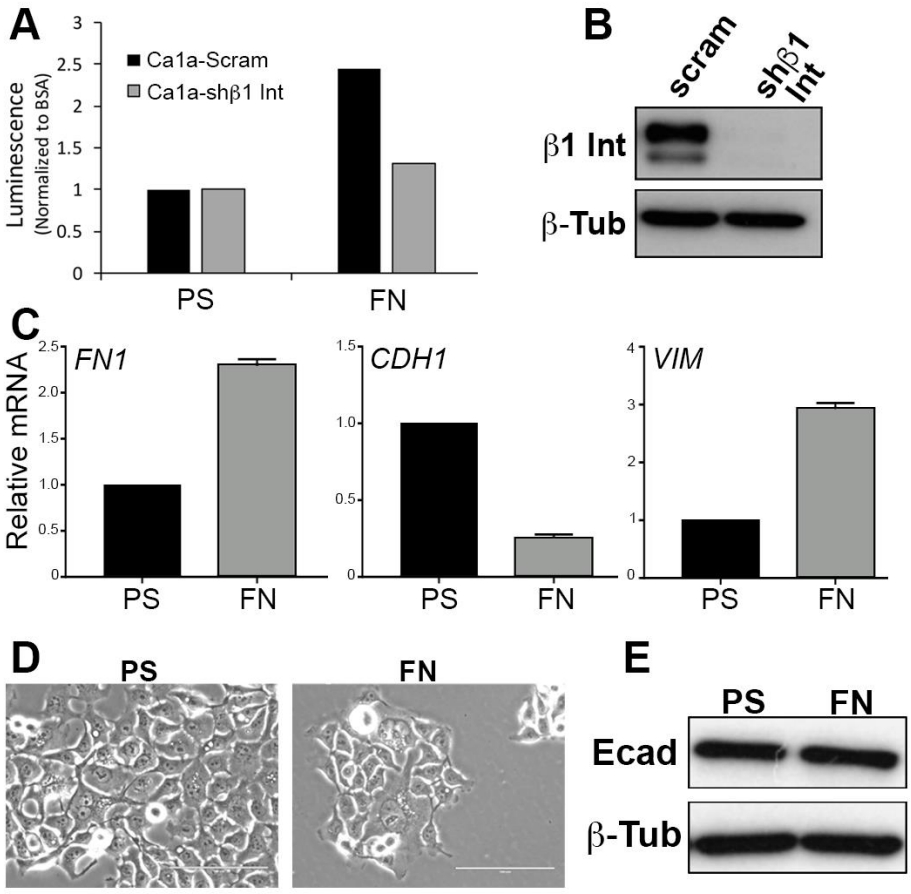

Figure 3.5: Fibronectin coated polystyrene induces a partial epithelial-mesenchymal transition**.**

(A) Control (scram) and β1 integrin depleted (shβ1 Int) Ca1a cells were cultured on BSA or FN-coated polystyrene for one hour, washed with PBS and cell-derived bioluminescence was measured. (B) Depletion of β1 integrin (β1 Int) was confirmed using immunoblot analysis. (C) Ca1a cells were cultured on FN-coated (FN) or uncoated polystyrene (PS) 2D surfaces for 6 passages, and mRNA transcripts for *FN1*, *CDH1* and *VIM* were quantified by RT-PCR. (D) Phase contrast images demonstrating the epithelial morphology of Ca1a cells cultured on FN-coated (FN) and uncoated polystyrene (PS). (E) Immunoblot analyses for Ecad from Ca1a cells cultured as described in panel D. Expression of β-tubulin served as a loading control. All data are representative of at least three independent analyses.

open spaces of the tessellated scaffold creating a controlled microenvironment for the culture of the Ca1a cells free of interference from the polymer scaffold (Figure 3.8A). Consistent with our coating of 2D polystyrene, Ca1a cells that remained on the solid support of the FN-coated scaffold-maintained cell-cell junctions (Figure 3.8A). However, the Ca1a cells that grew off the scaffold within the unsupported FN fibrils underwent an EMT-like morphological change, characterized by activation of the cytoskeleton, dissolution of adherent junctions, and detection of STAT3 phosphorylation (Figure 3.8A-3.8C and Figure 3.9). These effects of fibrillar FN required expression of β1 integrin in the Ca1a cells (Figure 3.8A-3.8C and Figure 3.9). We were able to use time-lapse microscopy to capture Ca1a cells migrating and proliferating on these pure FN fibrils.

To quantify this small subpopulation of cells growing within the FN fibrils, off the support of the scaffold, we assessed changes in the CD44 and CD24 populations by flow cytometry. A small but distinct population of Ca1a cells isolated from the FN-coated scaffolds demonstrated a mesenchymal $CD44^{hi}/CD24^{lo}$ phenotype as compared to those same cells harvested from 2D polystyrene (Figure 3.8D). This effect was again dependent on the expression of the FN receptor, β1 integrin (Figure 3.8D). Similar to the Ca1a cells, culture of immortalized human mammary epithelial (HMLE) cells on functionalized FN-coated scaffolds also resulted in the emergence of a $CD44^{hi}$, mesenchymal population that could be readily visualized upon return to 2D culture (Figure 3.10)[108,123].

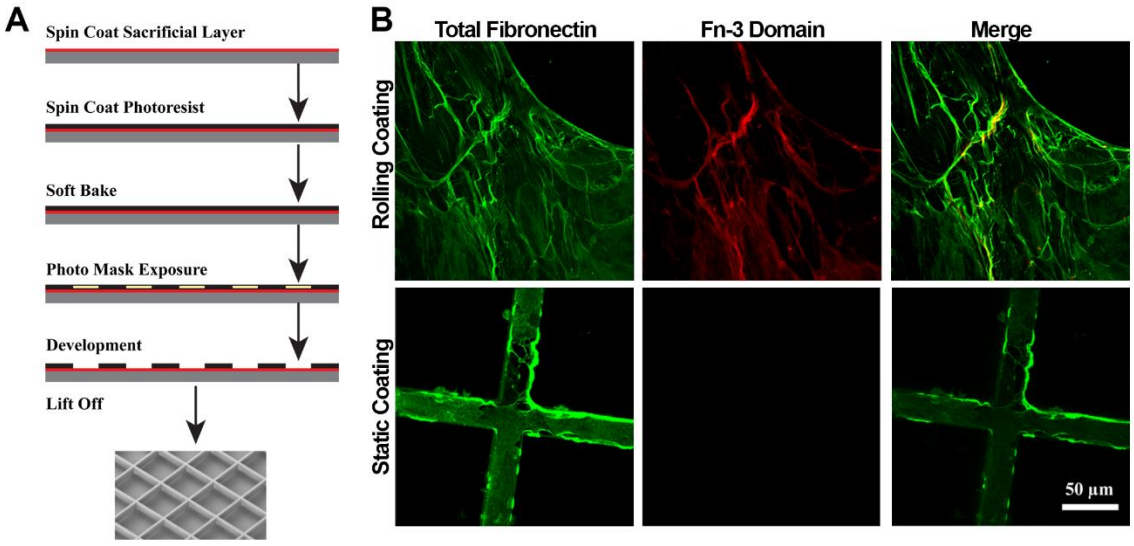

Figure 3.6: Fabrication and matrix coating of tessellated culture scaffolds.

(A) A sacrificial layer of omnicoat (red) is added to a silicon wafer (gray). Next, the negative resist SU-8 is coated onto the wafer (black), followed by a soft bake. After the soft bake the wafers are exposed to UV light, followed by the development of the wafer. After development, regions in the SU-8 layer that were not exposed to UV light are removed, leaving behind the scaffolds on the silicon wafer. The sacrificial layer is then removed, allowing for the release of the scaffolds from the silicon, which can then be used for cell culture applications. (B) These scaffolds were coated with fibronectin using both static surface adsorption as well as rotational coating. Static adsorption of the scaffolds with fibronectin resulted in a conformal layer of the protein, that was absent of fibrils. After rotational coating fibronectin fibrils formed, that spanned the free volume of the scaffolding. Immuno-staining revealed that surface adsorption of the scaffolds did not expose the cryptic binding domain of functionalized FN (Fn-3). However, after rotational coating, this domain is exposed.

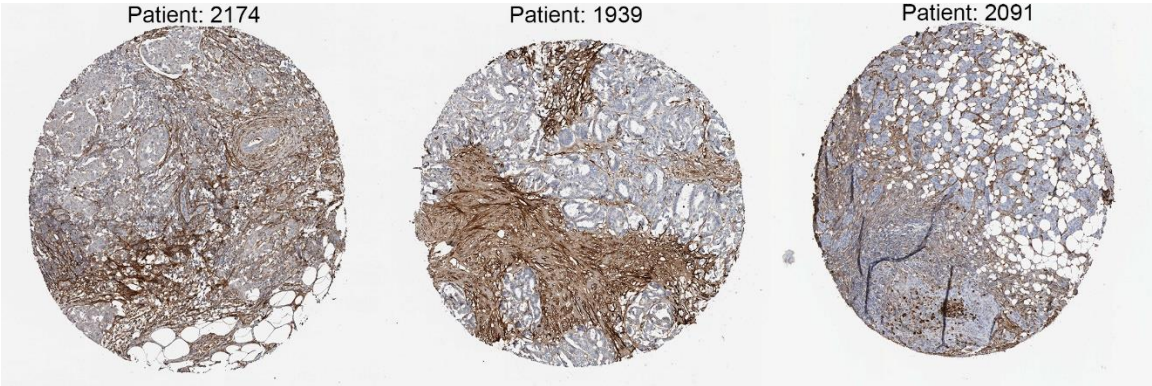

Figure 3.7: Fibronectin is in a fibular form in patient tumors.

Biopsies from the indicated patients were stained for FN and counterstained with hematoxylin to visualize nuclei. Images were obtained from the protein atlas (www.proteinatlas.org).

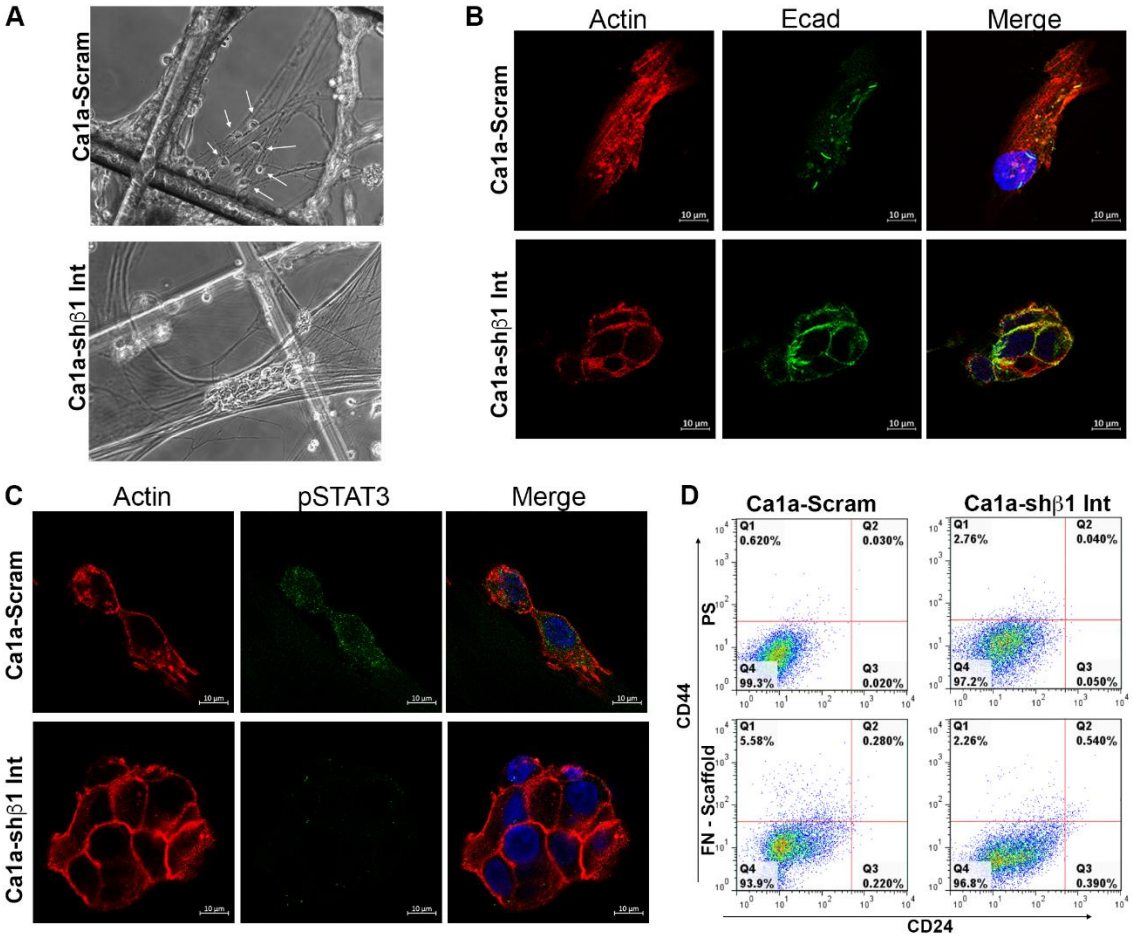

Figure 3.8: Functionalized fibronectin fibrils facilitate EMT and directional cellular migration.

(A) Control (scram) and β1 integrin depleted (shβ1 Int) Ca1a cells were cultured on fibronectin coated 3D scaffolds as described in the methods for 6 days and images were acquired using phase contrast microscopy. Arrows indicate single cells (scram) or cell clusters (shβ1 Int) growing off the solid support of the scaffold. (B and C) The cells cultured as described in panel A were stained with antibodies against Ecad in panel B or phospho-STAT3 in panel C. In both cases cells were counterstained with phalloidin (red) and dapi (blue) to visualize the actin cytoskeleton and the nucleus, respectively. (D) Control (scram) and β1 integrin depleted (shβ1 Int) Ca1a cells were cultured on fibronectin coated 3D scaffolds or polystyrene (PS) for 6 days and analyzed by flow cytometry for cell surface expression of CD44 and CD24.

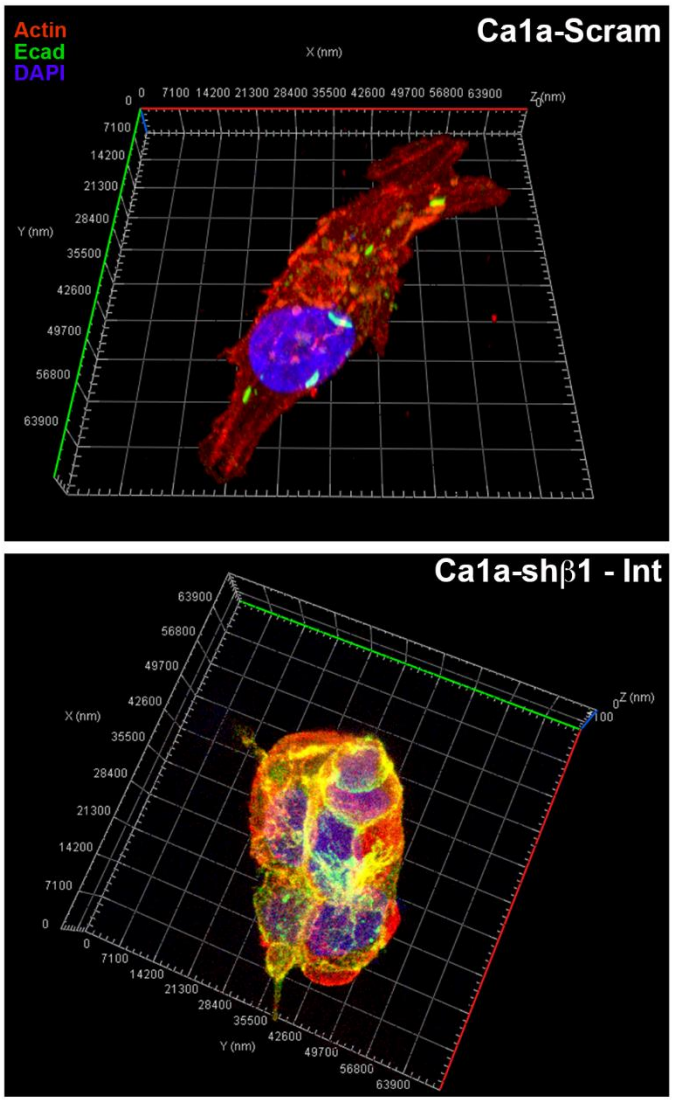

Figure 3.9: Fibrillar fibronectin induction of EMT is dependent on the expression of β1 integrin.

3D reconstructions cells are shown in Figure 7B. Control (scram) and β1 integrin depleted (sh β1-Int) Ca1a cells growing on fibrillar FN off of the solid support of our scaffold. Cells were stained with antibodies against Ecad (green), phalloidin (Red) and DAPI (blue).

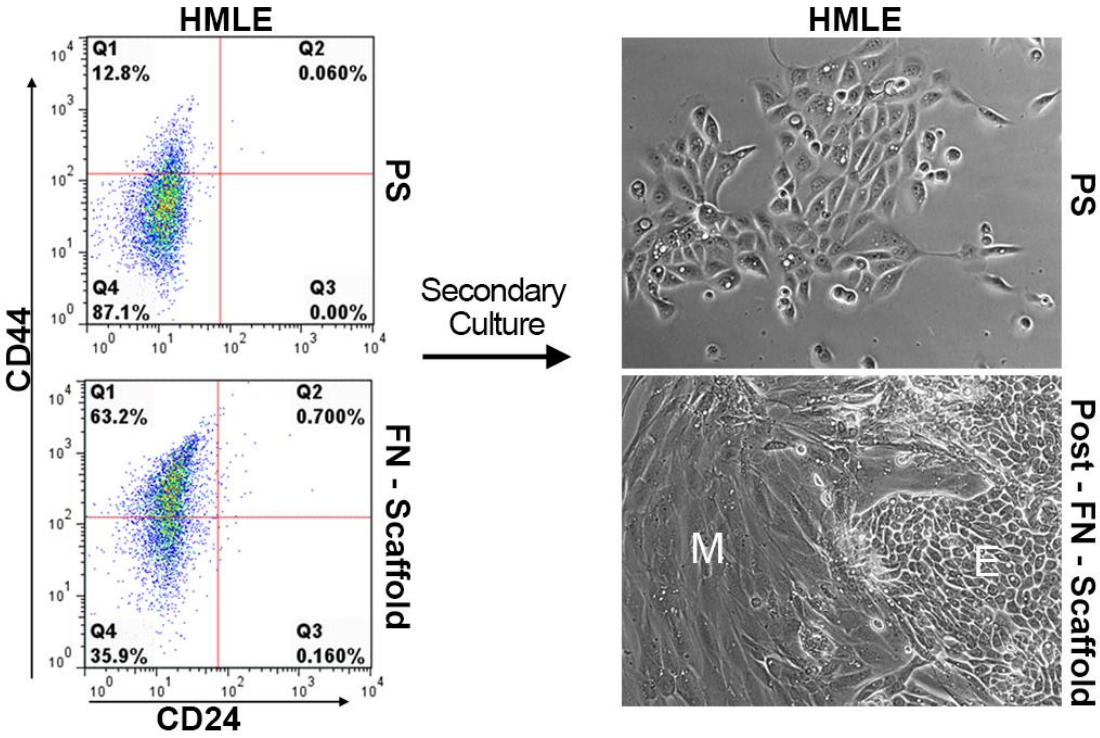

Figure 3.10: Fibrillar fibronectin induces a mesenchymal phenotype.

Human mammary epithelial (HMLE) cells were cultured on polystyrene (PS) or FN-coated scaffolds for 6 days and these cells were analyzed by flow cytometry for cell surface expression of CD44 and CD24. Subsets of these cells were returned to traditional 2D culture for three days and imaged by phase contrast microscopy to visualize the distinct epithelial (E) and mesenchymal (M) cell populations.

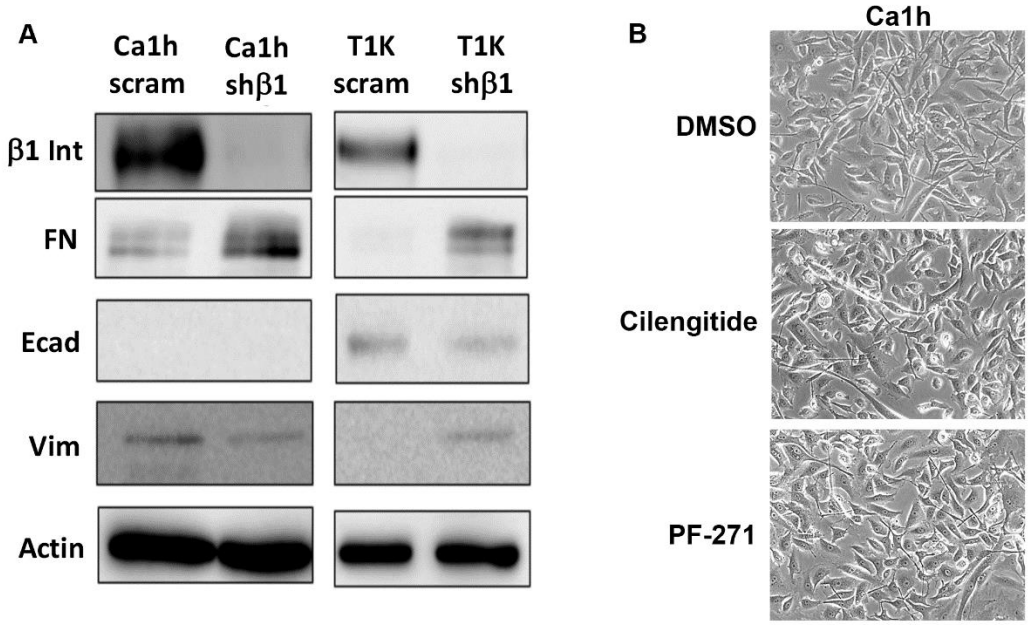

Figure 3.11: Depletion of β1 increases intracellular FN.

(A) Ca1h and their isogenic counterpart T1K cells were depleted for expression of β1 integrin via shRNA. Expression of intracellular FN, Ecad, and vimentin (Vim) was assessed by immunoblot analyses. Expression of actin and β1 integrin served as loading controls. (B) Ca1h cells were treated for 14 days with the integrin blocking cyclic peptide Cilengitide (1 μM) or the focal adhesion kinase inhibitor PF-562,271 (PF-271; 1 μM). Cells were subsequently imaged by phase contrast microscopy. No changes in cell morphology were observed with these inhibitors.

3.3.4 Autocrine expression of fibronectin stabilizes a constitutive mesenchymal phenotype

In contrast, to the requirement of β1 integrin for cellular response to fibrillar FN, depletion of β1 integrin or pharmacological inhibition of integrin:FAK signaling using cyclic peptides or small molecules kinase inhibitors in the Ca1h cells did not result in a return of epithelial characteristics (Figure 3.11-3.11B). In fact, shRNA-mediated depletion of β1 integrin led to increased levels of intracellular FN and diminution in Ecad expression in the T1K cells, an isogenic counterpart of the Ca1h cells (Figure 3.11A). Therefore, we sought to investigate potential integrin-independent functions of FN in EMT and metastasis that may be working in an intracellular fashion. Confocal microscopy confirmed strong colocalization of intracellular FN with the actin cytoskeleton (Figure 3.12). Depletion of FN in the Ca1h cells using two independent shRNAs led to increased transcript levels of the epithelial marker Ecad and loss of the mesenchymal marker vimentin, the intensity of which was consistent with the efficiency of FN depletion (Figure 3.13A). Additionally, depletion of FN caused altered protein expression of several but not all makers of MET including Ecad, Vimentin, Zeb1, Zo1, FGFR1 and cell surface expression of CD44 and CD24 (Figure 3.13B and 3.13C). Accompanying these phenotypic markers, depletion of FN also leads a robust morphological change in the Ca1h cells, resulting in the reduction of filamentous actin and the formation of adherent junctions (Figure 3.13D and 3.13E). Taken together, these data are consistent with the conclusion that autocrine FN functions in a β1 integrin-independent fashion to maintain a stable mesenchymal phenotype.

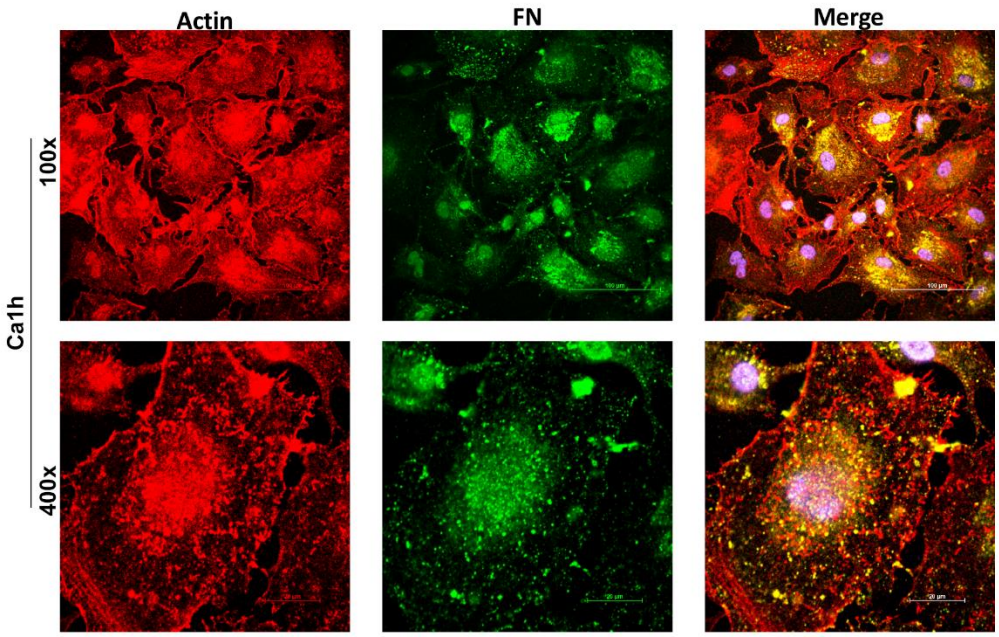

Figure 3.12: Intracellular FN colocalizes with the actin cytoskeleton.

Ca1h cells were stained with antibodies directed toward FN and phalloidin to visualize the actin cytoskeleton. These cells were visualized used confocal microscopy. Shown are single, mid-cell plains of focus.

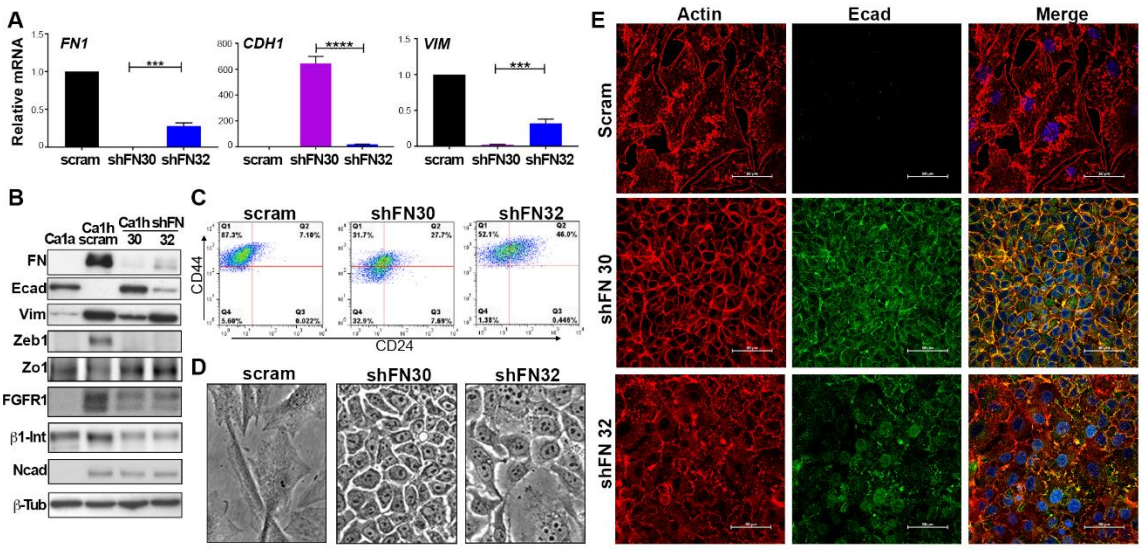

Figure 3.13: Expression of fibronectin stabilizes a mesenchymal phenotype.

(A) Control (scram) or two independent shRNAs, shFN30 or shFN32, targeting human *FN1* transcripts were stably expressed in the Ca1h cells. Transcript levels for fibronectin (*FN1*), E-cadherin (*CDH1*) and vimentin (*VIM*) were quantified relative to control Ca1h cells. (B) Immunoblot analyses for FN, Ecad and Vimentin (Vim), Zeb1, Zo1, FGFR1, β1 integrin, N-cadherin (Ncad), from control (scram) and FN-depleted Ca1h cells. Levels of these proteins in the Ca1a cells is shown as a reference. Expression of β-tubulin served as a loading control. (C) Control and FN-depleted Ca1h cells were analyzed by flow cytometry for cell surface expression of CD44 and CD24. (D) Phase contrast images showing the differential morphologies of control and FN-depleted Ca1h cells. (E) Control (scram), and FN-depleted (shFN30 and shFN32) Ca1h cells were immunostained for Ecad (green) and stained with phalloidin (red) and dapi (blue) to visualize the actin cytoskeleton and nuclei, respectively. Confocal images shown are z, x and y planes reconstructed from serial sections obtained throughout whole cells. All data are representative of at least three independent experiments.

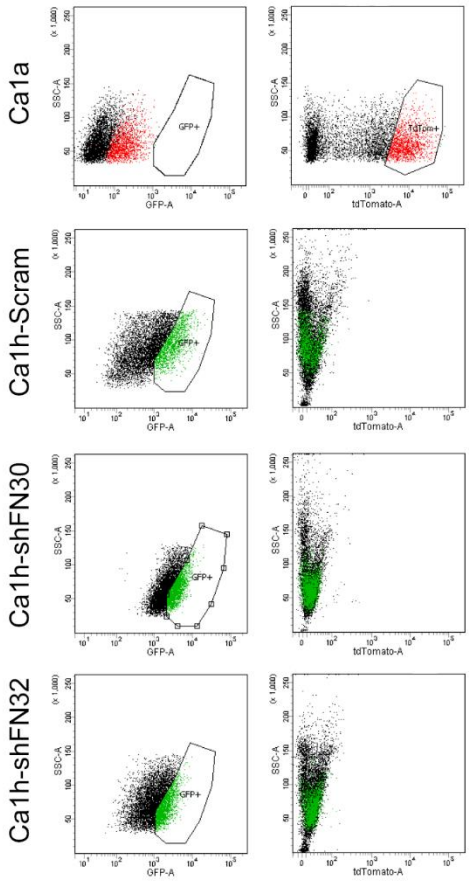

Figure 3.14: Differential fluorescent labeling of epithelial and mesenchymal cells.

Ca1a cells stably expressing a d-Tomato encoding vector were isolated from the indicated gate. Similarly, control (scram) and FN-depleted (shFN30, shFN32) Ca1h cells expressing an eGFP encoding vector were isolated from the indicated gates in the GFP channel.

3.3.5 Tumor cells expressing FN act in a stromal capacity to support the growth of other tumor cells

We next sought to characterize the interaction between FN-producing, constitutively mesenchymal tumor cells, and metastatic tumor cells. To this end, we differentially identified Ca1a and Ca1h cells via stable expression and fluorescence activated cell sorting for d-Tomato and eGFP, respectively (Figure 14). These cells were then cultured in a 3D hydrogel basement membrane matrix to assess the growth of the Ca1a cells alone or when in a heterogeneous coculture with the Ca1h cells. The growth of the Ca1a cells alone results in cell dense, spherical 3D structures (Figure 3.15A). However, coculture of the Ca1a cells with FN-expressing Ca1h cells resulted in a loss of the spherical morphology, heterogeneous cell interspersion, and enhanced invasion of the Ca1a cells into the surrounding matrix (Figure 3.15B, top panels). Additionally, even when cells grew in close physical proximity, they did not form interspersed structures and the spherical growth pattern of the Ca1a structures was maintained (Figure 3.15B, middle and bottom panels). Measuring bioluminescence production from the firefly luciferase expressing Ca1a cells allowed us to quantify their increased growth when in the presence of Ca1h cells (Figure 3.15C). Decreased formation of heterogeneous cell clusters prevented this stromal support upon FN depletion in the Ca1h cells (Figure 3.15C and 3.15D). These data suggest that FN expression by tumor cells allows them to act in a stromal fashion to physically support the growth of metastatic tumor cells.

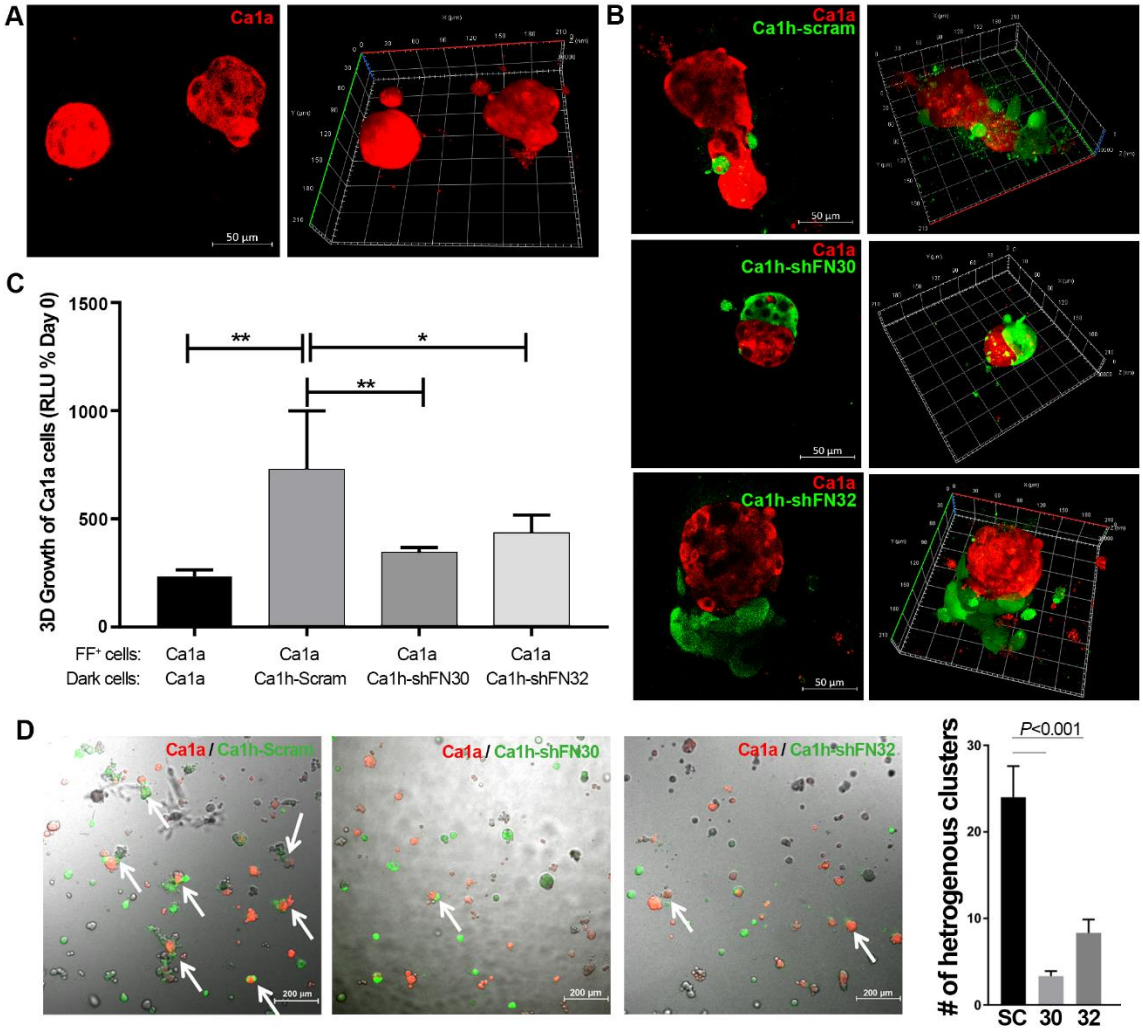

Figure 3.15: Depletion of FN decreases the stromal support capacity of breast cancer cells.

Confocal images of dTomato expressing Ca1a cells cultured for 16 days under 3D hydrogel conditions, alone (A) and with eGFP labeled Ca1h scram (B, top), shFN30 (B, middle), shFN32 (B, bottom) cells. (B) *Left panels*: Confocal images are z, x and y planes reconstructed from serial sections obtained throughout the entire cell cluster. *Right panels*: Three-dimensional projections of cell clusters imaged with confocal sectioning. (C) Bioluminescent Ca1a cells were cocultured with or without non-bioluminescent Ca1a, control Ca1h (scram), or FN depleted Ca1h (shFN30 or shFN32) cells under 3D hydrogel conditions in a 1:1 ratio. Data are day 16 Ca1a-derived luminescence values relative to the day 0 luminescence values. Data are the mean values (±SE) of at least three independent experiments completed in triplicate, resulting in the indicated P values. (D) Fluorescently labeled Ca1a and Ca1h cells were mixed at 1:1 ratio, cultured in a 3D hydrogel for 4 days and the numbers of heterogeneous cell clusters containing both d-Tomato and eGFP positive cells were quantified. Data are the mean (± SE) number of heterogeneous cell clusters per field of view over 9 separate fields resulting in the indicated P value.

3.3.6 Autocrine FN inhibits pulmonary tumor outgrowth

To more specifically characterize the autocrine versus the paracrine role of FN in tumor growth we cultured control and FN-depleted Ca1h cells on our 3D scaffolds lacking any exogenous matrix coating. Addition of the Ca1h cells to the 3D scaffolds led to the formation of cellular fibrils that crossed the open spaces of the culture scaffolds (Figure 3.16A). In contrast, Ca1h cells depleted in FN expression grew more robustly than control cells (Figure 3.16B). However, FN-depleted cells remained on the solid support of the scaffold in an epithelial fashion, generating very distinct cortical actin (Figure 3.16A-3.16C). Using our differentially labeled Ca1a and Ca1h cells, we were able to capture time lapse microscopy demonstrating the ability of the Ca1a cells to utilize Ca1h cellular fibrils to migrate away from the culture scaffold. These data clearly demonstrate the ability of mesenchymal tumor cells to produce FN-containing cellular fibrils that are capable of facilitating cellular migration of metastatic tumor cells.

The increased proliferation of FN-depleted cells suggested that autocrine FN actively inhibits the ability of tumor cells to grow in a 3D environment. Along these lines, FN is also constitutively expressed by the D2.OR cell model of systemic dormancy as compared to their isogeneic and fully metastatic, D2.A1, counterparts (Figure 3.17)[133]. Therefore, we conducted tail vein injection experiments to assess the *in vivo* capacity of control and FN-depleted Ca1h cells to initiate tumor growth within a physiologically relevant site of metastasis. Injection of control Ca1h cells resulted in detectable, but asymptomatic maintenance of these cells in the lungs over a period of 7 weeks (Figure 3.16D-3.16F). In contrast, FN-depleted Ca1h cells were capable of forming numerous macroscopic tumors within the pulmonary microenvironment (Figure 3.16D-3.16F). The

Figure 3.16: Autocrine FN inhibits pulmonary tumor formation.

(A) Control (scram) and FN depleted (shFN30 and shFN32) Ca1h cells were cultured on 3D scaffolds as described in the methods for 6 days and images were acquired using phase contrast microscopy. (B) Growth of control (scram) and FN-depleted (shFN30) Ca1h cells was quantified by cell titer glow assay at the indicated time points. Data are the mean arbitrary luminescence units (ALU) (±SE) for three independent experiments completed in triplicate resulting in the indicated P value. (C) Control (scram) and FN depleted (shFN30) Ca1h cells were cultured on the 3D scaffold system for 6 days and subsequently stained with antibodies against FN (green), phalloidin (red) and dapi (blue). z, x and y planes are shown from reconstructed serial sections obtained through whole cells. *Right panels*: three-dimensional projections of cells shown in the left panels. (D) Bioluminescent images of representative mice taken immediately (Day 0) and 35 days (Day 35) following tail vein injection of control (scram) and FN-depleted (shFN30) Ca1h cells. (E) The mean (±SE) pulmonary bioluminescence values normalized to the injected values (n=3 mice for scram, n=5 mice for shFN30) were quantified at the indicated time points, resulting in the indicated P value. (F) Resultant pulmonary tumors from control (scram) and FN-depleted (shFN30) Ca1h cells were analyzed by histology. Serial sections were stained with hematoxylin and eosin (H&E) or analyzed by immune staining for Vimentin, FN, and Ecad. (G) Ca1a cells were stably transduced with FN or GFP as a control. These cells along with Ca1h cells as a reference were assessed by immunoblot for the indicated markers of EMT. Expression of β-tubulin served as a loading control. (H) Control (GFP) and FN expressing Ca1a cells were plated onto uncoated tessellated scaffolds and fibril formation was assessed. (I) Growth of control (GFP) and FN-expressing (FN) Ca1a cells was quantified 12-days post plating. Data are the mean (±SE) luminescence units normalized to the plated values (T0) for three independent experiments completed in triplicate, resulting in the indicated P value. (J) Control (GFP) and FN expressing Ca1a cells expressing firefly luciferase ($1x10^6$) were injected into the lateral tail vein of NRG mice and pulmonary tumor growth was tracked by bioluminescence. The mean (±SE) pulmonary bioluminescence values normalized to the injected values (n=4 per group) were quantified at the indicated time points, resulting in the indicated P value. (Inset) Representative lungs from mice receiving tail injections of control (GFP) or FN expressing Ca1a cells.

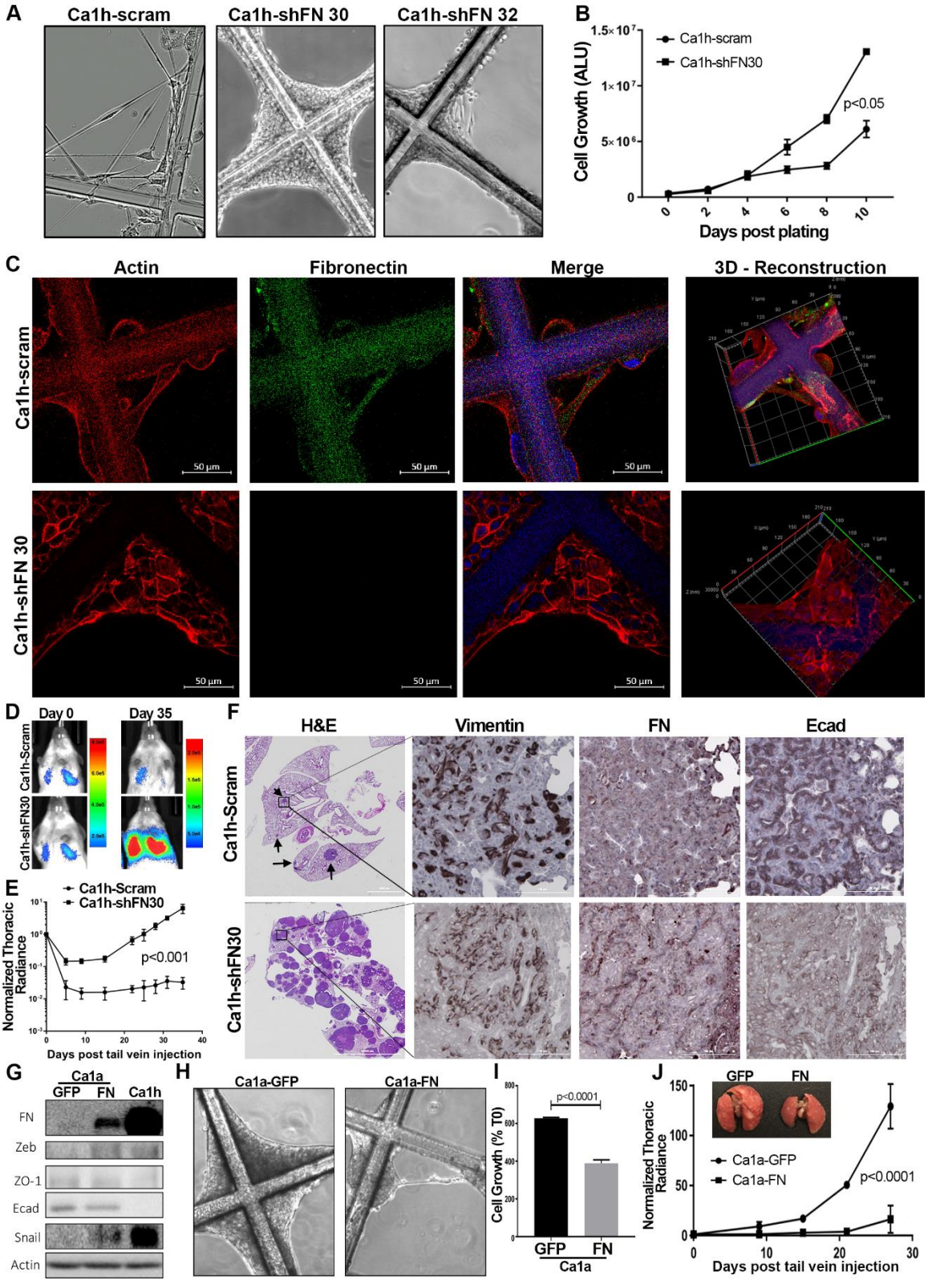
A
Ca1h-scram
Ca1h-shFN 30
Ca1h-shFN 32
B
Ca1h-scram
Ca1h-shFN30
p<0.05
Cell Growth (ALU)
Days post plating
C
Actin
Fibronectin
Merge
3D - Reconstruction
Ca1h-scram
Ca1h-shFN 30
50 µm
D
Day 0
Day 35
Ca1h-Scram
Ca1h-shFN30
E
Ca1h-Scram
Ca1h-shFN30
p<0.001
Normalized Thoracic Radiance
Days post tail vein injection
F
H&E
Vimentin
FN
Ecad
Ca1h-Scram
Ca1h-shFN30
G
Ca1a
GFP
FN
Ca1h
FN
Zeb
ZO-1
Ecad
Snail
Actin
H
Ca1a-GFP
Ca1a-FN
I
p<0.0001
Cell Growth (% T0)
GFP
FN
Ca1a
J
GFP
FN
Ca1a-GFP
Ca1a-FN
p<0.0001
Normalized Thoracic Radiance
Days post tail vein injection

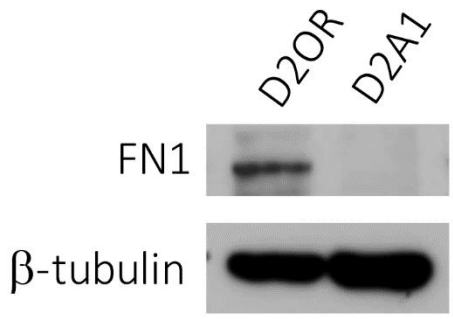

Figure 3.17: Systemically dormant cells express intracellular FN.

Whole cell lysates from systemically dormant D2.OR cells and their isogenic but fully metastatic counterpart D2.A1 cells were analyzed for expression of FN. β-tubulin served as a loading control.

bioluminescent signal from mice bearing control Ca1h cells were histologically located to a few small lesions within the lung (Figure 3.16F and 3.18). Consistent with our *in vitro* data, these smaller lesions that did form contained intracellular FN, but also demonstrated readily detectable levels of E-cadherin (Figure 3.16F). Finally, we were unable to achieve stable overexpress FN in the Ca1a cells to a level that was consistent with that of the Ca1h cells (Figure 3.16G). Nonetheless, even this moderate level of autocrine FN expression in the Ca1a cells was sufficient to modulate EMT markers, induce cellular fibril formation, decrease cell growth and inhibit pulmonary tumor formation upon tail injection (Figure 3.16G-3.16HJ). Taken together, these data suggest that when presented as a homogenous inoculum, highly mesenchymal cells can undergo MET in the pulmonary microenvironment and proceed to macroscopic pulmonary tumor formation. However, these events are clearly inhibited by autocrine expression of FN.

3.4 Discussion

Patient data presented here and elsewhere clearly demonstrate that high-level expression of FN within primary breast tumors is associated with decreased patient survival [106,136]. These clinical data are somewhat counter to data from tumor cell lines in which constitutive expression of autocrine FN corresponds to a non-metastatic phenotype. Our cell labeling data clearly demonstrates that FN produced by tumor cells that have undergone an EMT contributes to the invasion and metastasis of their epithelial counterparts. Furthermore, our genetic depletion and overexpression studies indicate that production of FN stabilizes a non-metastatic mesenchymal phenotype in an integrin-independent manner. The current study supports the concept of epithelial-mesenchymal

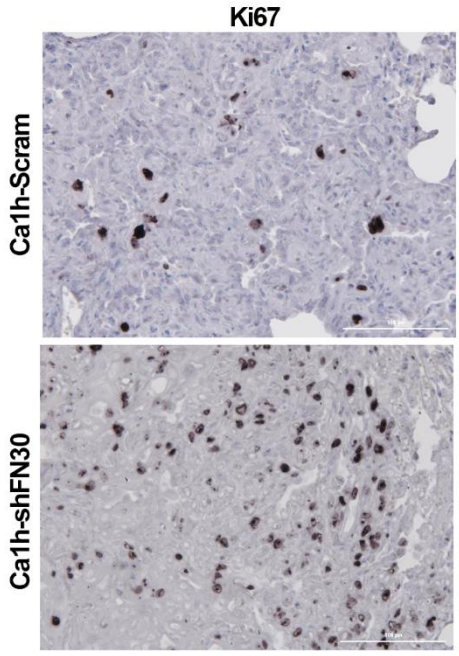

Figure 3.18: Depletion of FN increases pulmonary tumor proliferation.

The resultant pulmonary tumors formed 35 days after tail vein injection of control (scram) and FN-depleted (shFN30) Ca1h cells were analyzed by IHC staining for the proliferation marker Ki67.

heterogeneity (EMH). In this scenario, stably mesenchymal tumor cells lose their cell autonomous capacity for metastasis but still contribute to metastatic progression by taking on a stromal role within the tumor microenvironment.

Consistent with our previous studies, we demonstrate that β1 integrin is required for fibrillar FN to promote the phosphorylation of STAT3, a molecule that is known to participate in the induction of EMT[106,137]. However, our data also suggest that cellular binding to fibrillar FN physically distorts cell morphology promoting a more mechanically induced mesenchymal morphology. Further understanding of how fibrillar FN alters cell morphology and how these events relate to more transcriptionally driven EMT events induced by drugs and cytokines are clearly warranted. Additionally, our studies suggest the concept of intracrine FN signaling. Indeed, as opposed to its requirement for response to fibrillar FN, depletion of β1 integrin does not cause an epithelial reversion as we observe upon depletion of FN. In fact, depletion of β1 integrin increased the levels of intracellular FN and enhanced a mesenchymal phenotype. While depletion of β1 integrin can have pleiotropic effects on cells, these data are consistent with a mechanism by which integrins facilitate the secretion of FN, a process that remains poorly understood in epithelial-derived cells. Additionally, our microscopy studies suggest that intracellular FN directly interacts with the actin cytoskeleton, but more nanoscale analyses of these interactions are required. This and other potential mechanisms of how intracrine FN signaling may influence cell morphology and the molecular mechanisms that sustain constitutive FN expression in epithelial-derived tumor cells are areas of current investigation in our lab.

In addition to furthering our biological understanding of FN function and ECM-induced morphological changes, a major advance of the current study is development and implementation of our tessellated cell culture device capable of accurately recapitulating cellular and matrix phenotypes observed *in vivo*. Overall, our culture system represents advanced engineering that is easy to use and inexpensive to produce. As shown, cells cultured on ECM-coated or uncoated scaffolds can be readily grown and analyzed by immunofluorescence, harvested for immunoblot or mRNA analyses, trypsinized for flow cytometry, or passaged for continuous culture. All these procedures can be done using techniques that are completely analogous to those currently used for standard 2D cell culture. Therefore, while other 3D culture systems are cumbersome and/or cost prohibitive for the ongoing culture of stock cells our platform is well suited for long-term maintenance of cultured cell lines or primary, patient-derived tumor tissues.

3.5 Conclusions

In conclusion, we observed single-cell migration, loss of junctional Ecad, phosphorylation of STAT3 and gain of CD44 in cells cultured on FN fibrils. However, our studies do not rule out the possibility of tumor cells remaining in a transcriptionally epithelial state while migrating on cellular or FN fibrils. What is clear is that growth, migration and overall metastasis of epithelial-mesenchymal malleable tumor cells is enhanced when in the presence of constitutively mesenchymal, FN-expressing tumor cells. These combined concepts of epithelial-mesenchymal plasticity and heterogeneity are likely both at play during metastasis, and model-dependent reliance on one or the other likely explains discrepancies between studies as to whether or not EMT contributes to metastasis[108,136,138–140]

3.6 References

1. Yang, J. *et al.* Twist, a master regulator of morphogenesis, plays an essential role in tumor metastasis. *Cell* (2004). doi:10.1016/j.cell.2004.06.006
2. Mani, S. A. *et al.* The Epithelial-Mesenchymal Transition Generates Cells with Properties of Stem Cells. *Cell* (2008). doi:10.1016/j.cell.2008.03.027
3. Wendt, M. K., Taylor, M. A., Schiemann, B. J., Sossey-Alaoui, K. & Schiemann, W. P. Fibroblast growth factor receptor splice variants are stable markers of oncogenic transforming growth factor β1 signaling in metastatic breast cancers. *Breast Cancer Res.* (2014). doi:10.1186/bcr3623
4. Wendt, M. K., Taylor, M. A., Schiemann, B. J. & Schiemann, W. P. Down-regulation of epithelial cadherin is required to initiate metastatic outgrowth of breast cancer. *Mol. Biol. Cell* (2011). doi:10.1091/mbc.e11-04-0306
5. Li, R. *et al.* A mesenchymal-to-Epithelial transition initiates and is required for the nuclear reprogramming of mouse fibroblasts. *Cell Stem Cell* (2010). doi:10.1016/j.stem.2010.04.014
6. Schmidt, J. M. *et al.* Stem-cell-like properties and epithelial plasticity arise as stable traits after transient twist1 activation. *Cell Rep.* (2015). doi:10.1016/j.celrep.2014.12.032
7. Neelakantan, D. *et al.* EMT cells increase breast cancer metastasis via paracrine GLI activation in neighbouring tumour cells. *Nat. Commun.* (2017). doi:10.1038/ncomms15773
8. Wyckoff, J. *et al.* A paracrine loop between tumor cells and macrophages is required for tumor cell migration in mammary tumors. *Cancer Res.* (2004). doi:10.1158/0008-5472.CAN-04-1449
9. Keller, P. J. *et al.* Estrogen expands breast cancer stem-like cells through paracrine FGF/Tbx3 signaling. *Proc. Natl. Acad. Sci.* (2010). doi:10.1073/pnas.1007863107
10. Dieudonne, M. N. *et al.* Leptin mediates a proliferative response in human MCF7 breast cancer cells. *Biochem. Biophys. Res. Commun.* (2002). doi:10.1016/S0006-291X(02)00205-X

11. Sikandar, S. S. *et al.* Role of epithelial to mesenchymal transition associated genes in mammary gland regeneration and breast tumorigenesis. *Nat. Commun.* (2017). doi:10.1038/s41467-017-01666-2
12. Jolly, M. K., Ware, K. E., Gilja, S., Somarelli, J. A. & Levine, H. EMT and MET: necessary or permissive for metastasis? *Molecular Oncology* (2017). doi:10.1002/1878-0261.12083
13. Bani, D. & Nistri, S. New insights into the morphogenic role of stromal cells and their relevance for regenerative medicine. lessons from the heart. *J. Cell. Mol. Med.* (2014). doi:10.1111/jcmm.12247
14. Provenzano, P. P. *et al.* Collagen reorganization at the tumor-stromal interface facilitates local invasion. *BMC Med.* (2006). doi:10.1186/1741-7015-4-38
15. Balanis, N. *et al.* Epithelial to mesenchymal transition promotes breast cancer progression via a fibronectin-dependent STAT3 signaling pathway. *J. Biol. Chem.* (2013). doi:10.1074/jbc.M113.475277
16. Curtis, C. *et al.* The genomic and transcriptomic architecture of 2,000 breast tumours reveals novel subgroups. *Nature* (2012). doi:10.1038/nature10983
17. Santner, S. J. *et al.* Malignant MCF10CA1 cell lines derived from premalignant human breast epithelial MCF10AT cells. *Breast Cancer Res. Treat.* (2001). doi:10.1023/A:1006461422273
18. Park, J. & Schwarzbauer, J. E. Mammary epithelial cell interactions with fibronectin stimulate epithelial-mesenchymal transition. *Oncogene* (2014). doi:10.1038/onc.2013.118
19. Li, C. L. *et al.* Fibronectin induces epithelial-mesenchymal transition in human breast cancer MCF-7 cells via activation of calpain. *Oncol. Lett.* (2017). doi:10.3892/ol.2017.5896
20. Ruoslahti, E. Fibronectin in cell adhesion and invasion. *Cancer Metastasis Rev.* (1984). doi:10.1007/BF00047692
21. Moon, P.-G. *et al.* Fibronectin on circulating extracellular vesicles as a liquid biopsy to detect breast cancer. *Oncotarget* (2016). doi:10.18632/oncotarget.9561

22. To, W. S. & Midwood, K. S. Plasma and cellular fibronectin: Distinct and independent functions during tissue repair. *Fibrogenesis and Tissue Repair* (2011). doi:10.1186/1755-1536-4-21
23. Brown, W. S., Akhand, S. S. & Wendt, M. K. FGFR signaling maintains a drug persistent cell population following epithelial-mesenchymal transition. *Oncotarget* (2016). doi:10.18632/oncotarget.13117
24. Fernandez-Garcia, B. *et al.* Expression and prognostic significance of fibronectin and matrix metalloproteases in breast cancer metastasis. *Histopathology* (2014). doi:10.1111/his.12300
25. Marusyk, A. *et al.* Non-cell-autonomous driving of tumour growth supports sub-clonal heterogeneity. *Nature* (2014). doi:10.1038/nature13556
26. Fischer, K. R. *et al.* Epithelial-to-mesenchymal transition is not required for lung metastasis but contributes to chemoresistance. *Nature* (2015). doi:10.1038/nature15748
27. Zheng, X. *et al.* Epithelial-to-mesenchymal transition is dispensable for metastasis but induces chemoresistance in pancreatic cancer. *Nature* (2015). doi:10.1038/nature16064
28. Wendt, M. K., Balanis, N., Carlin, C. R. & Schiemann, W. P. STAT3 and epithelial–mesenchymal transitions in carcinomas. *JAK-STAT* (2014). doi:10.4161/jkst.28975

CHAPTER 4. EXOSOMES EXPRESSING TGM2 CROSSLINKED FUNCTIONALIZED FIBRILS PROMOTE BREAST CANCER METASTASIS

4.1 Abstract

Cancer cells derived exosomes have been implicated in cell survival and metastasis[1]. These exosomes contain extracellular matrix proteins and matrix enzymes including fibronectin (FN) and tissue transglutaminase 2 (TGM2), respectively. However, the definitive role of these proteins in breast cancer metastasis is unknown. In this study, we have utilized a HER2 transformation model to establish that TGM2 expression is essential and enough to convert non-metastatic into metastatic breast cancer cells. RNA sequence and qRT-PCR analysis of non-metastatic and metastatic cells confirmed that TGM2 is upregulated only in metastatic breast cancer cells following induction and reversion of epithelial-mesenchymal transition. Further, depletion of TGM2 inhibited breast cancer metastasis and promoted survival *in vivo*. Importantly, genetic knockout of TGM2 using a CRISPR approach in highly metastatic 4T1 cells inhibited metastatic tumor outgrowth. To investigate the mechanism through which TGM2 promote breast cancer metastasis, we isolated exosomes from both metastatic and non-metastatic breast cancer cells. Using immunoblot analysis, we confirmed exosomes derived from metastatic breast cancer cells express TGM2 and FN dimers compared to those derived from non-metastatic cells. Further, tensin 1 (TNS1) is also upregulated in exosomes derived from metastatic breast cancer cells. Immunoelectron micrographs of these exosomes suggest FN exists as a fibrillar structure on the surface of exosomes. Confocal microscopy images indicated the colocalization of TGM2 and FN fibrils on the surface of exosomes. Furthermore, genetic

or pharmacological inhibition of TGM2 downregulates TNS1 expression and FN fibril formation on the surface of exosomes. Additionally, genetic depletion of TNS1 reduces expression of TGM2 and FN fibrils. Using a novel 3D culture assay, we further demonstrate human pulmonary fibroblasts educated with metastatic breast cancer cells derived exosomes promote breast cancer cells growth. We also establish exosomes isolated from metastatic breast cancer cells induce pre-metastatic niche formation in naïve mice and subsequently promote metastatic breast cancer cells pulmonary growth. Overall, results from our studies imply a novel mechanism through which metastatic breast cancer cells derived exosomes promote premetastatic niche development and distant metastasis. Furthermore, our studies also suggest TGM2 as a promising target to treat metastatic breast cancer.

4.2 Introduction

Breast cancer is the second leading cause of mortality and morbidity in women. Even though the five-year survival rate for early stage breast cancer patients is 90%, the survival rate drops significantly to 22% for patients diagnosed with distant metastasis. Therefore, there is an unmet need to understand the underlying mechanism and develop targeted therapies to inhibit breast cancer metastasis. Recent studies have indicated that exosomes play an important role in cancer progression and metastasis by promoting intercellular communication, pre-metastatic niche formation and immune evasion[1–8]. Although, several studies suggest different mechanisms through which exosomes promote metastasis in liver, lung and pancreatic cancers, the processes through which exosomes promote breast cancer metastasis remains poorly understood[9–13].

Exosomes are nanosized (50-150 nm) membrane-enclosed extracellular vesicles and are generated when intermediate endocytic compartment known as multivesicular bodies shed them by fusing with the plasma membrane of cells[14–16]. Exosomes consist of different molecular cargoes like proteins and RNA belonging to their cells of origin[17–19]. Exosomes derived from metastatic cancer cells contain different proteins and RNA from those derived from non-metastatic cancer cells[19–21]. Exosomes shed by these metastatic cancer cells can transfer biomolecules and reprogram the cells in the immediate environment, which eventually create a favorable environment for their growth and survival[22]. Consequently, exosomes offer ways to cancer cells to communicate with their neighboring cells thereby promoting cancer progression[10,18,23–25]. Also, exosomes are more stable in the circulatory system than other extracellular vesicles[26] and therefore they can deliver biomolecules to distant organs and help in the creation of a premetastatic niche for secondary tumor formation.

Here we report that exosomes derived from metastatic breast cancer cells induce growth of breast cancer cells *in vitro* and promote tumor growth in lungs in xenograft models. Exosomes isolated from metastatic breast cancer cells express functionalized FN fibrils on their surface and promote significant growth of cancer cells compared with those isolated from non-metastatic breast cancer cells. Immunoblot analysis suggests metastatic breast cancer cells derived exosomes contain FN dimers crosslinked by TGM2. These FN dimers are assembled into FN fibrils by TNS1. Further, depletion of TGM2 inhibits FN dimerization and downregulates TNS1 expression, which inhibits FN fibrillogenesis on the surface of exosomes. Exosomes lacking FN fibrils on their surface due to lack of TGM2 or TNS1 were unable to promote cancer cells growth and metastasis. Taken together, our

data indicate that metastatic breast cancer cells secrete exosomes containing TGM2 to create a pre-metastatic niche and promote distant metastasis.

4.3 Results

4.3.1 Tissue transglutaminase 2 expression is associated with decreased patient survival

We performed RNA sequencing analysis on a previously established model of human mammary epithelial cells (HMLE) overexpressing HER2 (HME2), TGF-β treated HME2 (HME2-Post TGF-β) and bone metastases obtained from HME2-Post TGF-β xenograft model (HME2-BM) cells. Characterization of this metastatic progression series using RNA sequence analyses (GSE#115255) revealed mRNA expression of TGM2 is higher in HME2-BM (4.038717) than in HME2-Post TGF- β cells (1.695798) or HME2 cells (1.260098). Consistent with our RNA sequence analyses, qRT-PCR and immunoblot analyses confirmed increased TGM2 mRNA and protein levels in HME2-BM cells (Figure 4.1A-4.1B). In addition, HME2 cells can form primary tumors in mice but they are incapable of metastases. We have previously demonstrated an association between FN expression and decreased patient survival[27]. Since TGM2 is known to crosslink FN in the extracellular matrix and induce tissue fibrosis[28–31], we analyzed survival time in patients expressing both TGM2 and FN using Kaplan Meier plot[32]. Patients in high FN and TGM2 expression group demonstrate decreased survival rate compared to those patients in the low expression group (Figure 4.1C-4.1D). These data clearly indicate that high expression of TGM2 and FN is strongly associated with decreased patient survival.

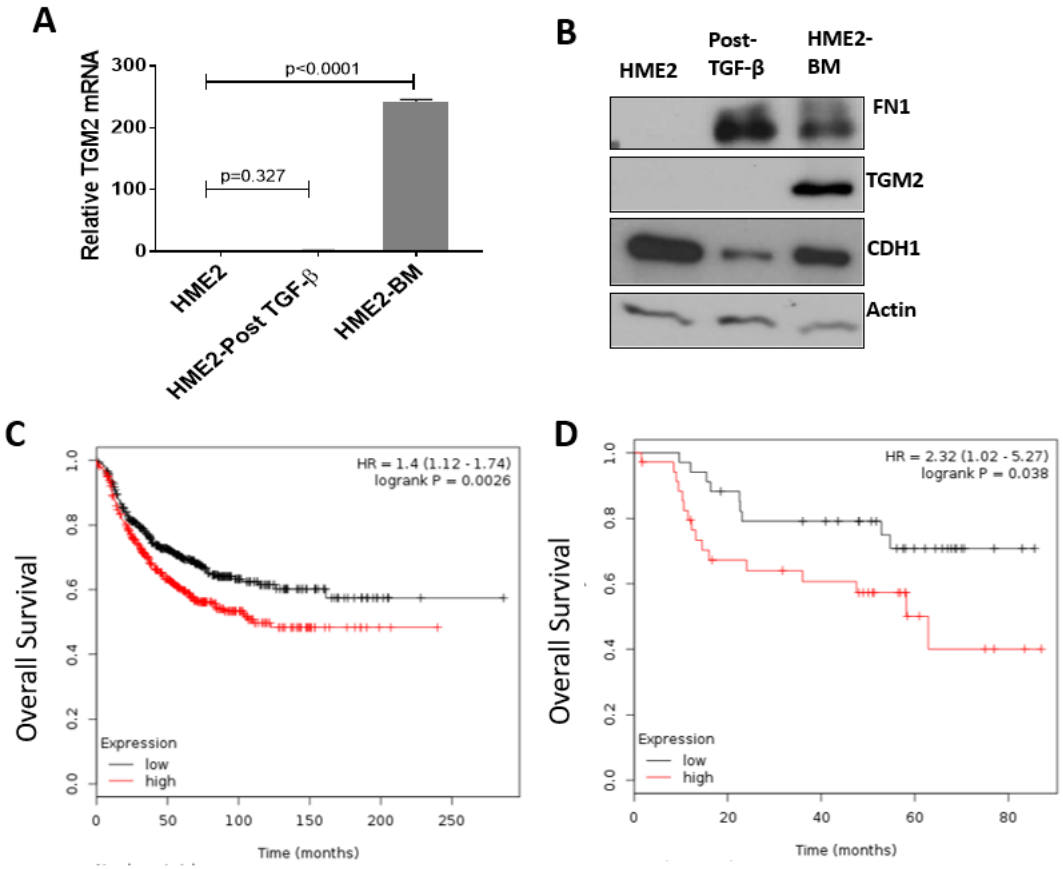

Figure 4.1: TGM2 expression is associated with decreased patient survival.

(A) Transcript levels for *TGM2* in HME2, HME2-Post TGF-β and HME2-BM were quantified using qRT-PCR relative to HME2 cells. (B) Immunoblot analyses for TGM2, FN1, and CDH1 in HME2, HME2-Post TGF-β and HME2-BM cells. Expression of β-tubulin served as a loading control. (C) Comparison of overall survival curve between patients (grade 3 tumor samples) expressing higher levels of both TGM2 and FN1 and those expressing low levels using Kaplan-Meier plot. (D) Comparison of overall survival curve between grade 3 HER2 positive patients (grade 3 tumor samples) expressing higher levels of both TGM2 and FN1 and those expressing low levels using Kaplan-Meier plot.

4.3.2 Depletion of TGM2 inhibits breast cancer metastasis and promote survival

To determine if TGM2 is important for breast cancer metastasis, we depleted TGM2 in HME2-BM cells (Figure 4.2A) and engrafted HME2-BM MT (control) or HME2-BM shTGM2 cells onto the mammary fat pad of immunocompetent NRG mice (Figure 4.2B). Depletion of TGM2 had minimal effect on primary tumor growth but inhibited lung metastasis and promoted metastasis-free survival (Figure 4.2C-H). Since we observed metastasis in both HME2-BM and shTGM2 groups, we isolated these metastatic cells from lymph node and cultured them *ex vivo*. The metastatic cells isolated from lymph nodes (HME2-BM MT Lym mets and HME2-BM shTGM2 Lym mets) express higher TGM2 and FN1 compared to the original (HME2-BM MT and HME2-BM shTGM2 respectively) cells and are highly heterogenous in nature as determined by immunoblot and CD44/24 flow cytometric analysis (Figure 4.2I-J). To further strengthen our conclusions, we overexpressed TGM2 in HME2 cells (Figure 4.3A) and performed similar *in vivo* experiments. Indeed, overexpression of TGM2 in HME2 cells promoted primary tumor growth and metastasis (Figure 4.3B-H). To extend these observations to different breast cancer models, we deleted TGM2 using a CRISPR mediated gene editing approach in highly metastatic 4T1 murine breast cancer cells (Figure 4.4A). Consistent with our previous results, deletion of TGM2 hindered efficient growth of 4T1 in a complaint 3D culture environment (Figure 4.4B and 4.5A). Deletion of TGM2 further inhibited primary tumor growth and overall metastasis (Figure 4.4C-G and 4.5B). These results imply TGM2 is required and sufficient for breast cancer metastasis and its expression increases with secondary metastasis along with the increase in FN expression.

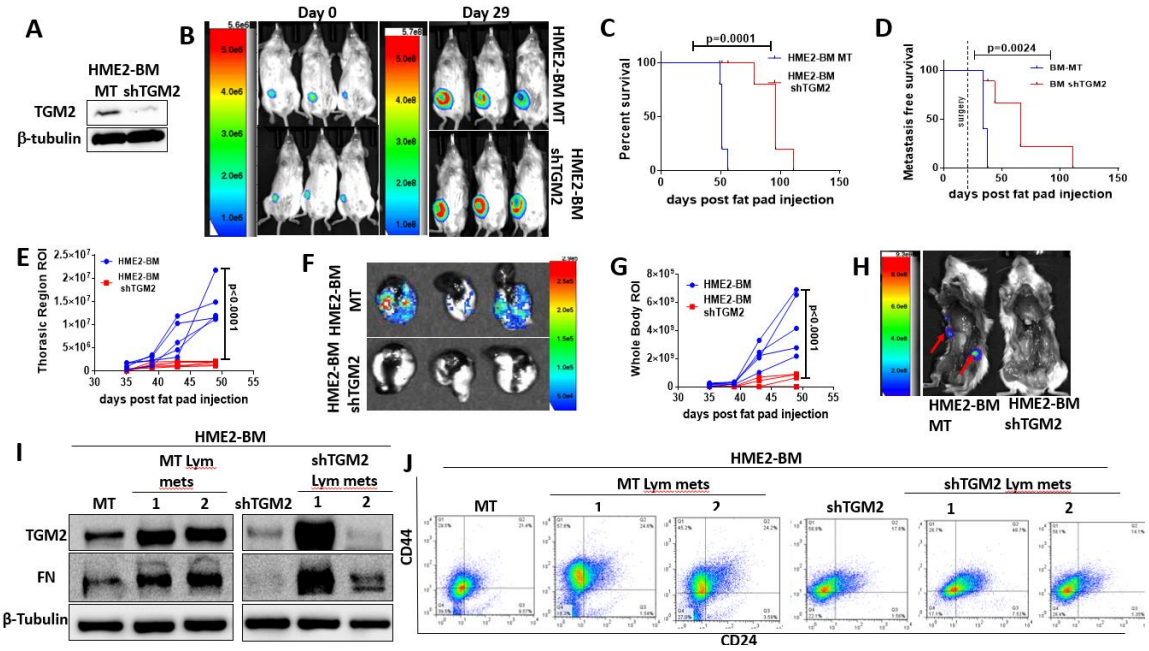

Figure 4.2: Depletion of TGM2 inhibits breast cancer metastasis and promotes survival.

(A) Immunoblot analyses for TGM2 depleted HME2-BM cells. (B) HME2-BM MT and HME2-shTGM2 were engrafted onto the mammary fat pad of two separate groups of mice. Bioluminescent images were taken immediately after engraftment (Day 0) and 29 days later (Day 29). (C) Comparison of overall survival between HME2-BM MT and HME2-BM shTGM2 tumor-bearing mice. (D) Comparison of metastasis-free survival between HME2-BM MT and HME2-BM shTGM2 tumor-bearing mice. (E and G) Bioluminescent intensity (Radiance) measurements of a thoracic and whole-body region of control (MT) or shTGM2-depleted (shTGM2) HME2-BM tumor-bearing mice. (F and H) Primary mammary tumors were removed 32 days after engraftment and lungs and whole mouse bioluminescence at day 39 was used to quantify metastatic recurrence. (I) Immunoblot analyses of whole cell lysates of lymph node metastatic cells obtained from HME2-BM MT and HME2-BM shTGM2 and their respective controls for TGM2 and FN1. β-Tubulin was used as a loading control. (J) Lymph node metastatic cells were analyzed by flow cytometry for cell surface expression of CD44 and CD24.

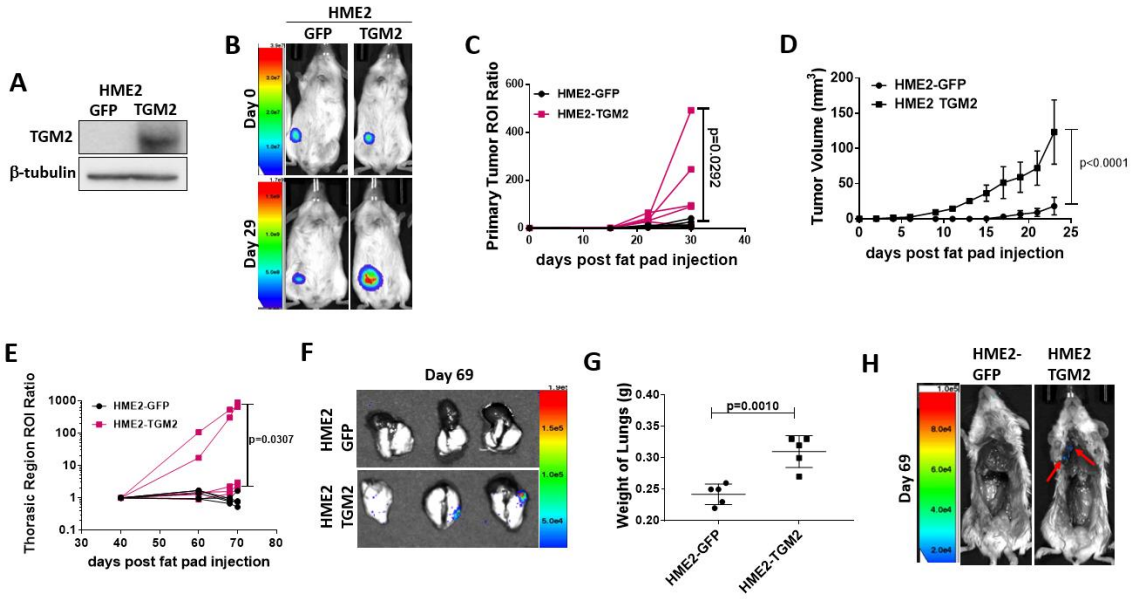

Figure 4.3: Overexpression of TGM2 promotes primary tumor growth and breast cancer metastasis.

(A) Immunoblot analyses of TGM2 overexpressed in HME2 cells. (B) HME2 cells were engrafted onto the mammary fat pad via an intraductal inoculation and primary tumor growth was measured by bioluminescent intensity (Radiance) measurements at the indicated time points. (C-D) Primary tumor growth of control (GFP) or TGM2-overexpressed (TGM2) HME2 tumor-bearing mice was quantified by bioluminescence and caliper measurements (E) Bioluminescent intensity (Radiance) measurements of thoracic of control (GFP) or TGM2-overexpressed (TGM2) HME2 tumor-bearing mice. (Data are presented as the natural log (LN) of the bioluminescent radiance for each mouse (n=5 mice per group), resulting in the indicated P value. (G) Control (GFP) and TGM2 expressing HME2 cells were engrafted onto the mammary fat pad and lungs were removed and weighed after mice were sacrificed at Day 69. (F and H) lungs and whole mouse bioluminescence at day 69 were used to quantify metastatic recurrence.

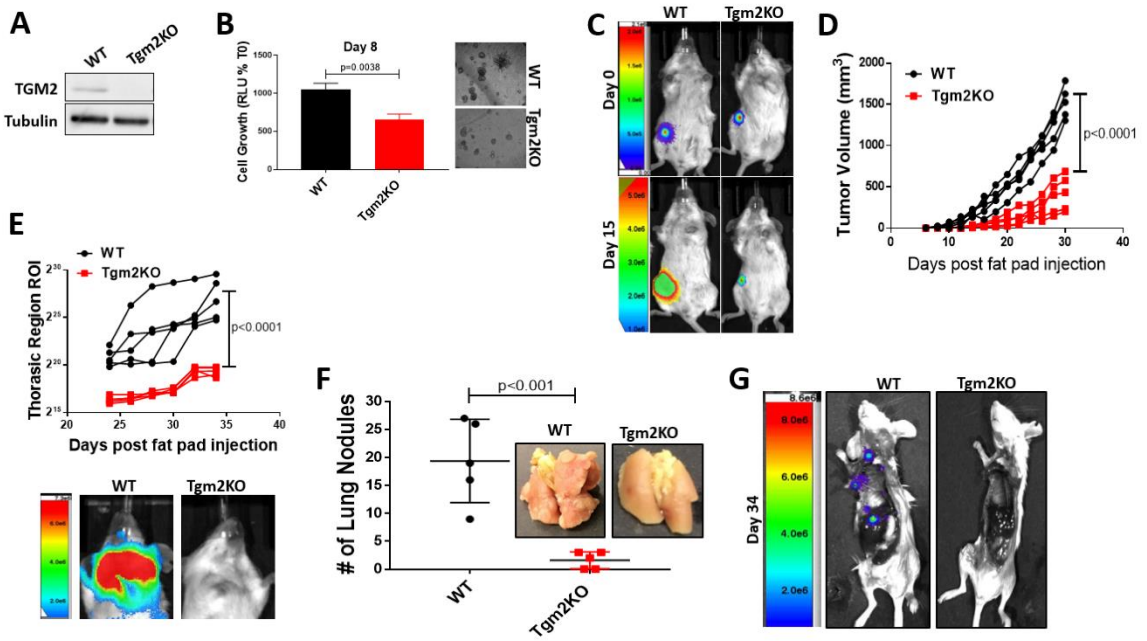

Figure 4.4: Deletion of TGM2 inhibits 3D growth and overall metastasis in 4T1.

(A) Genetic knockout of Tgm2 (Tgm2KO) in the 4T1 cells was verified by immunoblot. (B) Control (WT) and Tgm2KO 4T1 cells were grown under single cell 3D culture conditions. Longitudinal cellular outgrowth was quantified by bioluminescence at Day 8. Data are normalized to the plated values and are the mean ±SD of three independent analyses resulting in the indicated P-value. (C and D) Control (WT) and Tgm2KO 4T1 cells were engrafted onto the mammary fat pad and primary tumor growth was quantified by bioluminescence and caliper measurements. Data are normalized to the injected values. (E) Quantification of bioluminescent radiance from the pulmonary region at the indicated time points and bioluminescent images of lungs from control 4T1 (WT) tumor-bearing mice and those bearing Tgm2KO tumors. (F) Upon necropsy, the numbers of pulmonary metastatic nodules were quantified the corresponding gross anatomical views of lungs from control 4T1 (WT) tumor-bearing mice and Tgm2KO 4T1 tumor-bearing mice. (G) The lungs of mice injected with control (WT) and Tgm2 deleted (Tgm2KO) 4T1 cells were removed upon necropsy and the carcasses were immediately imaged. Shown are representative images from each group. For panels D, E, and F, data are the mean ±SE of 5 mice resulting in the indicated P values.

.

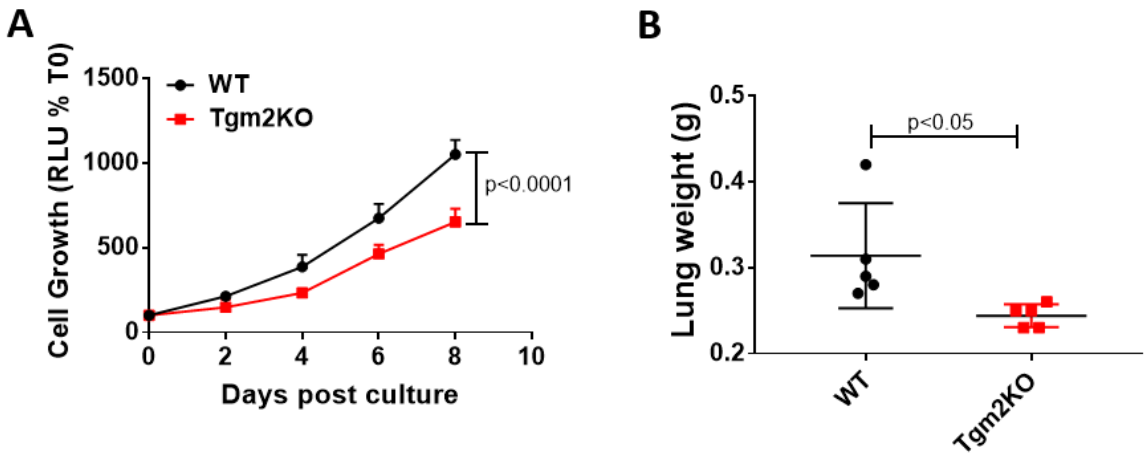

Figure 4.5: Deletion of TGM2 inhibits 3D growth in 4T1

(A) Control (WT) and Tgm2KO 4T1 cells were grown under single cell 3D culture conditions. Longitudinal cellular outgrowth was quantified by bioluminescence at the indicated time points. Data are normalized to the plated values and are the mean ±SD of three independent analyses resulting in the indicated P-value. (B) Control (WT) and Tgm2 deleted 4T1 cells were engrafted onto the mammary fat pad and lungs were removed and weighed after mice were sacrificed at Day 34

4.3.3 Tissue transglutaminase 2 is important for FN fibril formation on the surface of exosomes

Cancer cells can transform neighboring primary cells through the delivery of microvesicles containing TGM2 crosslinked FN[33]. TGM2 is known to exist in exosomes and promote cellular processes important for cancer cells growth and survival[34–36]. We, therefore, analyzed TGM2 and FN expression in both exosomes and whole cell lysates (WCL) derived from non-metastatic and metastatic breast cancer cells (Figure 4.6A-4.7A-B). Consistent with our previous results, FN dimers existed only in exosomes isolated from metastatic breast cancer cells (Figure 4.6A). Further, FN dimers were absent in WCL obtained from both non-metastatic and metastatic cells (Figure 4.7A).

Genetic depletion of TGM2 or pharmacological inhibition of TGM2 by NC9 inhibited FN dimer formation while overexpression of TGM2 promoted dimerization of FN in exosomes (Figure 4.6A and 4.7C). These results imply TGM2 is crucial for the formation of FN dimers in exosomes. FN dimers are important for the formation of FN fibrils. FN is functional only in its fibrillar form. Recently, we demonstrated that mesenchymal cells producing functionalized FN fibrils promote EMT and growth of metastatic competent epithelial cells[37]. Therefore, we hypothesize that FN exists in the fibrillar form on the surface of exosomes. Immuno-electron micrographs and confocal microscopy images confirmed the presence of FN fibrils on the surface of exosomes (Figure 4.6B - 4.6C). Further, FN fibrillogenesis is dependent on the TGM2 expression in exosomes (Figure 4.6B-4.6D). Taken together, these data indicate FN is assembled into FN fibrils on the surface of exosomes and formation of FN fibrils is dependent on TGM2 crosslinking activity.

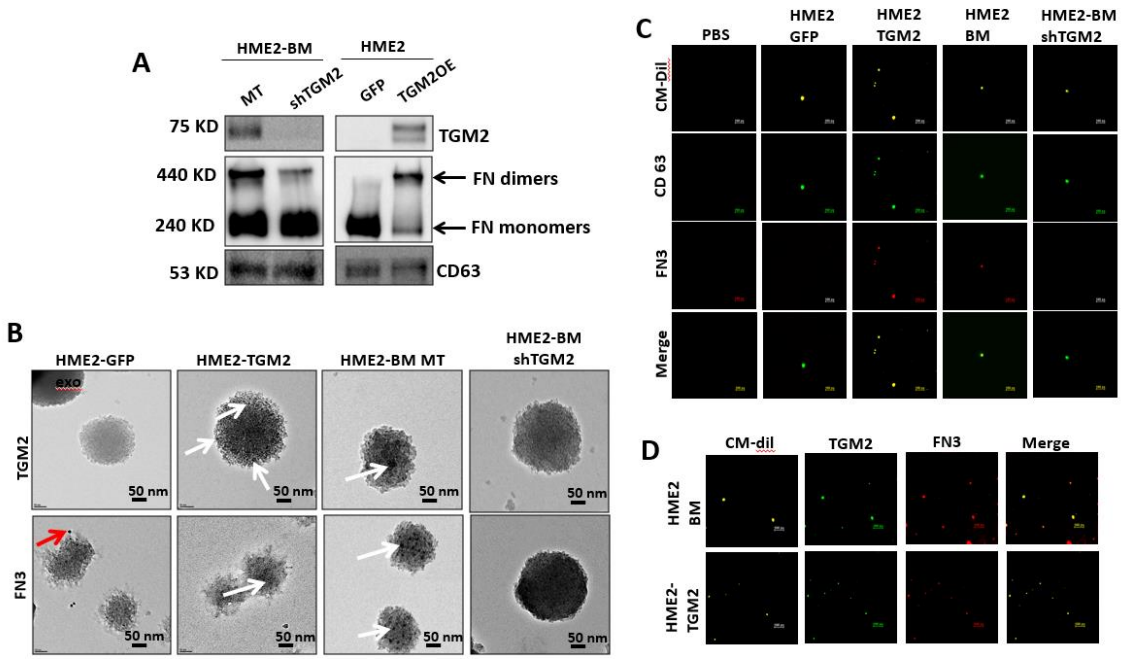

Figure 4.6: TGM2 is important for FN fibril formation on the surface of exosomes.

(A) Immunoblot analysis of exosomes derived from HME2-GFP, HME2-TGM2, HME2-BM MT or HME2-BM shTGM2 for TGM2 and FN. CD63 served as a loading control. (B) Immuno-electron micrographs of exosomes derived from HME2-GFP, HME2-TGM2, HME2-BM MT or HME2-BM shTGM2. White arrows point to black dots on exosomes indicating TGM2 and FN fibrils detected by TGM2 and FN3 antibody respectively. Red arrow points to black dots suggesting non-specific binding. (C) Exosomes derived from HME2-GFP, HME2-TGM2, HME2-BM MT or HME2-BM shTGM2 were stained with CM-Dil (yellow), CD63 (green) and FN3 (red) and imaged using confocal microscope. Merge displays overlay of green (CD63) and red (FN3) channels.A blank control sample, a confocal image of Alexa Fluor 488, Alexa Fluor 647 and CM-Dil. Scale bar is 500 nm. (D) Exosomes derived from HME2-BM MT or HME2-TGM2 cells were stained with CM-Dil (yellow), TGM2 (green) and FN3 (red) and imaged using a confocal microscope. Merge displays overlay of green (TGM2) and red (FN3) channels. Blank control sample, confocal image of Alexa Fluor 488, Alexa Fluor 647 and CM-Dil dye.

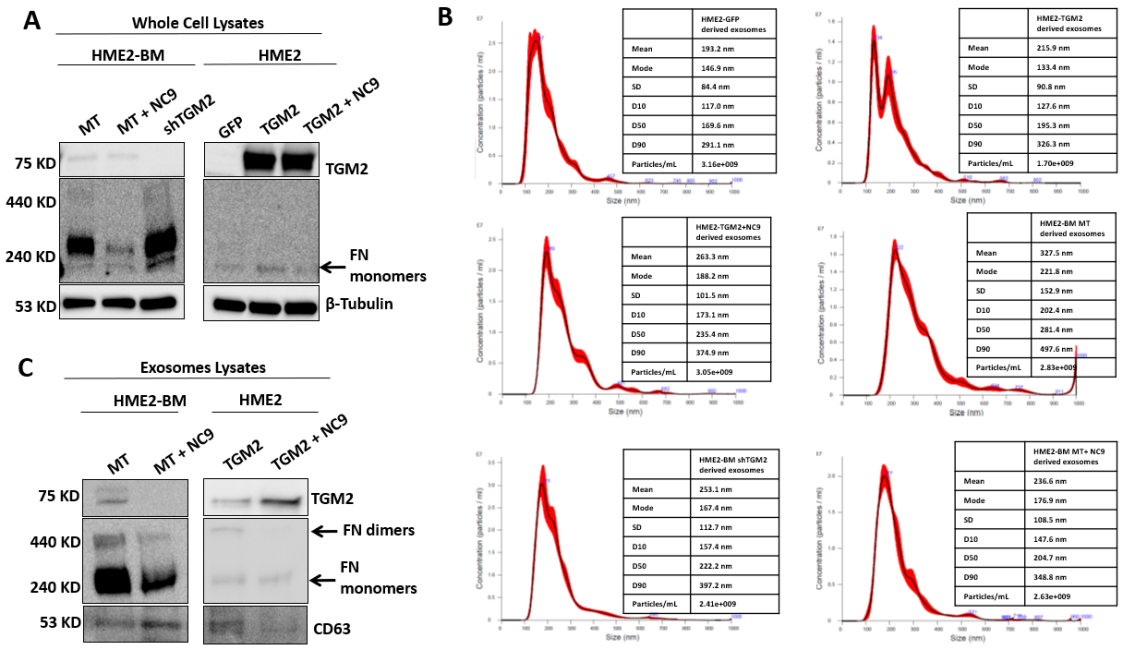

Figure 4.7: NC9 inhibits FN dimerization in exosomes.

(A) Immunoblot analysis of whole cell lysates derived from HME2-BM MT, HME2-BM shTGM2, HME2-BM MT treated with NC9, HME2-GFP, HME2-TGM2 and HME2-TGM2 treated with NC9 for TGM2 and FN1. β-Tubulin served as a loading control. (B) Nanosight analysis of exosomes derived from HME2-BM MT, HME2-BM shTGM2, HME2-BM MT treated with NC9, HME2-GFP, HME2-TGM2 and HME2-TGM2 treated with NC9. (C) Immunoblot analysis of exosomes derived from HME2-BM MT, HME2-BM MT treated with NC9, HME2-TGM2, and HME2-TGM2 treated with NC9 for TGM2 and FN1. CD63 served as a loading control.

4.3.4 Metastatic breast cancer cells derived exosomes promote pre-metastatic niche formation

Since we observed metastasis in breast cancer cells expressing TGM2, we reasoned these cells may secret exosomes containing TGM2 to establish a pre-metastatic niche and promote distant metastasis. To test our hypothesis, we developed a novel 3D culture assay to mimic *in vivo* conditions[37]. We cultured human pulmonary fibroblasts (HPF) on the tessellated scaffolds described in chapter 3 to allow fibrillar structure formation that recapitulates *in vivo* pulmonary microenvironment (Figure 4.8A). Human pulmonary fibroblasts were treated with indicated exosomes for 3 weeks. Indeed, HPF cells treated with exosomes eexpressing TGM2 promoted Ca1a FF growth both in 3D and 2D culture conditions (Figure 4.8B and 4.9A-4.9C). To confirm metastatic breast cancer cells derived exosomes promote pre-metastatic niche formation, NSG mice were given intraperitoneal injections of indicated exosomes for 3 weeks. These mice were then given tail vein injections of Ca1a cells. Consistent with our *in vitro* 3D culture results, only mice injected with HME2-BM MT exosomes supported faster growth of Ca1a cells in lungs (Figure 4.8C-E and 4.9D-E). Altogether, these results suggest exosomes containing TGM2 reprogram pulmonary fibroblasts cells to form pre-metastatic formation and promote pulmonary metastasis.

4.3.5 Tissue transglutaminase 2 promotes functionalized FN fibrils formation through upregulation of TNS1

Tensin 1 (TNS1) plays an important role in FN fibrillogenesis and ECM remodeling[38–40]. It is also essential for tissue fibrosis, an important process linked to cancer [38]. So, we decided to analyze TNS1 expression in metastatic breast cancer cells derived

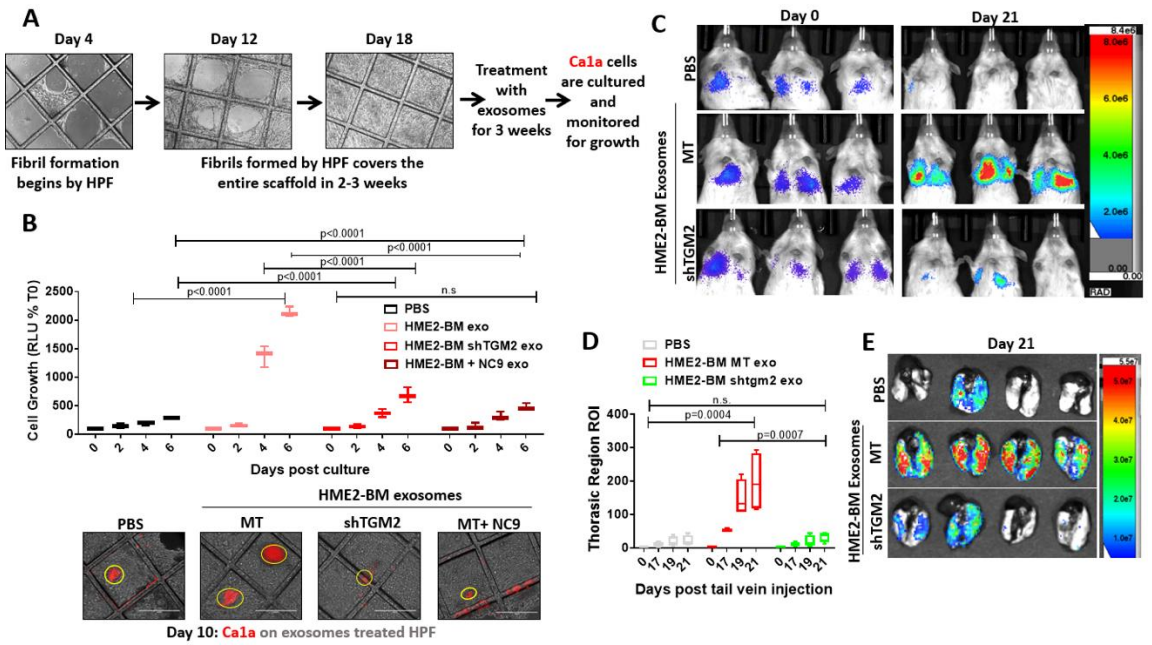

Figure 4.8: Metastatic breast cancer cells derived exosomes promote pre-metastatic niche formation.

(A) Schematic illustration of the development of 3D scaffold assay. HPF cells were cultured on 3D scaffolds as described in methods and allowed to form fibrils throughout the scaffolds. After 2-3 weeks, HPF cells were treated with indicated exosomes for 3 weeks and Ca1a FF dTomato were cultured on these scaffolds. (B) Growth of Ca1a FF dTomato cells was quantified by bioluminescence at indicated time points. Data are the mean arbitrary luminescence units (ALU) (±SE) for three independent experiments completed in triplicate resulting in the indicated P value. Red colored spots indicate growth of Ca1a on grey colored (HPF) background. (C) Mice were pretreated with indicated exosomes for 3 weeks prior to tail vein injection of Ca1a FF cells. Bioluminescent images of representative mice taken immediately (Day 0) and 21 days (Day 21) following tail vein injection of Ca1a FF cells. (D) The mean (±SE) pulmonary bioluminescence values normalized to the injected values (n=4 mice in each group were quantified at the indicated time points, resulting in the indicated P value. (E) Mice were sacrificed at day 21 and lungs were imaged using bioluminescence to quantify metastatic recurrence.

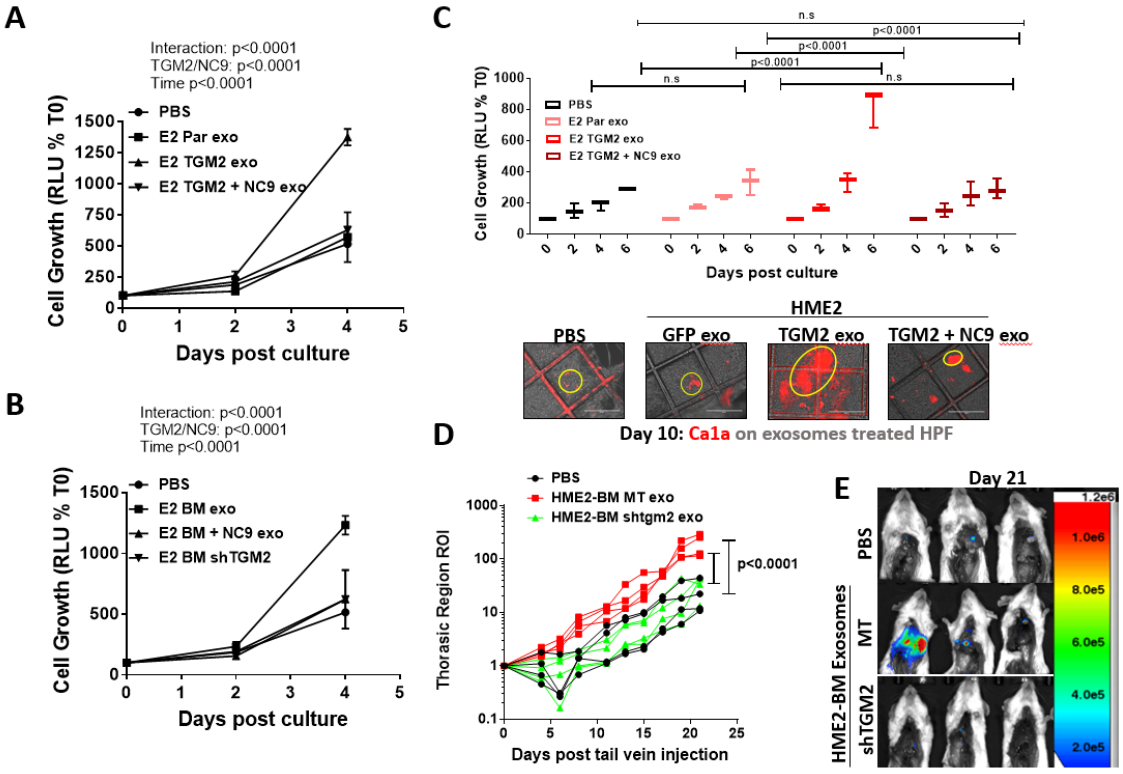

Figure 4.9: Metastatic breast cancer cells derived exosomes promote Ca1a's growth *in vitro* and pulmonary tumor formation *in vivo*.

(A, B) HPF cells were cultured in 96 well plates as described in methods and treated with indicated exosomes for 3 weeks. Ca1a FF dTomato were cultured on HPF and growth of Ca1a FF dTomato cells was quantified by bioluminescence at the indicated time points. Data are the mean arbitrary luminescence units (ALU) (±SE) for three independent experiments completed in triplicate resulting in the indicated P value. (C) HPF cultured on 3D scaffolds were treated with indicated exosomes for another 3 weeks and Ca1a FF dTomato were cultured on these scaffolds. The growth of Ca1a FF dTomato cells was quantified by bioluminescence at the indicated time points. Data are the mean arbitrary luminescence units (ALU) (±SE) for three independent experiments completed in triplicate resulting in the indicated P value. Red colored spots indicate growth of Ca1a on grey colored (HPF) background. (D) The mean (±SE) pulmonary bioluminescence values normalized to the injected values (n=4 mice in each group were quantified at the indicated time points, resulting in the indicated P value. (E) Mice were sacrificed at day 21 and the whole body was imaged using bioluminescence to quantify metastatic recurrence.

exosomes. Deletion of TGM2 inhibited TNS1 expression, FN dimerization and fibrils formation on the surface of exosomes derived from 4T1 cells (Figure 4.10A and 4.10C and 4.11A). However, FN expression remained unaffected in 4T1 Tgm2KO WCL (Figure 4.11B). Further, depletion of TGM2 in other breast cancer cells resulted in reduced TNS1 expression in both whole cell and exosomes lysates (Figure 4.11C-4.11H). In addition, overexpression of TGM2 in HMLE cells increased expression of TNS1 in WCL and FN dimers in exosomes (Figure 4.11E and 4.11H). Next, to confirm the role of TNS1 in FN fibrillogenesis, we depleted TNS1 using lentiviral approach (Figure 4.10B). Depletion of TNS1 increased TGM2 expression in WCL but decreased secretion of TGM2 and formation of FN dimers in exosome lysates. Depletion of TNS1 further inhibited FN fibrillogenesis on the surface of exosomes (Figure 4.10C-D). This result implies TNS1 is important for TGM2 secretion in exosomes and remodeling of FN dimers into fibrils on the surface of exosomes. Also, HPF treated with 4T1 WT exosomes promoted Ca1a's growth while exosomes lacking either TNS1 or TGM2 were unable to support Ca1a's growth; indicative of the role of FN fibrils present on the surface of exosomes (Figure 4.10E). To further determine the role of TNS1 in breast cancer metastasis, we performed 3D growth and 4T1 metastasis assay. Depletion of TNS1 inhibited branching structure formation in 3D culture and growth of 4T1 in both 2D and 3D environment (Fig 4.10F and 4.11 I). Even though 4T1 shTns1 cells showed similar primary tumor growth rate to control 4T1 cells (Figure 4.10G and 4.11J), lung metastasis was significantly inhibited in 4T1 shTns1 tumor-bearing mice as shown in Figure 4.10H-4.10I. Taken together, these findings imply TNS1 assembles FN dimers (crosslinked by TGM2) into fibrils on the the surface of exosome to establish intercellular communication and promote distant metastasis.

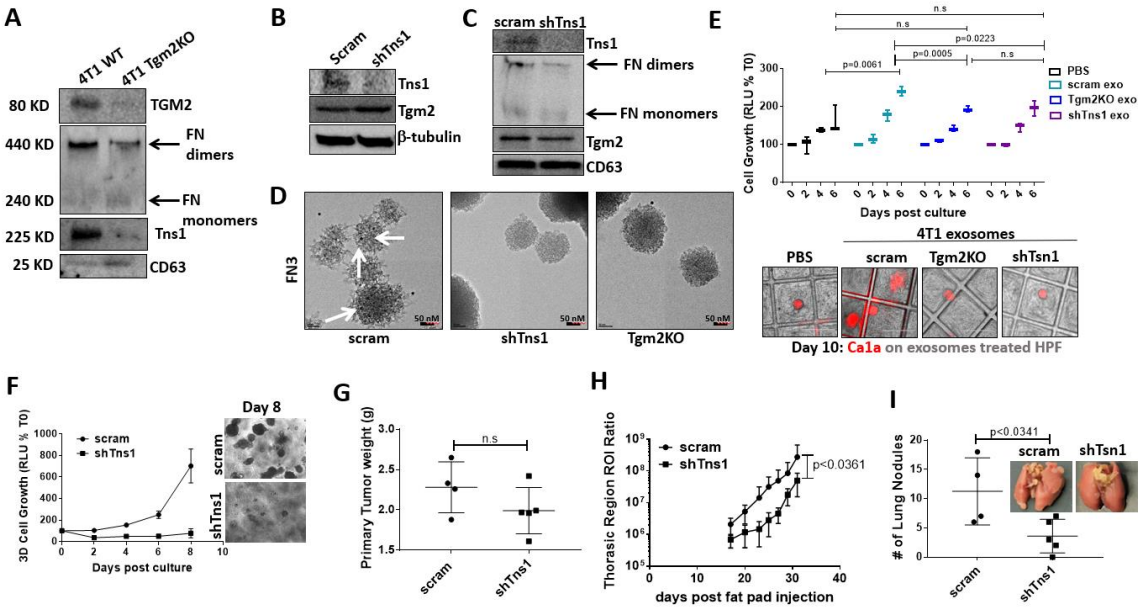

Figure 4.10: TNS1 is required for assembly of FN fibrils on the surface of exosomes and 4T1 metastasis.

(A) Immunoblot analysis of exosomes derived from 4T1 WT and 4T1 Tgm2KO for TGM2, FN1, and TNS1. CD63 served as a loading control. (B) Immunoblot analysis of whole cell lysates derived from 4T1 scram and Tns1 depleted 4T1 for TNS1, TGM2. β-Tubulin served as a loading control. (C) Immunoblot analysis of exosomes derived from 4T1 WT and 4T1 shTns1 for TNS1, TGM2, and FN1. CD63 served as a loading control. (D) Immuno-electron micrographs of exosomes derived from 4T1 WT, 4T1 shTns1, and Tgm2KO. White arrows point to black dots on exosomes indicating FN fibrils as detected by TGM2 and FN3 antibody respectively. (E) HPF cultured on 3D scaffolds for 3 weeks were treated with indicated exosomes for another 3 weeks and Ca1a FF dTomato were cultured on these scaffolds. The growth of Ca1a FF dTomato cells was quantified by bioluminescence at the indicated time points. Data are the mean arbitrary luminescence units (ALU) (±SE) for three independent experiments completed in triplicate resulting in the indicated P value. Red colored spots indicate growth of Ca1a on grey colored (HPF) background. (F) Control (scram) and shTns1 4T1 cells were grown under single cell 3D culture conditions. Longitudinal cellular outgrowth was quantified by bioluminescence at Day 8. Data are normalized to the plated values and are the mean ±SD of three independent analyses resulting in the indicated P-value. (G) Control (scram) and shTns1 4T1 cells were engrafted onto the mammary fat pad and primary tumors were removed and weighed after mice were sacrificed at Day 31. (H) Quantification of bioluminescent radiance from the pulmonary region at the indicated time points and bioluminescent images of lungs from control 4T1 scram tumor-bearing mice and those bearing shTns1 tumors. (I) Upon necropsy, the numbers of pulmonary metastatic nodules were quantified. (Inset) Corresponding gross anatomical views of lungs from control 4T1 (scram) tumor-bearing mice and 4T1 shTns1 tumor-bearing mice.

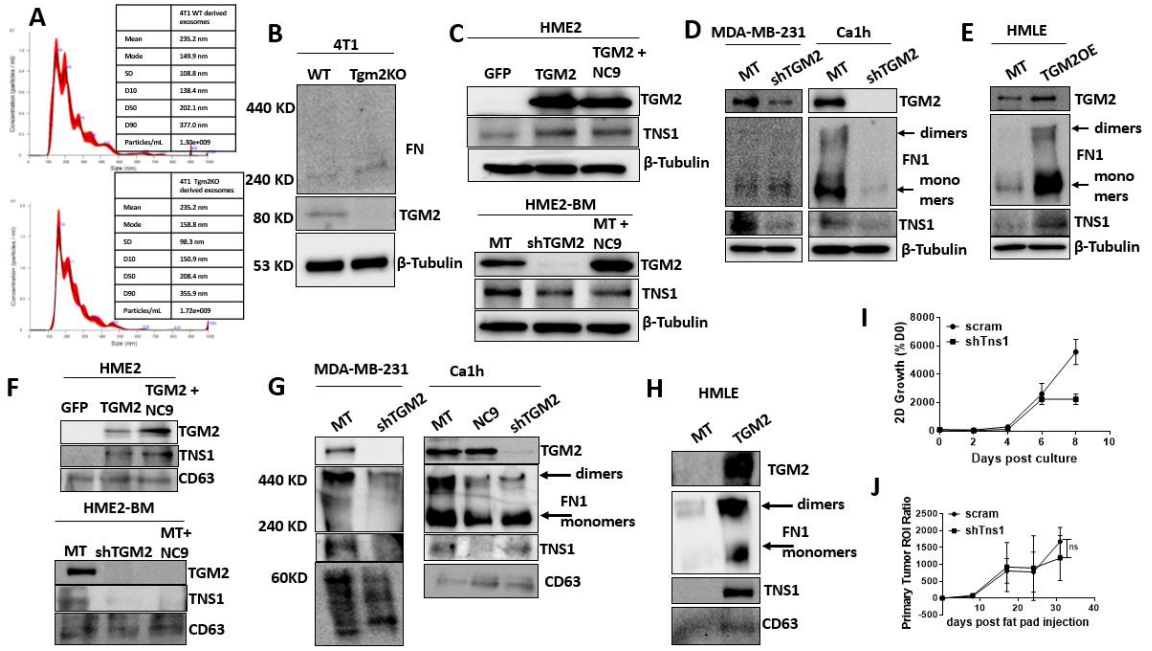

Figure 4.11: Inhibition of TGM2 downregulates TNS1.

(A) Nanosight analysis of exosomes derived control (WT) and Tgm2KO 4T1 cells. (B) Immunoblot analysis of whole cell lysates derived from control (WT) and Tgm2KO 4T1 cells for TGM2 and FN1. (C) Immunoblot analysis of whole cell lysates derived from HME2-BM MT, HME2-BM shTGM2, HME2-BM MT treated with NC9, HME2-GFP, HME2-TGM2 and HME2-TGM2 treated with NC9 for TGM2, FN1, and TNS1. (D) Immunoblot analysis of whole cell lysates derived from control (MT) and TGM2 depleted MDA-MB-231or Ca1h cells for TGM2, FN1, and TNS1. (E) Immunoblot analysis of whole cell lysates derived from control (MT) and TGM2 expressing HMLE cells for TGM2, FN1, and TNS1. β-Tubulin served as a loading control for whole cell lysates. (F) Immunoblot analysis of exosomes derived from HME2-BM MT, HME2-BM shTGM2, HME2-BM MT treated with NC9, HME2-GFP, HME2-TGM2 and HME2-TGM2 treated with NC9 for TGM2, FN1, and TNS1. (G) Immunoblot analysis of exosomes derived from control (MT) and TGM2 depleted MDA-MB-231or Ca1h cells and Ca1h MT cells treated with NC9 for TGM2, FN1, and TNS1. (H) Immunoblot analysis of exosomes derived from control (MT) and TGM2 expressing HMLE cells for TGM2, FN1, and TNS1. CD63 served as a loading control for exosomes lysates. (I) Control (scram) and shTns1 4T1 cells were grown in traditional 2D culture condition and growth were quantified by bioluminescence at indicated time points. Data are normalized to the plated values and are the mean ±SD of three independent analyses resulting in the indicated P-value. (J) Bioluminescent intensity (Radiance) measurements of primary tumor of control (scram) or TNS1 depleted (shTns1) 4T1 tumor-bearing mice.

4.4 Discussion

Cancer cell-derived exosomes are involved in the development of the premetastatic niche to support metastasis[19]. Since exosomes derived from cancer cells contain multiple biologically active molecules including proteins, nucleic acids, and lipids, they can alter local stroma to support disease associated microenvironment[2]. Studies suggest both FN and TGM2 are present in exosomes derived from breast cancer cells[33]. Further, FN exists in the dimeric form in these vesicles. The formation of FN dimers is essential for the generation of FN fibrils[42], the functional form of FN. Recently, our group established fibrillar FN is capable of inducing EMT in metastatic competent breast cancer cells and cells expressing intracellular FN acts in stromal fashion to support metastases of these cells through the formation of FN-containing cellular fibrils[37]. Whether exosomes express fibrillar FN to promote construction of premetastatic niche is unknown. In this study, we report exosomes derived from metastatic breast cancer cells exhibit fibrillar FN on their surface to foster metastases of breast cancer cells.

In recent years, several studies have investigated the role of TGM2 and FN in tumor progression and therapeutic resistance in different cancer types[43–47]. Nevertheless, there are few studies reporting the exact role of TGM2 and FN in breast cancer metastasis[48–50]. In this work, we observed patients with higher expression of TGM2 and FN have a lower survival rate than those with lower expression of TGM2 and FN. In addition, RNA sequence and immunoblot analysis of non-metastatic HME2 and metastatic HME2-BM cells revealed high TGM2 and FN expression in HME2-BM cells compared to those in HME2 cells. This implies TGM2 and FN functioning together to drive tumor progression. Our metastasis assays also confirmed only breast cancer cells expressing TGM2 can form distant metastases. Also, HME2-TGM2 primary tumors grew faster compared to HME2

GFP (control) tumors. In order to determine the metastases capacity of these cells, HME2-GFP primary tumors were allowed to grow to the same size as HME2-TGM2 primary tumors before they were removed surgically. Still, HME2 GFP (control) cells were incapable of forming secondary tumors. These data imply the expression of TGM2 is enough to promote breast cancer metastasis.

Tumor cells secrete exosomes that act as key players in establishing intercellular communication[2,51,52]. Intravenous injection of exosomes derived from melanoma cells can exit the circulation and localize in general melanoma metastatic sites to encourage the development of premetastatic niche in these organs[12]. Kuffer cells upon uptake of exosomes derived from highly metastatic pancreatic ductal adenocarcinomas (PDACs) exhibit increase FN production and foster a fibrotic environment to promote liver metastases[9]. Our data are consistent with such findings as mice pretreated with exosomes consisting TGM2 can support faster pulmonary tumor growth of breast cancer cells than mice pretreated with PBS (control) or exosomes lacking TGM2. These results suggest metastatic breast cancer cells secrete exosomes containing TGM2 to establish intercellular communication with distant organs to prime them for metastases.

Tissue transglutaminase 2 can crosslink FN into dimers that are crucial for FN fibrillogenesis. Both TGM2 and FN are known to exist in extracellular vesicles and that FN is crosslinked into dimers by TGM2[33]. Indeed, we observed FN dimers in exosomes isolated from breast cancer cells expressing TGM2. We also observed FN exist in the fibrillar form on the surface of exosomes derived from metastatic breast cancer cells. Formation of both FN dimers and fibrils are dependent on TGM2 expression. Moreover, expression of tensin 1, a cytoplasmic protein essential for FN fibrillogenesis[39,40,56], is also

dependent on the expression of TGM2. Depletion of TNS1 or TGM2 in 4T1 cells inhibited FN fibrillogenesis on the surface of exosomes. Depletion of TNS1 alone downregulated expression of TGM2 and FN dimers in exosomes. In addition, HPF pretreated with exosomes lacking TGM2 or TNS1 were unable to support the growth of metastatic breast cancer cells *in vitro*. These results suggest TGM2 crosslinks FN into dimers, which are assembled into functionalized fibrils by TNS1 on the surface of exosomes. Thus, we demonstrate TGM2 promotes FN fibrillogenesis on the surface of exosomes by upregulating TNS1 expression and reprograms HPF to support the growth of breast cancer cells. Whether TGM2 regulates TNS1 transcriptionally is currently under investigation in our lab. Further studies are necessary to determine how TGM2 upregulates TNS1 and other proteins associated with cellular adhesions and migration to promote breast cancer metastasis.

4.5 Conclusions

Taken together, our findings reveal a novel mechanism through which metastatic breast cancer cells derived exosomes foster the creation of a premetastatic niche and promote metastasis of breast cancer cells (Figure 4.12). These exosomes express functionalized FN fibrils crosslinked by TNS1, a TGM2 dependent process, on their surface. Further, TGM2 is enough to transform non-metastatic breast cancer cells into metastatic breast cancer cells. In addition, NC9 can potentially inhibit TGM2 crosslinking activity and curb interactions of TGM2 with FN; therefore, NC9 could be utilized as a potent TGM2 inhibitor to inhibit breast cancer metastasis.

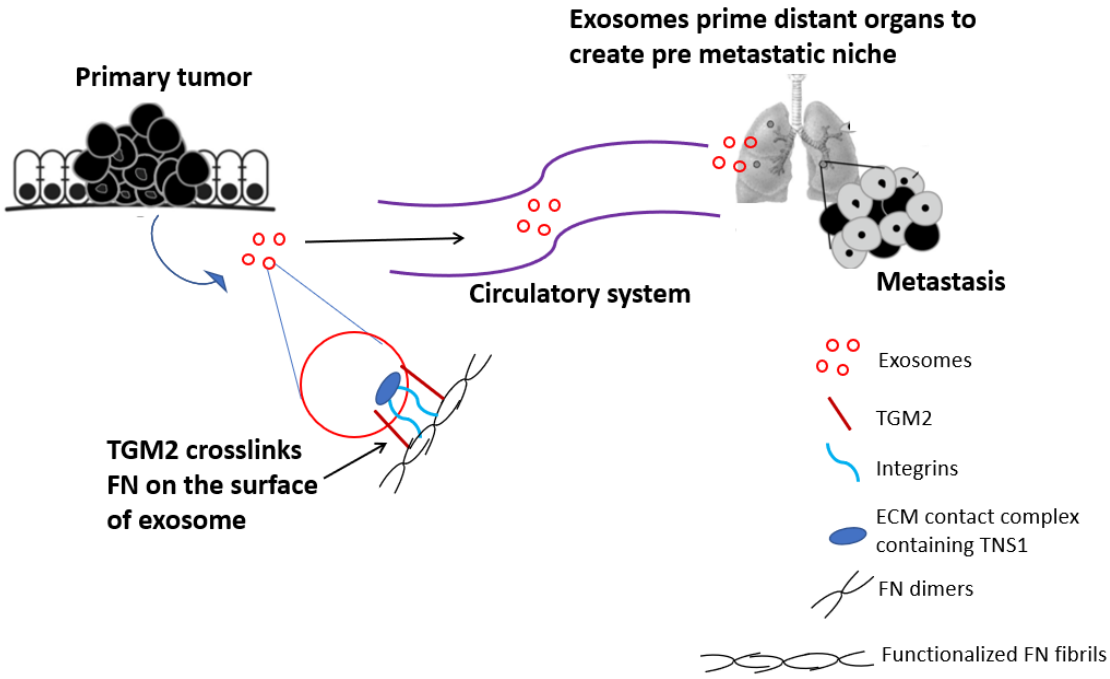

Figure 4.12: Model describing the mechanism through which TGM2 on exosomes promotes metastasis of breast cancer cells

4.6 References

1. Alderton, G. K. Metastasis: Exosomes drive premetastatic niche formation. *Nature Reviews Cancer* (2012). doi:10.1038/nrc3304
2. Milane, L., Singh, A., Mattheolabakis, G., Suresh, M. & Amiji, M. M. Exosome mediated communication within the tumor microenvironment. *J. Control. Release* (2015). doi:10.1016/j.jconrel.2015.06.029
3. Zhang, H., Garcia-Santos, G., Peinado, H. & Lyden, D. C. Microenvironmental regulation of metastasis by exosomes. in *Emerging Concepts of Tumor Exosome-Mediated Cell-Cell Communication* (2013). doi:10.1007/978-1-4614-3697-3_9
4. Liu, Y. *et al.* Tumor Exosomal RNAs Promote Lung Pre-metastatic Niche Formation by Activating Alveolar Epithelial TLR3 to Recruit Neutrophils. *Cancer Cell* (2016). doi:10.1016/j.ccell.2016.06.021
5. Zhang, Y. & Wang, X. F. A niche role for cancer exosomes in metastasis. *Nature Cell Biology* (2015). doi:10.1038/ncb3181
6. Greening, D. W., Gopal, S. K., Xu, R., Simpson, R. J. & Chen, W. Exosomes and their roles in immune regulation and cancer. *Seminars in Cell and Developmental Biology* (2015). doi:10.1016/j.semcdb.2015.02.009
7. Bobrie, A. & Théry, C. Exosomes and communication between tumours and the immune system: are all exosomes equal? *Biochem. Soc. Trans.* (2013). doi:10.1042/BST20120245
8. Simons, M. & Raposo, G. Exosomes - vesicular carriers for intercellular communication. *Current Opinion in Cell Biology* (2009). doi:10.1016/j.ceb.2009.03.007
9. Costa-Silva, B. *et al.* Pancreatic cancer exosomes initiate pre-metastatic niche formation in the liver. *Nat. Cell Biol.* (2015). doi:10.1038/ncb3169
10. Zhang, H. *et al.* Exosome-delivered EGFR regulates liver microenvironment to promote gastric cancer liver metastasis. *Nat. Commun.* (2017). doi:10.1038/ncomms15016
11. J., K. & T., L. Exosomes derived from carcinoma-associated fibroblasts induce premetastatic niche formation in lung. *J. Extracell. Vesicles* (2017). doi:10.1080/20013078.2017.1310414

12. Peinado, H. *et al.* Melanoma exosomes educate bone marrow progenitor cells toward a pro-metastatic phenotype through MET. *Nat. Med.* (2012). doi:10.1038/nm.2753
13. Yu, Z. *et al.* Pancreatic cancer-derived exosomes promote tumor metastasis and liver pre-metastatic niche formation. *Oncotarget* (2017). doi:10.18632/oncotarget.18831
14. Colombo, M., Raposo, G. & Théry, C. Biogenesis, Secretion, and Intercellular Interactions of Exosomes and Other Extracellular Vesicles. *Annu. Rev. Cell Dev. Biol.* (2014). doi:10.1146/annurev-cellbio-101512-122326
15. Stoorvogel, W., Kleijmeer, M. J., Geuze, H. J. & Raposo, G. The biogenesis and functions of exosomes. *Traffic* (2002). doi:10.1034/j.1600-0854.2002.30502.x
16. Cocucci, E. & Meldolesi, J. Ectosomes and exosomes: Shedding the confusion between extracellular vesicles. *Trends in Cell Biology* (2015). doi:10.1016/j.tcb.2015.01.004
17. Fevrier, B. *et al.* Cells release prions in association with exosomes. *Proc. Natl. Acad. Sci.* (2004). doi:10.1073/pnas.0308413101
18. Gross, J. C., Chaudhary, V., Bartscherer, K. & Boutros, M. Active Wnt proteins are secreted on exosomes. *Nat. Cell Biol.* (2012). doi:10.1038/ncb2574
19. Whiteside, T. L. Tumor-Derived Exosomes and Their Role in Cancer Progression. in *Advances in Clinical Chemistry* (2016). doi:10.1016/bs.acc.2015.12.005
20. Minciacchi, V. R., Freeman, M. R. & Di Vizio, D. Extracellular Vesicles in Cancer: Exosomes, Microvesicles and the Emerging Role of Large Oncosomes. *Seminars in Cell and Developmental Biology* (2015). doi:10.1016/j.semcdb.2015.02.010
21. Lyden, D. Exosomes: Tumor-derived exosomes promote pre-metastatic niche formation and organotropism. *SABCS* (2013).
22. Li, K., Chen, Y., Li, A., Tan, C. & Liu, X. Exosomes play roles in sequential processes of tumor metastasis. *International Journal of Cancer* (2018). doi:10.1002/ijc.31774
23. Yan, W. *et al.* Cancer-cell-secreted exosomal miR-105 promotes tumour growth through the MYC-dependent metabolic reprogramming of stromal cells. *Nat. Cell Biol.* (2018). doi:10.1038/s41556-018-0083-6

24. Chivet, M. *et al.* Exosomes secreted by cortical neurons upon glutamatergic synapse activation specifically interact with neurons. *J. Extracell. Vesicles* (2014). doi:10.3402/jev.v3.24722
25. Horibe, S., Tanahashi, T., Kawauchi, S., Murakami, Y. & Rikitake, Y. Mechanism of recipient cell-dependent differences in exosome uptake. *BMC Cancer* (2018). doi:10.1186/s12885-017-3958-1
26. Kamerkar, S. *et al.* Exosomes facilitate therapeutic targeting of oncogenic KRAS in pancreatic cancer. *Nature* (2017). doi:10.1038/nature22341
27. Balanis, N. *et al.* Epithelial to mesenchymal transition promotes breast cancer progression via a fibronectin-dependent STAT3 signaling pathway. *J. Biol. Chem.* (2013). doi:10.1074/jbc.M113.475277
28. Olsen, K. C. *et al.* Transglutaminase 2 and its role in pulmonary fibrosis. *Am. J. Respir. Crit. Care Med.* (2011). doi:10.1164/rccm.201101-0013OC
29. Maiuri, L. *et al.* Tissue Transglutaminase Activation Modulates Inflammation in Cystic Fibrosis via PPAR Down-Regulation. *J. Immunol.* (2008). doi:10.4049/jimmunol.180.11.7697
30. Cardoso, I. *et al.* Dissecting the interaction between transglutaminase 2 and fibronectin. *Amino Acids* (2017). doi:10.1007/s00726-016-2296-y
31. Collighan, R. J. & Griffin, M. Transglutaminase 2 cross-linking of matrix proteins: Biological significance and medical applications. *Amino Acids* (2009). doi:10.1007/s00726-008-0190-y
32. Győrffy, B. *et al.* An online survival analysis tool to rapidly assess the effect of 22,277 genes on breast cancer prognosis using microarray data of 1,809 patients. *Breast Cancer Research and Treatment* (2010). doi:10.1007/s10549-009-0674-9
33. Antonyak, M. A. *et al.* Cancer cell-derived microvesicles induce transformation by transferring tissue transglutaminase and fibronectin to recipient cells. *Proc. Natl. Acad. Sci.* (2011). doi:10.1073/pnas.1017667108
34. Diaz-Hidalgo, L. *et al.* Transglutaminase type 2-dependent selective recruitment of proteins into exosomes under stressful cellular conditions. *Biochim. Biophys. Acta - Mol. Cell Res.* (2016). doi:10.1016/j.bbamcr.2016.05.005

35. Zemskov, E. A., Mikhailenko, I., Hsia, R. C., Zaritskaya, L. & Belkin, A. M. Unconventional secretion of tissue transglutaminase involves phospholipid-dependent delivery into recycling endosomes. *PLoS One* (2011). doi:10.1371/journal.pone.0019414

36. Furini, G. *et al.* Proteomic Profiling Reveals the Transglutaminase-2 Externalization Pathway in Kidneys after Unilateral Ureteric Obstruction. *J. Am. Soc. Nephrol.* (2018). doi:10.1681/ASN.2017050479

37. Shinde, A. *et al.* Autocrine Fibronectin Inhibits Breast Cancer Metastasis. *Mol. Cancer Res.* (2018). doi:10.1177/159101991301900212

38. Bernau, K. *et al.* Tensin 1 is essential for myofibroblast differentiation and extracellular matrix formation. *Am. J. Respir. Cell Mol. Biol.* (2017). doi:10.1165/rcmb.2016-0104OC

39. Pankov, R. *et al.* Integrin dynamics and matrix assembly: Tensin-dependent translocation of α5β1 integrins promotes early fibronectin fibrillogenesis. *J. Cell Biol.* (2000). doi:10.1083/jcb.148.5.1075

40. Sottile, J. Fibronectin Polymerization Regulates the Composition and Stability of Extracellular Matrix Fibrils and Cell-Matrix Adhesions. *Mol. Biol. Cell* (2002). doi:10.1091/mbc.E02-01-0048

41. Hoshino, A. *et al.* Tumour exosome integrins determine organotropic metastasis. *Nature* (2015). doi:10.1038/nature15756

42. Schwarzbauer, J. E. & Sechler, J. L. Fibronectin fibrillogenesis: A paradigm for extracellular matrix assembly. *Current Opinion in Cell Biology* (1999). doi:10.1016/S0955-0674(99)00017-4

43. Nurminskaya, M. V. & Belkin, A. M. Cellular Functions of Tissue Transglutaminase. *Int. Rev. Cell Mol. Biol.* (2012). doi:10.1016/B978-0-12-394305-7.00001-X

44. Akar, U. *et al.* Tissue Transglutaminase Inhibits Autophagy in Pancreatic Cancer Cells. *Mol. Cancer Res.* (2007). doi:10.1158/1541-7786.MCR-06-0229

45. Tucholski, J., Lesort, M. & Johnson, G. V. W. Tissue transglutaminase is essential for neurite outgrowth in human neuroblastoma SH-SY5Y cells. *Neuroscience* (2001). doi:10.1016/S0306-4522(00)00482-6

46. Yuan, L. Tissue transglutaminase 2 inhibition promotes cell death and chemosensitivity in glioblastomas. *Mol. Cancer Ther.* (2005). doi:10.1158/1535-7163.MCT-04-0328

47. Oh, K., Moon, H.-G., Lee, D.-S. & Yoo, Y.-B. Tissue transglutaminase-interleukin-6 axis facilitates peritoneal tumor spreading and metastasis of human ovarian cancer cells. *Lab. Anim. Res.* (2015). doi:10.5625/lar.2015.31.4.188

48. Mangala, L. S., Fok, J. Y., Zorrilla-Calancha, I. R., Verma, A. & Mehta, K. Tissue transglutaminase expression promotes cell attachment, invasion and survival in breast cancer cells. *Oncogene* (2007). doi:10.1038/sj.onc.1210035

49. Oh, K. *et al.* Transglutaminase 2 facilitates the distant hematogenous metastasis of breast cancer by modulating interleukin-6 in cancer cells. *Breast Cancer Res.* (2011). doi:10.1186/bcr3034

50. Agnihotri, N., Kumar, S. & Mehta, K. Tissue transglutaminase as a central mediator in inflammation-induced progression of breast cancer. *Breast Cancer Research* (2012). doi:10.1186/bcr3371

51. Roma-Rodrigues, C., Fernandes, A. R. & Baptista, P. V. Exosome in tumour microenvironment: Overview of the crosstalk between normal and cancer cells. *BioMed Research International* (2014). doi:10.1155/2014/179486

52. Syn, N., Wang, L., Sethi, G., Thiery, J. P. & Goh, B. C. Exosome-Mediated Metastasis: From Epithelial-Mesenchymal Transition to Escape from Immunosurveillance. *Trends in Pharmacological Sciences* (2016). doi:10.1016/j.tips.2016.04.006

53. R Goulet, C. *et al.* Exosomes Induce Fibroblast Differentiation into Cancer-associated Fibroblasts through TGFβ Signaling. *Mol. Cancer Res.* (2018). doi:10.1158/1541-7786.MCR-17-0784

54. Chowdhury, R. *et al.* Cancer exosomes trigger mesenchymal stem cell differentiation into pro-angiogenic and pro-invasive myofibroblasts. *Oncotarget* (2015). doi:10.18632/oncotarget.2711

55. Webber, J., Steadman, R., Mason, M. D., Tabi, Z. & Clayton, A. Cancer exosomes trigger fibroblast to myofibroblast differentiation. *Cancer Res.* (2010). doi:10.1158/0008-5472.CAN-10-1722

56. McCleverty, C. J., Lin, D. C. & Liddington, R. C. Structure of the PTB domain of tensin1 and a model for its recruitment to fibrillar adhesions. *Protein Sci* (2007). doi:10.1110/ps.072798707

57. Howe, J. D. The Role of Tensin in Cell Migration and Fibronectin Fibrillogenesis. (2009)

58. Chen, H., Duncan, I. C., Bozorgchami, H. & Lo, S. H. Tensin1 and a previously undocumented family member, tensin2, positively regulate cell migration. *Proc Natl Acad Sci U S A* (2002). doi:10.1073/pnas.022518699

CHAPTER 5. GENERAL DISCUSSION AND FUTURE DIRECTIONS

The extracellular matrix (ECM) is enriched with various proteins and can support tissue structure, cell adhesion, cell-cell communication, and differentiation[1]. Several studies implicate the aberrant expression of ECM proteins in different cancers and their active participation in metastasis[2]. Once such matrix protein which is abnormally expressed in many cancers is FN. Fibronectin plays an essential role in various processes to maintain normal homeostasis. These processes include cell growth, differentiation, migration, wound healing and blood coagulation[3]. Altered expression of fibronectin in cancers is known to promote tumor growth, invasion, proliferation, migration, and resistance to therapy [4–9]. In many cancers, along with FN, its receptor α5β1 is also upregulated. For instance, FN and the extra domain (ED)-A (a splice variant of fibronectin) are linked to higher α5β1 levels in malignant as compared to normal breast epithelial cells[5]. Fibronectin also increases the invasion capacity of MDA-MB-231 cells cultured atop collagen hydrogels[4]. Furthermore, interactions of FN with syndecans (other receptors) increase cell adhesion and migration of MDA-MB-231 cells cultured on collagen and increase proliferation on FN matrices[10]. These studies imply the extracellular role of FN in breast cancer. However, there are still open questions regarding cancer cells that express FN—How do these cancer cells utilize fibronectin for their own survival? How do they support the growth of heterogenous tumors?

5.1 Role of intracellular FN in breast cancer metastasis

This dissertation is focused on the role of intracellular FN and exosomes expressing FN in breast cancer metastasis. In chapter 3, we demonstrated network formation of intracellular FN with actin cytoskeleton in mesenchymal cells. Mesenchymal cells expressing intracellular FN make functionalized FN fibrils to support the growth of metastatic competent cells. We also reported the ability of external functionalized FN to cause phosphorylation of STAT3, a β1 integrin-dependent process, to promote EMT in Ca1a cells. Whether or not FN requires STAT3 to drive EMT is unknown. In order to investigate the importance of STAT3 in FN driven EMT, STAT3 could be depleted in Ca1a cells using lentiviral approach and cultured on 3D scaffolds coated with FN. These scaffolds could be stained with phalloidin for actin cytoskeleton and E-cadherin to observe adherent junctions. Further, staining with p-FAK and p-Src antibodies will help investigate if functionalized FN activates FAK/Src/STAT3 pathway to promote EMT and migration. The above experiment could also be performed in the presence of stattic (a STAT3 inhibitor) to pharmacologically inhibit STAT3 phosphorylation and determine its effect on FN induced cell proliferation and EMT. Since FN also binds β3 integrin, it is beneficial to investigate the involvement of β3 integrin in FN driven EMT. This could be achieved by depleting β3 integrin in Ca1a cells using lentiviral approach. β3 integrin depleted Ca1a cells could be cultured on FN-coated 3D scaffolds to determine if they can undergo EMT. Alternatively, Ca1a cultured on FN-coated 3D scaffolds could be treated with cilengitide (β3-integrin activity inhibitor) and stained for E-cadherin. Overall, the above experiments will be useful in determining the mechanism through which intracellular and extracellular FN induce EMT in breast cancer cells.

Next, we demonstrated depletion of β1 integrin in Ca1a cells increases FN expression and enhances mesenchymal phenotype. Neither genetic nor pharmacological inhibition of β1 integrin in Ca1h cells induced MET and, therefore, no morphological changes were observed, implying the role of intracrine FN signaling (Chapter 3). Additional studies are required to understand how fibrillar FN drives mesenchymal cell morphology and how these events relate to more transcriptionally driven EMT events induced by drugs and cytokines.

Data presented in Chapter 3 is consistent with the fact that integrins are important for the secretion of FN, however, this process is under-investigated in epithelial-derived cells. β1 integrin is required for unconventional secretion of TGM2. In addition, TGM2 binds to β1 integrin in recycled endosomes prior to its secretion as a complex with β1 integrin[11]. TGM2 can bind to integrins and FN simultaneously to strengthen FN interactions with β1 integrin[2]. Therefore, depletion of β1 integrin can cause accumulation of TGM2 bound to FN inside the cell and increase expression of TGM2 and FN in cells. It is, therefore, crucial determining if depletion of β1 integrin or TGM2 inhibits FN secretion. To investigate the role of TGM2, we depleted TGM2 in Ca1h cells (Appendix Figure 1A-B). We did not observe MET or change in morphology of TGM2 depleted cells. However, both mRNA and protein expression were reduced in whole cell lysates of TGM2 depleted Ca1h cells. We overexpressed TGM2 in LAPR (lapatinib resistant HME2 cells) and BMAR (afatinib resistant HME2-BM cells) to study the effect of TGM2 on FN expression and cell morphology. Drug-resistant cells overexpressing TGM2 expressed FN dimers in whole cell lysates (Appendix Figure 1C) and exhibited a mesenchymal phenotype. This result implies TGM2 can crosslink FN intracellularly to foster mesenchymal morphology.

It would be further essential to determine if drug-resistant cells can form cellular FN fibrils on our 3D scaffold culture system to support the growth of breast cancer cells. This will help to gain insights into how chemotherapy, when not successful, can paradoxically promote tumor progression and metastasis[12,13].

Tensin 1(TNS1) is a cytoplasmic phosphoprotein located in integrin-mediated focal adhesion kinases and plays an important role in FN fibrillogenesis[14,15]. Tensin 1 is also required for fibronectin deposition and assembly by myofibroblast and human lung fibroblasts[16]. Given that TNS1 has an actin-binding domain and binds to actin during fibrillogenesis[17,18], it may foster FN interactions with the actin cytoskeleton and promote mesenchymal morphology. Therefore, it is important to investigate if TNS1 is responsible for the intracellular fibrillar organization of FN. To achieve the above goal, TNS1 could be depleted in mesenchymal breast cancer cells and examined for morphological change and their capacity to form FN fibrils.

Tensin 1 requires TGF-β receptor 1 to promote FN matrix deposition by myofibroblasts[16]. Transforming growth factor upregulates both FN and TGM2 expression during EMT to promote mesenchymal morphology[19–21]. Therefore, it would be also useful to determine if cells lacking TNS1 could undergo EMT in response to TGF-β treatment. To achieve this, cells lacking TNS1 could be treated with TGF-β and examined for morphological change and expression of mesenchymal markers. The above experiment will help establish the role of TNS1 in promoting FN driven mesenchymal morphology.

5.2 Application of 3D scaffold model

In addition to fostering our biological understanding of FN function and ECM-stimulated morphological changes, a major advance of the current study is the development

and implementation of our tessellated cell culture device. This novel 3D scaffold cell culture system is capable of accurately reiterating cellular and matrix phenotypes observed *in vivo*. In Chapter 3, we demonstrated WT Ca1h form fibrils across the empty spaces in the scaffolds. This novel 3D scaffold model could be further used to distinguish differences between EMT driven by cytokines and chemotherapeutics based on their fibrils forming capacity on uncoated 3D scaffolds. This would further help us to understand if cells that have undergone EMT in response to chronic drug treatment are capable of promoting growth and metastasis of metastatic competent epithelial cells.

Our 3D scaffold model can be used to understand how different matrix proteins induce resistance to chemotherapeutics in breast cancer cells. Our lab is mainly interested in investigating how FN is involved in drug resistance. Our unique 3D scaffolds can be utilized to gain better insights into interactions between cells and individual matrix proteins that are responsible for promoting drug resistance. For instance, we investigated the response of HME2-BM cells to different concentrations of neratinib (a HER2 kinase inhibitor) using the traditional approach (FN-coated 2D tissue culture (TC) plates) and FN-coated 3D scaffolds. We observed that HME2-BM cells cultured on FN-coated 3D scaffolds were more resistant to higher concentrations of neratinib (IC50= 442.5 nM) than those cultured on FN-coated 2D TC plates (IC50 65.28nM) or non-coated TC plates (Appendix Figure 2). The above experiment suggests FN existing in functionalized fibrillar structure can promote drug resistance. However, additional studies are required to understand the mechanism through which these fibrils promote resistance to chemotherapy.

5.3 Role of exosomes containing TGM2 in breast cancer metastasis

In Chapter 4, we reported exosomes derived from metastatic breast cancer cells containing FN fibrils modify HPF to promote the growth of Ca1a cells. Findings from our study also suggest exosomes derived from metastatic breast cancer cells promote Ca1a tumor formation in the lungs. According to previous studies, exosomes secreted by cancer cells can transform primary fibroblasts into cancer-associated fibroblasts through TGF-β1 signaling[22–24]. Hence, it is crucial investigating if depletion of TGM2 affects TGF-β1 expression in these exosomes. This may be achieved by detecting TGF-β1 levels in exosomes using Human TGF-β quantikine ELISA kit. It is possible that we may not detect a difference in TGF-β1 levels between exosomes derived from cells expressing TGM2 and those lacking TGM2. This result will indicate that TGF-β1 is acting upstream of TGM2 and therefore, requires TGM2 to exert its effect.

Previous studies imply that TGF-β1 driven EMT is dependent on the expression of TGM2 in mammary breast cancer cells[20,25]. Further, TGF-β1 upregulates TGM2 expression during EMT[20,25]. In order to determine if TGF-β1 is functional in exosomes expressing TGM2, exosomes derived from HME2-BM cells should be incubated with anti-TGF-β1 antibody and used to treat HPF cells cultured on 3D scaffolds. Following treatment with exosomes, the growth of Ca1a FF-dTomato cells cultured on these scaffolds could be tracked using bioluminescence. A global proteomic analysis of reprogrammed HPF cells may be performed to detect the modifications occurred in HPF following treatment with exosomes. In addition, global proteomic and RNA sequence analysis of exosomes derived from metastatic breast cancer cells can provide important information about the expression of other growth factors, ECM degrading enzymes, cytokines, and micro-RNAs that are regulated by TGM2 expression. Since cancer cells derived exosomes are known to alter

the immune response for their survival and growth[26–28], it is imperative to understand if TGM2 in exosomes is a factor in this phenomenon of immune evasion.

We also investigated if TGM2 is essential for biogenesis and secretion of exosomes under normal cell culture conditions. We did not observe a decrease in exosomes quantity, which indicated TGM2 does not affect the biogenesis of exosomes (data not shown). According to a recent study, TGM2 is released in exosomes derived from primary cells cultured under hypoxic or stressful conditions[29]. Given that TGM2 is a stress response gene, its expression may increase in cells cultured under stressful conditions like hypoxia, treatment with cytokines like TGF-β or chemotherapeutic drugs. Supporting this notion, 4T1 cells cultured in glutamine-free full growth media expressed higher TGM2 protein levels (Appendix Figure 3A). Furthermore, treatment of 4T1 cells with TGF-β1 or SYK inhibitor (R406) or both elevated TGM2 expression (Appendix Figure 3B). Treatment of 4T1 TGM2KO cells with TGF-β1 or SYK inhibitor (R406) or both induced stress (Appendix Figure 3C). Also, 4T1 TGM2KO cells treated with TGF-β1 failed to undergo EMT (Appendix Figure 3C). This ability of 4T1 cells to survive in a stressful environment may arise from exosomes with increased levels of TGM2. Further studies are required to understand the mechanism through which TGM2 is secreted in the exosome and the factors that drive TGM2 expression under stressful conditions.

In chapter 4, we demonstrated exosomes containing TGM2 promote pre-metastatic niche formation and support the pulmonary tumor growth of metastatic competent Ca1a cells *in vivo*. Given the role of TGM2 in crosslinking various matrix proteins specifically FN and collagen[30–32], exosomes expressing TGM2 may modify extracellular matrix to support the growth of breast cancer cells. Supporting this hypothesis, HPF pretreated with

exosomes expressing TGM2 promoted the growth of breast cancer cells (Chapter 4). Whereas, HPF cells pretreated with exosomes derived from breast cancer cells pretreated with NC9 were unable to promote the growth of Ca1a cells (Chapter 4). Future animal studies using NC9 could help to determine its efficacy *in vivo.* For instance, mice could be given intraperitoneal injections of exosomes expressing or lacking TGM2 or exosomes derived from cells treated with NC9. The lungs harvested from these mice could be analyzed for FN and collagen rearrangement using immunohistochemistry. The outcome of the above experiment will help to determine the underlying mechanisms of pre-metastatic niche formation by exosomes derived metastatic breast cancer cells. Further, it will also help us understand how breast cancer cells expressing TGM2 in exosomes are capable of metastasizing compared to those lacking TGM2 in exosomes.

5.4 Tissue transglutaminase 2 as a promising therapeutic target for breast cancer treatment

Tissue transglutaminase 2 has active participation in tumor progression, metastasis and resistance development to cancer therapeutics[33–35]. Its expression is highly upregulated in multiple cancer types, specifically those selected for resistance to chemotherapy and radiotherapy, and those acquired from metastatic sites[36–38]. In this dissertation, we establish that expression of TGM2 is adequate to transform non-metastatic breast cancer cells into malignant type (chapter 4). Our results also implicate TGM2 as an effective therapeutic target for the treatment of breast cancer metastasis.

To understand the role of TGM2 in driving EMT, we overexpressed TGM2 in primary mammary epithelial cells using lentiviral approach and generated HMLE-TGM2 cells (Appendix Figure 4A). HMLE-TGM2 cells cultured in HMLE media exhibited

epithelial morphology like HMLE MT (control) cells, whereas HMLE-TGM2 cells passaged in full growth media (DMEM + 10% FBS) underwent EMT and exhibited mesenchymal phenotype (Appendix Figure 4B-C). However, HMLE MT (control) cells were unable to survive in full growth media. In addition, HMLE-TGM2 cells cultured in full growth media can deposit fibrillar FN matrix like HPF cells and secrete soluble FN (Appendix Figure 5). The above findings imply TGM2 expression helps HMLE cells in surviving stressful conditions by promoting EMT and fibronectin matrix deposition. Next, to test the efficacy of NC9, we derived ECM from HMLE TGM2 cells treated with NC9 for 6 days. HMLE TGM2 cells treated with NC9 were incapable of depositing FN matrix (Appendix Figure 6). Although we didn't observe any changes in FN and TGM2 expression in whole cell lysates, both TGM2 and FN expressions were inhibited in extracellular matrix lysates. The above results indicate NC9 successfully inhibits TGM2 activity and FN matrix deposition.

Given the role of TGM2 in promoting drug resistance, it is important investigating if inhibition of TGM2 in drug-resistant breast cancer cells improves their sensitivity to chemotherapeutics. Previously our lab demonstrated HME2-Post TGF-β cells are resistant to HER2 kinase inhibitors including lapatinib. HME2-Post TGF-β cells express TGM2 and therefore, could be a good model to study mechanisms through which TGM2 promotes drug resistance in these cells. A possible experiment could be depleting TGM2 in HME2-Post TGF-β cells using lentiviral approach and testing their sensitivity to lapatinib and neratinib. *In vivo* drug combination experiments using NC9 and neratinib inhibitors could further help us determining if NC9 is able to sensitize HME2-Post TGF-β cells to neratinib and improve survival. Furthermore, the capacity of these inhibitors to promote metastasis

could be determined using bioluminescence. The outcomes of the above experiments will help to establish an effective treatment for metastatic breast cancer and develop a combination therapy to reduce breast cancer resistance to chemotherapeutics utilized in breast cancer therapy.

5.5 Summary and Significance

Breast cancer metastasis is one of the leading causes of death among women[39]. One of the important processes involved in tumor progression and metastasis is EMT. So, EMT is a promising target in cancer therapy. Epithelial-mesenchymal transition process can be targeted using different potential pharmacological strategies to inhibit or prevent metastasis; these strategies include preventing the initiation of EMT, eradicating the invasive mesenchymal cells and promoting dormancy by blocking MET. Recently we establish repurposing of fostamatinib, a clinically approved spleen tyrosine kinase inhibitor, as an effective treatment for the prevention of metastatic recurrence in breast cancer through maintenance of disseminated cells in an asymptomatic state of dormancy[40]. More broadly, our work highlights an exit from the traditional pharmacological goal of total tumor cell eradication and instead posits the concept of forced tumor dormancy for the management of stage IV breast cancer[40]. Still, extensive evaluation of these pharmaceuticals in combination with other therapies is essential to achieve successful inhibition or prevention of tumor progression and metastasis recurrence.

Epithelial-mesenchymal transition allows cancerous epithelial cells to acquire invasive and migratory properties and transform them into a mesenchymal phenotype that helps them in intravasation[41]. These mesenchymal cells are capable of secreting matrix proteins like fibronectin which has significant involvement in most steps of tumor

progression and metastasis[1]. Therefore, these mesenchymal proteins could be exploited as potential targets, which may provide a mechanism through which prevailing metastatic cancer cells could be eliminated in patients with a metastatic form of the disease. However, compounds that inhibit the mesenchymal state could also promote MET and, therefore may induce the formation of metastatic tumors. Therefore, in order to develop stage-particular anti-EMT inhibitors for more individualized cancer therapy, it is crucial to investigate more into the above approach for targeting EMT in cancer.

In this dissertation, we demonstrate non-metastatic breast cancer cells express intracellular FN that drives them into stable non-metastatic mesenchymal phenotype. In contrast to the tumor-promoting functions of FN within the ECM, our data imply autocrine fibronectin production inhibits the metastatic potential of mesenchymal tumor cells. The above findings suggest FN could be exploited as a potential target to prevent breast cancer metastasis. However, our study also demonstrates non-metastatic mesenchymal cells expressing FN act in stromal capacity to foster the metastasis of metastatic competent epithelial breast cancer cells. Further, these mesenchymal cells form functionalized FN fibrils to support the growth of these metastatic competent cells. Therefore, targeting other proteins along with fibronectin is important to prevent breast cancer metastasis. This may be achieved by targeting proteins that interact with FN to drive FN associated cell signaling pathways. Fibronectin primarily associates with integrins present on the cell surface to activate signaling pathways necessary for cancer cell survival. Integrins are present on the cell surface and can be easily blocked by pharmacological agents. Therefore, targeting integrins could offer a beneficial therapeutic approach in cancer therapy. Along with integrins, FN also binds to TGM2. Tissue transglutaminase 2 crosslinks FN in the

extracellular matrix and supports FN-integrin interactions. Further, including integrins and FN, TGM2 is also upregulated in many cancers specifically in metastatic tumors. Therefore, developing strategies to inhibit TGM2 or FN-TGM2 interactions might open a unique therapeutic window to treat patients in the late stage of cancer. But in order to target these proteins, more investigation is necessary to understand the mechanism through which they promote metastasis.

Prior to our work, the role played by TGM2 in breast cancer metastasis was ambiguous. Data attained in this dissertation have expanded this paradigm wherein inhibition of TGM2 is enough to inhibit breast cancer metastasis and prolong survival of HER2 transformed metastatic breast cancer model. Both FN and TGM2 are known to exist in exosomes, however, their role in metastatic breast cancer is poorly understood. Data shown here establish metastatic breast cancer cells secrete exosomes expressing functionalized FN fibrils crosslinked by TGM2 on their surface. Exosomes derived from metastatic breast cancer cells promote premetastatic niche formation in the lungs, a TGM2 dependent process, and support the tumor growth of breast cancer cells. Using an inhibitor of TGM2, we inhibit FN-TGM2 interactions and growth of breast cancer cells. Thus, through this dissertation, we successfully demonstrate TGM2 as a promising therapeutic target for the treatment of metastatic breast cancer. These insights will contribute to establishing new drugs to target TGM2 or FN-TGM2 interactions aimed at reducing breast cancer metastasis and breast cancer associated mortality.

5.6 References

1. Koulu, M., Penttinen, R., Jarvelainen, H., Wight, T. N. & Sainio, A. Extracellular Matrix Molecules: Potential Targets in Pharmacotherapy. *Pharmacol. Rev.* (2009). doi:10.1124/pr.109.001289
2. Wang, J. P. & Hielscher, A. Fibronectin: How its aberrant expression in tumors may improve therapeutic targeting. *Journal of Cancer* (2017). doi:10.7150/jca.16901
3. Pankov, R. Fibronectin at a glance. *J. Cell Sci.* (2002). doi:10.1242/jcs.00059
4. Mierke, C. T., Frey, B., Fellner, M., Herrmann, M. & Fabry, B. Integrin {alpha}5{beta}1 facilitates cancer cell invasion through enhanced contractile forces. *J Cell Sci* (2011). doi:10.1242/jcs.071985
5. Nam, J. M., Onodera, Y., Bissell, M. J. & Park, C. C. Breast cancer cells in three-dimensional culture display an enhanced radioresponse after coordinate targeting of integrin α5β1 and fibronectin. *Cancer Res.* (2010). doi:10.1158/0008-5472.CAN-09-2319
6. Lou, X. *et al.* SOX2 targets fibronectin 1 to promote cell migration and invasion in ovarian cancer: new molecular leads for therapeutic intervention. *OMICS* (2013). doi:10.1089/omi.2013.0058
7. Wei, P. L. *et al.* Nicotine enhances colon cancer cell migration by induction of fibronectin. *Ann. Surg. Oncol.* (2011). doi:10.1245/s10434-010-1504-3
8. Kenny, H. A. *et al.* Mesothelial cells promote early Ovarian cancer metastasis through fibronectin secretion. *J. Clin. Invest.* (2014). doi:10.1172/JCI74778
9. Knowles, L. M. *et al.* Integrin avb3 and fibronectin upregulate slug in cancer cells to promote clot invasion and metastasis. *Cancer Res.* (2013). doi:10.1158/0008-5472.CAN-13-0602
10. Huang, W., Chiquet-Ehrismann, R., Orend, G., Moyano, J. V. & Garcia-Pardo, A. Interference of tenascin-C with syndecan-4 binding to fibronectin blocks cell adhesion and stimulates tumor cell proliferation. *Cancer Res.* (2001).
11. Zemskov, E. A., Mikhailenko, I., Hsia, R. C., Zaritskaya, L. & Belkin, A. M. Unconventional secretion of tissue transglutaminase involves phospholipid-dependent delivery into recycling endosomes. *PLoS One* (2011). doi:10.1371/journal.pone.0019414

12. Keklikoglou, I. *et al.* Chemotherapy elicits pro-metastatic extracellular vesicles in breast cancer models. *Nat. Cell Biol.* (2019). doi:10.1038/s41556-018-0256-3
13. Karagiannis, G. S. *et al.* Neoadjuvant chemotherapy induces breast cancer metastasis through a TMEM-mediated mechanism. *Sci. Transl. Med.* (2017). doi:10.1126/scitranslmed.aan0026
14. Pankov, R. *et al.* Integrin dynamics and matrix assembly: Tensin-dependent translocation of α5β1 integrins promotes early fibronectin fibrillogenesis. *J. Cell Biol.* (2000). doi:10.1083/jcb.148.5.1075
15. McCleverty, C. J., Lin, D. C. & Liddington, R. C. Structure of the PTB domain of tensin1 and a model for its recruitment to fibrillar adhesions. *Protein Sci* (2007). doi:10.1110/ps.072798707
16. Bernau, K. *et al.* Tensin 1 is essential for myofibroblast differentiation and extracellular matrix formation. *Am. J. Respir. Cell Mol. Biol.* (2017). doi:10.1165/rcmb.2016-0104OC
17. Lo, S. H., Janmey, P. A., Hartwig, J. H. & Chen, L. B. Interactions of tensin with actin and identification of its three distinct actin-binding domains. *J. Cell Biol.* (1994). doi:10.1083/jcb.125.5.1067
18. Singh, P., Carraher, C. & Schwarzbauer, J. E. Assembly of Fibronectin Extracellular Matrix. *Annu. Rev. Cell Dev. Biol.* (2010). doi:10.1146/annurev-cellbio-100109-104020
19. Willis, B. C. & Borok, Z. TGF-β-induced EMT: mechanisms and implications for fibrotic lung disease. *Am. J. Physiol. Cell. Mol. Physiol.* (2007). doi:10.1152/ajplung.00163.2007
20. Fuchshofer, R., Birke, M., Welge-Lussen, U., Kook, D. & Lütjen-Drecoll, E. Transforming growth factor-β2 modulated extracellular matrix component expression in cultured human optic nerve head astrocytes. *Investig. Ophthalmol. Vis. Sci.* (2005). doi:10.1167/iovs.04-0649
21. Xu, J., Lamouille, S. & Derynck, R. TGF-B-induced epithelial to mesenchymal transition. *Cell Research* (2009). doi:10.1038/cr.2009.5

22. R Goulet, C. *et al.* Exosomes Induce Fibroblast Differentiation into Cancer-associated Fibroblasts through TGFβ Signaling. *Mol. Cancer Res.* (2018). doi:10.1158/1541-7786.MCR-17-0784
23. Webber, J., Steadman, R., Mason, M. D., Tabi, Z. & Clayton, A. Cancer exosomes trigger fibroblast to myofibroblast differentiation. *Cancer Res.* (2010). doi:10.1158/0008-5472.CAN-10-1722
24. Chowdhury, R. *et al.* Cancer exosomes trigger mesenchymal stem cell differentiation into pro-angiogenic and pro-invasive myofibroblasts. *Oncotarget* (2015). doi:10.18632/oncotarget.2711
25. Ayinde, O., Wang, Z. & Griffin, M. Tissue transglutaminase induces Epithelial-Mesenchymal-Transition and the acquisition of stem cell like characteristics in colorectal cancer cells. *Oncotarget* (2017). doi:10.18632/oncotarget.15370
26. Muller, L., Mitsuhashi, M., Simms, P., Gooding, W. E. & Whiteside, T. L. Tumor-derived exosomes regulate expression of immune function-related genes in human T cell subsets. *Sci. Rep.* (2016). doi:10.1038/srep20254
27. Bobrie, A. & Théry, C. Exosomes and communication between tumours and the immune system: are all exosomes equal? *Biochem. Soc. Trans.* (2013). doi:10.1042/BST20120245
28. Fanini, F. & Fabbri, M. Cancer-derived exosomic microRNAs shape the immune system within the tumor microenvironment: State of the art. *Seminars in Cell and Developmental Biology* (2017). doi:10.1016/j.semcdb.2016.12.004
29. Diaz-Hidalgo, L. *et al.* Transglutaminase type 2-dependent selective recruitment of proteins into exosomes under stressful cellular conditions. *Biochim. Biophys. Acta - Mol. Cell Res.* (2016). doi:10.1016/j.bbamcr.2016.05.005
30. Akimov, S. S. & Belkin, A. M. Cell-surface transglutaminase promotes fibronectin assembly via interaction with the gelatin-binding domain of fibronectin: a role in TGFbeta-dependent matrix deposition. *J. Cell Sci.* (2001).
31. Nurminskaya, M. V. & Belkin, A. M. Cellular Functions of Tissue Transglutaminase. *Int. Rev. Cell Mol. Biol.* (2012). doi:10.1016/B978-0-12-394305-7.00001-X

32. Akimov, S. S., Krylov, D., Fleischmana, L. F. & Belkin, A. M. Tissue transglutaminase is an integrin-binding adhesion coreceptor for fibronectin. *J. Cell Biol.* (2000). doi:10.1083/jcb.148.4.825

33. Huang, L., Xu, A. M. & Liu, W. Transglutaminase 2 in cancer. *Am. J. Cancer Res.* (2015).

34. Mehta, K., Kumar, A. & Kim, H. I. Transglutaminase 2: A multi-tasking protein in the complex circuitry of inflammation and cancer. *Biochemical Pharmacology* (2010). doi:10.1016/j.bcp.2010.06.029

35. Siegel, M. & Khosla, C. Transglutaminase 2 inhibitors and their therapeutic role in disease states. *Pharmacology and Therapeutics* (2007). doi:10.1016/j.pharmthera.2007.05.003

36. Agnihotri, N. & Mehta, K. Transglutaminase-2: evolution from pedestrian protein to a promising therapeutic target. *Amino Acids* (2017). doi:10.1007/s00726-016-2320-2

37. Budillon, A., Carbone, C. & Di Gennaro, E. Tissue transglutaminase: A new target to reverse cancer drug resistance. *Amino Acids* (2013). doi:10.1007/s00726-011-1167-9

38. Mehta, K., Fok, J., Miller, F. R., Koul, D. & Sahin, A. A. Prognostic significance of tissue transglutaminase in drug resistant and metastatic breast cancer. *Clin. Cancer Res.* (2004). doi:10.1158/1078-0432.CCR-04-1107

39. Breastcancer.org. U.S. Breast Cancer Statistics. *Web Page* (2018). doi:10.1080/14786437308217452

40. Shinde, A. *et al.* Spleen tyrosine kinase-mediated autophagy is required for epithelial-mesenchymal plasticity and metastasis in breast cancer. *Cancer Res.* (2019). doi:10.1158/0008-5472.CAN-18-2636

41. Gugnoni, M., Sancisi, V., Manzotti, G., Gandolfi, G. & Ciarrocchi, A. Autophagy and epithelial-mesenchymal transition: an intricate interplay in cancer. *Cell death & disease* (2016). doi:10.1038/cddis.2016.415

APPENDIX

Supplemental Figures

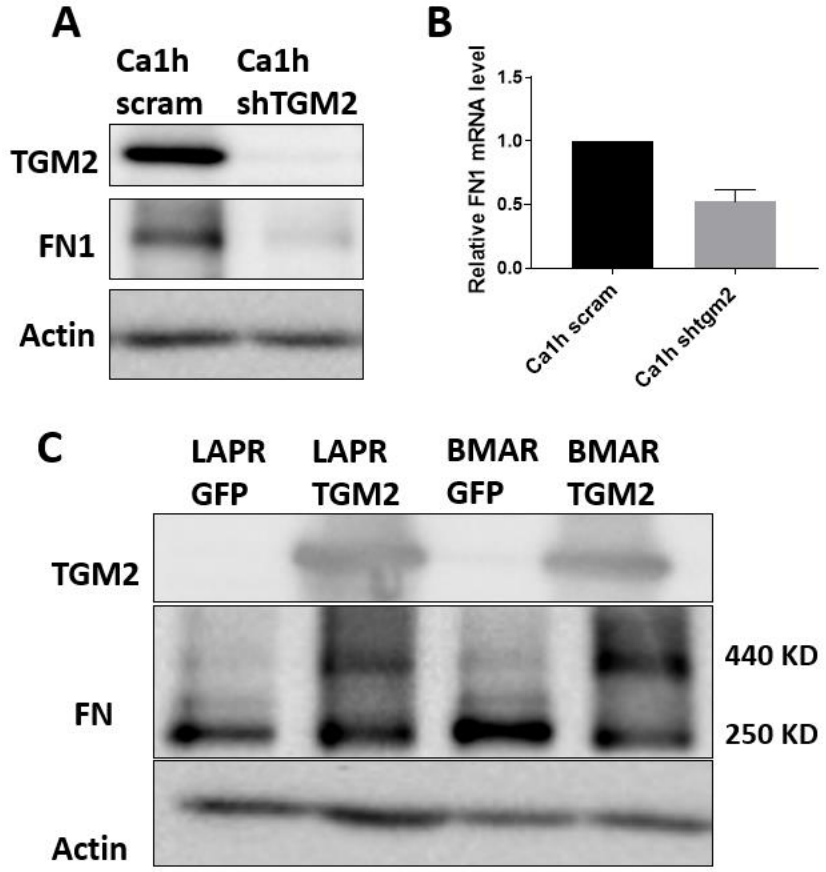

Appendix Figure 1: TGM2 drives FN expression in mesenchymal cells.

(A) Immunoblot analyses for TGM2 depletion and FN expression in Ca1h cells. Actin served as a loading control. (B) Transcript levels for tissue *FN1* in Ca1h shTGM2 cells were quantified using qRT-PCR relative to Ca1h scram (control) cells. (C) Immunoblot analysis of whole cell lysates derived from control (LPAR GFP and BMAR GFP), LPAR TGM2 and BMAR TGM2 cells for TGM2 overexpression and FN1 monomer and dimer expression.

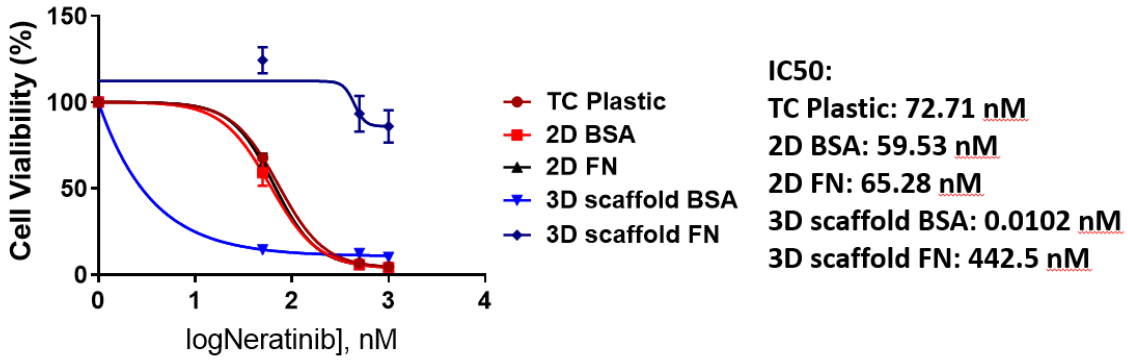

Appendix Figure 2: Functionalized FN fibrils promote neratinib resistance in HME2-BM cells.

HME2-BM were cultured on either non-coated tissue culture plates (TC plastic) or BSA or FN-coated 2D tissue culture plates (2D BSA or 2D FN) or 3D scaffolds coated with BSA or FN (3D scaffold BSA or 3D scaffold FN) in the presence of different concentrations of Neratinib (0 - 1000 nM) and cell viability was determined at day 4 using bioluminescence. Non-linear regression log(inhibitor) vs response-variable slope (four parameters) was used to analyze the IC50.

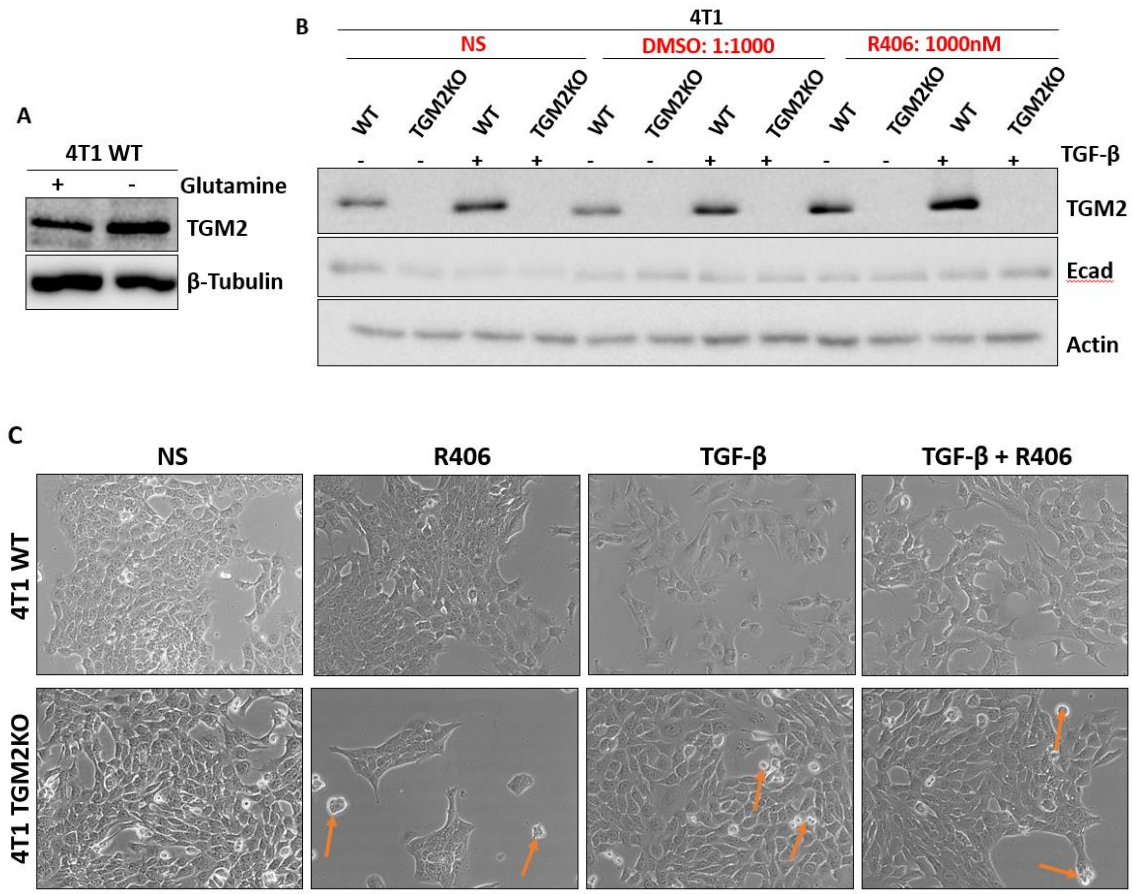

Appendix Figure 3: TGM2 expression increases in 4T1 WT cells in stressful conditions.

(A) 4T1 WT were cultured in full growth media with or without L-Glutamine for 8 days. (B) 4T1 WT or TGM2KO cells were treated with TGF- β1 for 8 days to induce EMT. NS or TGF- β1 treated cells were treated with R406 (1μM) for 48h and lysates were collected to perform immunoblot analysis for TGM2 and E-cadherin (Ecad). β-tubulin and actin served as loading controls. (C) Light microscopy images were taken on Day 8. Red arrow indicates stressed cells.

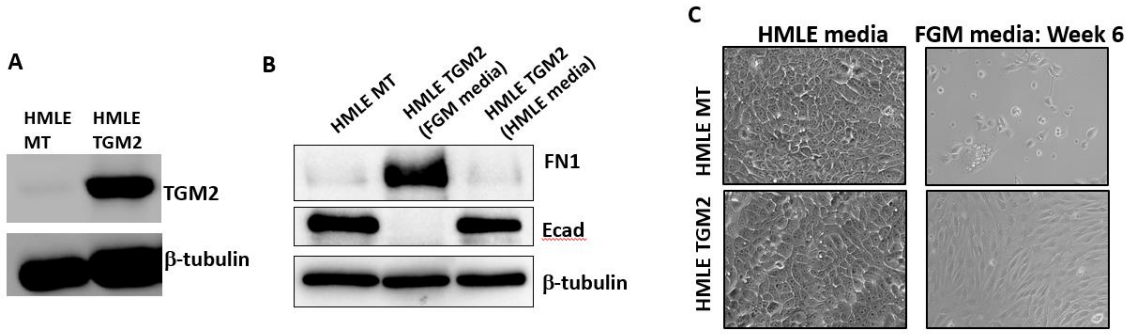

Appendix Figure 4: Expression of TGM2 drives EMT in primary mammary epithelial cells and promotes mesenchymal morphology.

(A) Immunoblot analyses of TGM2 overexpressed in HMLE cells. (B) Immunoblot analysis of whole cell lysates derived from HMLE MT and HMLE TGM2 cultured in HMLE media and whole cell lysates derived from HMLE TGM2 cells cultured in full growth media (FGM) for FN1 and E-cadherin. β-tubulin served as a loading control (C) Light microscopy images displaying epithelial morphology of HMLE MT and HMLE TGM2 cultured in HMLE media and mesenchymal morphology of HMLE TGM2 cultured in FGM.

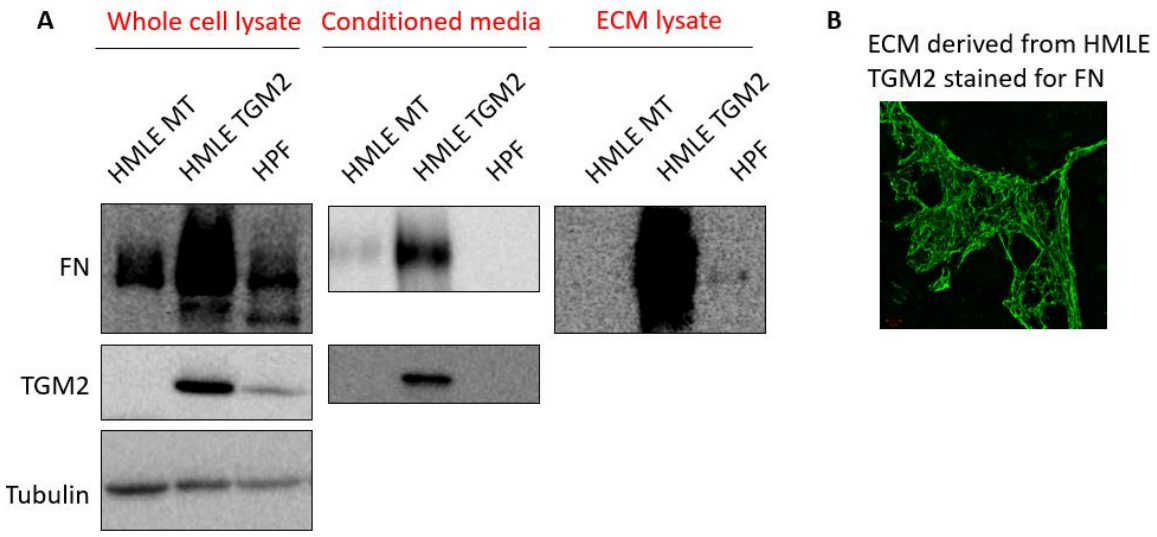

Appendix Figure 5: HMLE TGM2 deposit FN matrix as well as secret soluble FN.

(A) Immunoblot analysis of the whole cell, ECM and conditioned media lysates derived from HMLE MT, HMLE TGM2 and HPF for FN and TGM2. β-tubulin served as a loading control. (B) Confocal microscopy image of ECM derived from HMLE TGM2.

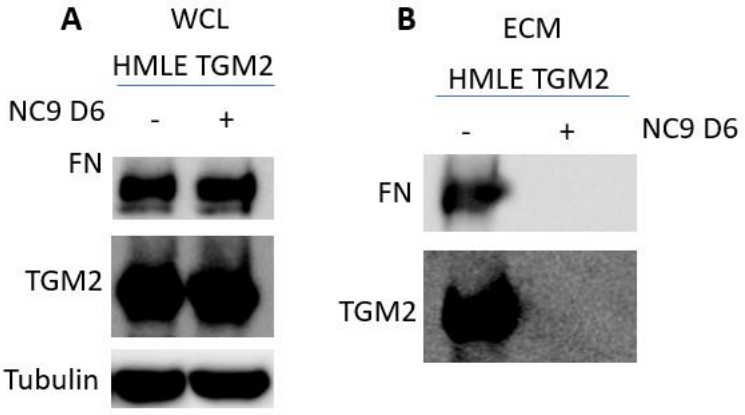

Appendix Figure 6: Treatment of HMLE-TGM2 with NC9 inhibits TGM2 activity and secretion.

(A) Immunoblot analysis of whole cell lysates derived from HMLE TGM2 cultured in the presence or absence of NC9 for TGM2 and FN. β-tubulin served as a loading control. (B) Immunoblot analysis of ECM lysates derived from HMLE TGM2 cultured in the presence or absence of NC9 for TGM2 and FN.

VITA

Aparna Shinde, daughter of Apeksha and Bhagwan Shinde, was born on November 14, 1987 in Mumbai, India. She graduated with B.Sc in biotechnology from the University of Mumbai, India. In 2009, she moved to the United States to pursue her Masters in Biochemistry from California State University Long Beach (CSULB), CA. In 2011, Aparna joined Dr. Katarzyna Slowinska's lab in the Department of Chemistry and Biochemistry at CSULB. In Slowinska's lab, her research focused on developing novel peptide carriers based on collagen peptides for cancer drug delivery. During her master studies, she earned American Chemical Society Graduate Student Travel Award and California State University Annual Biotechnology Symposium Travel Grant. She also published her master's research work as a lead author in *Journal of Peptide Sciences.* Following completion of her master's degree, she joined Purdue University Life Science Interdisciplinary program at Purdue University, West Lafayette, IN. In May 2014, she joined Dr. Candace Tsai's lab in School of Human and Health Sciences at Purdue University. Aparna's work in Tsai's lab focused on determining the effects of chronic exposure to carbon nanomaterials on human health. While working in Tsai's lab, Aparna received American Industrial Hygiene Foundation Scholarship, Eli Lilly and Company Industrial Hygiene Scholarship, AIHce Student and Young Professional Sponsorship, Individual Research Grant from the University of Cincinnati for NIOSH Pilot Project, and Best Oral and Poster presentation award at AIHce. In December 2015, she joined Dr. Michael K. Wendt's lab in Department of Medicinal Chemistry and Molecular Pharmacology at Purdue University's College of Pharmacy. Aparna's work in Wendt's lab focused on studying the role of tumor microenvironment in breast cancer metastasis. During her Ph.D. studies, Aparna earned Cancer Prevention Internship Program Fellowship, Bilsland Dissertation Fellowship, AAiPS Graduate Student Research Scholar Award and College of Pharmacy Graduate Student Travel Award. Aparna's first author publication in *Mol Can Res Journal* was featured as cover page of October 2018 Issue and special collection on the tumor microenvironment and immunobiology of *Mol Can Res Journal*. Aparna also completed a summer internship at Genentech, Inc. in 2017. In addition to her time in the lab, Aparna was actively involved in Purdue's Science in School,

ASHA Purdue, and Purdue NanoDays organizations to improve the graduate experience for all. Following completion of her Ph.D., Aparna will be joining the Global Biologics Department in Abbvie Discovery Organization based in Worcester, MA at Abbvie, Inc. working as a Post-Doctoral Scientist: Elucidation/ Investigation of Intracellular Trafficking Pathways towards Designing Targeted Biotherapeutics under Dr. Michael J. McPherson.

PUBLICATIONS

1. **A. Shinde** and C. Tsai, Toxicity mechanism in fetal lung fibroblast cells for multi-walled carbon nanotubes defined by chemical impurities and dispersibility", Toxicology Research, 2016, 5
2. S.Hardy, **A. Shinde**, *et al*, "Regulation of epithelial-mesenchymal transition and metastasis by TGF-beta, P-bodies, SYK, and autophagy", Oncotarget, 2017
3. T. Wilmanski*, X. Zhou*, W. Zheng, **A. Shinde** *et al*, "Inhibition of pyruvate carboxylase by 1α,25-dihydroxyvitamin D promotes oxidative stress in early breast cancer progression", Cancer Letters, 2017
4. **A. Shinde *et al*** "Autocrine fibronectin inhibits breast cancer metastasis", Molecular Cancer Research, 2018
5. **A. Shinde *et al*** "Pyruvate carboxylase drives pulmonary tropism of breast cancer", Breast Cancer Research, 2018
6. **A. Shinde *et al*** "Syk kinase-mediated autophagy is required for epithelial-mesenchymal plasticity", Cancer Research, 2019